THE ROLE OF WNT SIGNALING DURING REGENERATIVE NEUROGENESIS IN THE ZEBRAFISH OLFACTORY EPITHELIUM

by

Sema Elif Eski

B.S., Molecular Biology and Genetics, Boğaziçi University, 2016

Submitted to the Institute of Graduate Studies in
Science and Engineering in partial fulfillment of
the requirements for the degree
Master of Science

Graduate Program in Molecular Biology and Genetics
Boğaziçi University
2019

ACKNOWLEDGMENT

I would like to thank various people for their support and contribution to this project; Dr. Stefan H. Fuss, for being a role model as a supervisor and for his valuable guidance, critiques, optimism and enthusiastic encouragement during this research, and for developing Fiji macro which saved me many times from long nights of cell counting; Yiğit Kocagöz, for firstly being messy and wooly-minded, then being always around to calm me down when I messed something up; Mehmet Can Demirler, for warning me when I blab something out and for keeping the serious lab environment when we need to do experiments; Uğurcan Sakızlı, for being the opposite of Mehmet Can Demirler as a master distractive colleague and for sharing his music with me; Metin Özdemir, for being annoying and obsessive like me about the organization in the lab and for sharing his knowledge and experience with us; Kardelen Güler, for being my first and talented intern and for her valuable efforts in inhibitor trials and qPCR experiments; Emir Erkol, for teaching me western blotting and for being always challenging and displeased, but also, a supportive partner. Finally, I wish to extend my thanks to my family for being understanding and patient when I missed the chance of spending time with them at the weekends.

Work on this thesis was supported by Boğaziçi University Research Fund Grant Number 12980 (Project code 17B01P8).

ABSTRACT

THE ROLE OF WNT SIGNALING DURING REGENERATIVE NEUROGENESIS IN THE ZEBRAFISH OLFACTORY EPITHELIUM

The peripheral olfactory epithelium (OE) is a potentially insightful exception to the limited capacity of neurogenesis in the adult nervous system. The OE undergoes continuous generation of olfactory sensory neurons (OSNs) to replace senescent and dying neurons by maintenance neurogenesis. In addition, the OE is capable of rapid regeneration upon traumatic injury by repair neurogenesis. Yet, the molecular signals that contribute to these two modes of neurogenesis are not well established. Transcriptome profiling of gene expression during OE regeneration revealed that components and downstream target genes of the Wnt/β-catenin signaling pathway are strongly upregulated following OE injury. This suggests that Wnt/β-catenin signaling may critically contribute to the regulation of OE neurogenesis by triggering mitotic activity in relevant stem/progenitor cells. To examine the role of Wnt/β-catenin signaling for both maintenance and repair neurogenesis, Wnt activity was manipulated in the intact and damaged OE by using pharmacological agonists and antagonists. Pharmacological activation of the Wnt pathway induced massive proliferation responses across the entire OE, including the sensory OE, which resembled the neurogenesis pattern during OE regeneration. Inhibition of the pathway, on the other hand, had a minor effect on maintenance neurogenesis in the intact OE, however, resulted in the partial suppression of damage-induced proliferation. Importantly, anti-β-catenin immunostaining revealed the presence of Wnt-responsive cells in regions of active maintenance neurogenesis in the intact OE, while in agonist-treated OE the β-catenin expression pattern resembled expression observed under damage conditions. The specificity and efficiency of the agonists were validated by examining the changes in the expression levels of components and downstream genes of the Wnt pathway by a semi-quantitative RT-PCR approach. These results suggest that Wnt/β-catenin signaling is necessary and sufficient for maintenance and repair neurogenesis and that Wnt pathway activity induces cell proliferation from two types of progenitor cell populations in the zebrafish OE.

ÖZET

WNT SİNYAL YOLAĞININ ZEBRABALIĞI KOKU ALMA EPİTELİNDEKİ REJENERATİF NÖROGENEZDEKİ ROLÜ

Periferik koku alma epiteli (OE), yetişkin sinir sistemindeki sınırlı nörojenez kapasitesine potansiyel bir istisnadır. OE, yaşlanan ve ölen nöronların yerini alması için bakım nörojeneziyle sürekli koku alma duyusu nöronları üretir. Ek olarak, OE onarım nörojenezi ile travmatik yaralanma üzerine hızlı rejenerasyon yeteneğine sahiptir. Ancak, bu iki nörojenez moduna katkıda bulunan moleküler sinyaller iyi çalışılmamıştır. OE rejenerasyonu sırasındaki gen ekspresyonunun transkriptom profili, Wnt/β-katenin sinyal yolağının bileşenlerinin ve hedef genlerinin, OE yaralanmasından sonra kuvvetle artan şekilde regüle edildiğini ortaya koydu. Bu, Wnt/β-katenin sinyalinin, ilgili kök/progenitör hücrelerde mitotik aktiviteyi tetikleyerek OE nörojenezinin düzenlenmesine kritik derecede katkıda bulunabileceğini göstermektedir. Wnt/β-katenin sinyalinin hem bakım hem de onarım nörojenezindeki rolünü incelemek için, Wnt aktivitesi farmakolojik agonistler ve antagonistler kullanılarak sağlam ve hasar görmüş OE'de manipüle edildi. Wnt yolağının farmakolojik aktivasyonu, OE rejenerasyonu sırasındaki nörojenez düzenine benzeyen duyusal OE dahil olmak üzere, tüm OE boyunca büyük proliferasyon tepkilerini indüklemiştir. Öte yandan, yolağın inhibisyonu, sağlam OE'de bakım nörogenezi üzerinde küçük bir etkiye sahipti, ancak hasara bağlı proliferasyonun kısmen baskılanmasıyla sonuçlandı. Önemli bir şekilde, anti-β-katenin immün boyaması, sağlam OE'de aktif bakım nörojenezi bölgelerinde Wnt-duyarlı hücrelerin varlığını ortaya çıkarırken, agonistle muamele edilmiş OE'de ise β-katenin ekspresyon paterni hasar koşulları altında gözlenen ifadeye benziyordu. Agonistlerin seçiciliği ve etkinliği, yarı nicel bir RT-PCR yaklaşımı ile Wnt yolağının bileşenlerinin ve hedef genlerinin ekspresyon seviyelerindeki değişiklikler incelenerek doğrulandı. Bu sonuçlar, Wnt/β-katenin sinyalinin, bakım ve onarım nörojenezisi için gerekli ve yeterli olduğunu ve Wnt yolağı aktivitesinin, zebra balığı OE'sinde iki tip progenitör hücre popülasyonundan hücre proliferasyonunu indüklediğini gösterir.

TABLE OF CONTENTS

LIST OF FIGURES

LIST OF TABLES

LIST OF SYMBOLS

°C	Celcius
g	Gram
h	Hours
l	Liter
µg	Microgram
µl	Microliter
µm	Micrometer
µM	Micromolar
mg/l	Milligram/liter
ml	Milliliter
mM	Millimolar
min	Minutes
ng	Nanogram
sec	Seconds
v/v	Volume/volume
w/v	Weight/volume

LIST OF ACROYNMS/ABBREVIATIONS

BrdU	5’-Bromo-2’-Deoxyuridine
BSA	Bovine Serum Albumin
cDNA	Complementary DNA
CNS	Central Nervous System
DG	Dentate Gyrus
DMSO	Dimethyl Sulfoxide
DNA	Deoxyribonucleic Acid
dpf	Days Post-Fertilization
GBC	Globose Basal Cell
GSK3β	Glycogen Synthase Kinase 3-Beta
HBC	Horizontal Basal Cell
hpf	Hours Post-Fertilization
ILC	Interlamellar Curve
IP	Intraperitoneal
LiCl	Lithium Chloride
Mdn	Median
mRNA	Messenger RNA
OE	Olfactory Epithelium
OSN	Olfactory Sensory Neuron
PBS	Phosphate Buffered Saline
PBST	Phosphate Buffered Saline with Tween 20
PCR	Polymerase Chain Reaction
PFA	Paraformaldehyde
qRT-PCR	Quantitative Reverse Transcription PCR
RNA	Ribonucleic Acid
RT	Room Temperature
S/NS	Sensory/Non-Sensory
SC	Sustentacular Cell

SEM	Standard Error Mean
TCF/LEF	T Cell Factor/ Lymphocyte Enhancer Factor
UV	Ultraviolet

1. INTRODUCTION

1.1. Adult neurogenesis: the death of an early dogma

During most of the 20th century, neurogenesis, defined here as the generation of neurons from a repertoire of stem or lineage-restricted progenitor cells, was believed to occur only during embryonic and early postnatal development and to cease after development is completed (Ming and Song, 2005). For this reason, nerve cells in the central nervous system (CNS) were believed to be unable to undergo renewal or replacement in the adult brain (Ramon y Cajal, 1928). However, the past two decades have witnessed immense progress in our understanding of the brain and the underlying developmental processes in particular through the development of new technologies. As a result of these new abilities and findings, the once central dogma of neurobiology, which described the lack of regeneration in the adult CNS, was broken.

Pioneering studies by (Altman and Das, 1965) showed that new cells can be generated in the dentate gyrus (DG) of the hippocampus in adult rat brains, suggesting that the adult CNS has a much larger regenerative potential than previously anticipated. Later studies showed that the newly formed cells in the hippocampus and olfactory bulb of adult rat present all of the structural characteristics of neurons, such as dendrites and axons and that these cells are distinct from surrounding glial cells (Kaplan and Hinds, 1977). However, even though these studies are widely celebrated as a major breakthrough in neuroscience from today's perspective, they faced strong opposition and were disregarded by most neuroscientists until the early 1990s. This was primarily the case because ^{3}H-thymidine autoradiography was used to label newly synthesized DNA of proliferating neuronal precursors, which is a difficult technique for developing an effective and reliable methodology. The introduction of specific markers for the identification of maturing or differentiating neurons in combination with the development of the non-radioactive thymidine analog bromodeoxyuridine (BrdU) to birthdate cells and to trace cell lineages marked two substantial innovations that further elevated studies of adult neurogenesis (Kuhn *et al.*, 1996). Only subsequent reports of the functional integration of newly generated

neurons into the adult CNS of songbirds (Paton and Nottebohm, 1984), the hippocampus of monkeys (Gould *et al.*, 1999), and the human brain (Eriksson *et al.*, 1998) finally resulted in the widespread acceptance of the phenomenon of adult neurogenesis.

Although a large variety and number of distinct neurons and glial cells are generated during embryonic development, the rate of gliogenesis and neurogenesis in the adult mammalian brain is still relatively low (Alvarez-Buylla and Kirn, 1997; Doetsch and Scharff, 2001; Rakic, 2002). Despite the occurrence of life-long continuous neurogenesis in the vertebrate brain, active neurogenesis in the adult CNS is spatially restricted to two distinct neurogenic areas. In rodents, the most prominent neurogenic region is the ventricular-subventricular zone of the lateral ventricles, which generates new neurons, which migrate rostrally along the rostral migratory stream and differentiate into interneurons of the olfactory bulb (Altman, 1969; Hack *et al*., 2005; Luskin, 1993). A second active neurogenic area can be found in the previously described subgranular zone of the hippocampus, in which new granule cells are formed from multipotent precursors within the innermost DG cell layer (Altman and Das, 1965). Neuroblasts generated in the subgranular zone only migrate a short distance to more apical granular cell layers into which they integrate and where they become functional neurons (Cameron *et al.*,, 1993; Kaplan and Bell, 1984). In songbirds, however, newly formed neurons are integrated into multiple regions of the telencephalon that are related to song learning and production (Alvarez-Buylla *et al.*, 1994; Goldman and Nottebohm, 1983). The best-studied area among those regions is the higher vocal center, which undergoes seasonal changes in cell number, which correlate directly with the bird's ability to learn new songs or to vocalize (Kirn *et al.*, 1991). In contrast to the rodents, migrating neuroblasts in the bird brain travel along the rostral migratory stream to basal ganglia, not to the olfactory bulb (Alvarez-Buylla *et al*., 1994). Somehow, the ability to generate new neurons is inversely correlated with the level of evolution and simpler organisms, such as amphibians and fish appear to have more active regions of adult neurogenesis. Adult neurogenesis in the fish brain has been studied in detail in three teleost species: the stickleback *Gasterosteus aculeatus* (Ekström *et al.*, 2001), the electric knife fish *Apteronotus leptorhynchus* (Zupanc and Horschke, 1995), and the zebrafish *Danio rerio* (Grandel *et al.*, 2006). In these species, a total of 16 distinct neurogenic areas have been

identified, which include, among other regions, the olfactory bulb, the telencephalon, the hypothalamus, the cerebellum, and the spinal cord.

While the phenomenon of adult neurogenesis is now widely accepted in a multitude of species, the controversy continues for adult hippocampal neurogenesis in the human brain, and two recent publications presented opposite results. While in one of the studies, which included brain samples ranging from gestational week 14 to 79 years of age, the authors showed that hippocampal neurogenesis persisted throughout the entire human life (Boldrini *et al*., 2018), the other study demonstrated that humans appear to lack DG neurogenesis beyond 13 years of age (Sorrells *et al.*, 2018). The cause for the discrepancy is not clear and additional studies will be required to settle the dispute as to whether the human brain has the innate capacity to generate new nerve cells at adult age.

1.2. Regenerative neurogenesis

Neurogenesis is a complex process, which includes the proliferation and expansion of neural progenitor/stem cells but also the maturation, differentiation, and integration of the newly generated cells into existing and functioning neural circuits (Goldman, 2005). In response to changes in environmental conditions, learning, and traumatic injury, the brain is capable of adjusting and refining its neuronal circuitry, which may include the activation of neural progenitor/stem cells to adapt to changing functional requirements (Johansson, 2007). By activation of multipotent precursors, progenitor cells, or stem cells, new neurons and glia can be generated in the CNS that either enhance functionality or restore function in response to injury or degenerative processes (Chojnacki and Weiss, 2008; Goldman, 2005; Sohur *et al.*, 2006).

Conceptually, the process of adult neurogenesis can be subcategorized into two distinct modes: constitutive (or maintenance) and regenerative (or repair) neurogenesis. Throughout this

thesis, these two modes will be highlighted as they became active under different tissue conditions, may be regulated by different factors, and contribute to different outcomes. Maintenance neurogenesis defines the process during which an active stem/progenitor cell population divides continuously to support turnover of the neuronal population in the intact nervous system. On the other hand, regenerative neurogenesis is the process during which dormant stem/progenitor cell populations are transiently triggered to undergo mitotic divisions to replenish neurons that have been lost upon traumatic injury.

It should be mentioned that injuries to the nervous system, of all vertebrates, including the CNS of mammals, may also result in compensatory proliferation of non-neuronal cells in parallel to increased neurogenesis to heal the damaged tissue (Goldman, 2005; Zhang *et al.*, 2005). Many times, glia cell proliferation and glial scar formation is detrimental to functional recovery after CNS injury (Yiu and He, 2006). Of the non-mammalian vertebrate species, fish and amphibians appear to have the greatest regenerative capacity in response to CNS injuries and this ability parallels their increased capacity for constitutive neurogenesis (Doetsch and Scharff, 2001; García-Verdugo *et al*., 2002; Zupanc, 2001). Various experimental models of physical CNS lesion have been developed to elucidate the mechanisms and limitations of the regenerative capacities of post-embryonic teleost brains. A classic series of experiments during which parts or entire lobes of the optic tectum were removed in juvenile and adult *Carassius carassius* highlighted the importance of specific proliferative or "matrix" zones for successful neuroregeneration (Kirsche and Kirsche, 1961). As long as these matrix zones remained intact, the optic tectum was able to reconstitute with high regenerative activity. A pioneering study to elucidate the regenerative abilities of the teleost brain showed compensatory proliferation of constitutively active proliferation areas of the dorsal and ventral telencephalon of the guppy (*Poecilia reticulata*) in response to stab wounds (Richter, 1965). During the process, newly born cells migrate towards the dorsal telencephalon in order to restore the lesioned sites. Taken together, these studies have illustrated the presence and activity of specific proliferation areas and that these specific regions are crucial for neuroregeneration to take place in the lesioned pre-embryonic teleost brain. However, regenerative capacities may be age dependent and appear to be severely reduced in adult compared to developing brains. For instance, certain amphibians

can show remarkable regenerative capacities, especially in the peripheral nervous system, the tail, and limbs (Brockes and Kumar, 2002), however, juvenile frogs successfully regenerate even severe telencephalic lesions (Yoshino and Tochinai, 2004), while post-metamorphic frogs lack proliferative responses (Filoni *et al.*, 1995).

In line with the central dogma it has long been assumed that the mammalian brain also cannot produce new neurons following a lesion. However, recent studies revealed that in response to a lesion or during neurodegenerative diseases, compensatory proliferation can occur in the brain of mammals (Goldman, 2005). It has been reported that the subventricular zone and subgranular zone in the adult rodent brain show increased proliferation and migration of neural precursors in response to ischemic brain injury (Jin *et al.*, 2003; Nakatomi *et al*., 2002). In sum, neuroregenerative studies on the adult mammalian brain showed limited and spatially restricted regenerative abilities, along with compensatory neurogenesis. These findings open the exciting possibility that neuronal repair in inactive proliferative regions of the human CNS may be triggered if the correct factors are supplied to stimulate dormant or constitutively active progenitor pools.

1.3. Anatomical structure and function of the olfactory epithelium

From an evolutionary perspective, olfaction is considered to be an ancient sense that, similar to other specialized sensory systems, strongly depends on the unique organization of its neural and anatomical structure (Price, 1990). More than any other sensory modality, olfaction has fundamental importance for life, which includes the ability to find food, to recognize potential mates, and to avoid predators. Generally, chemical stimuli from the environment, called odorants, are detected by specialized olfactory sensory neurons (OSNs) that each express a single member of the odorant receptor gene family of seven transmembrane receptors (Song *et al.*, 2008). OSNs are embedded in an epithelial sheet, the olfactory epithelium (OE), which is a pseudostratified tissue that is composed of a limited number of neuronal and non-neuronal cell types, which each serves characteristic functions (Schwob, 2002). The OE tissue lines the nasal

cavity and, inherent to its function, is in direct contact with the external environment, a position that makes OE cells vulnerable to damage or insult by various chemicals, toxins and infectious agents. Probably because of this high level of vulnerability, OSNs have a short lifespan and the OE has maintained a remarkably efficient neurogenic capacity to preserve sensory function over the lifetime of an organism (Schultz, 1941). Specific stem/progenitor cell populations have been identified in the OE that are responsible for this capacity. Axonal projection from OSNs connect to the olfactory bulb of the forebrain, which in turn relays information to the piriform cortex and other higher processing centers by bypassing thalamic relay neurons (Mori *et al.*, 1999; Tham *et al.*, 2009). Interestingly, OSNs that express the same olfactory receptor, and therefore have the same ligand specificity, specifically connect to the same (pair of) glomeruli in the olfactory bulb. Thus, new OSNs that have been generated during adult life also need to reestablish these highly specific connections to maintain proper function.

1.3.1. Cellular constituents of the olfactory epithelium

Most of the structural and molecular insight on the OE comes from the histological analysis in rodents, especially mouse and rat. The OE is organized in a laminar pattern in the form of a pseudostratified epithelium that spans from the basal lamina to the apical surface, which is in contact with the outside environment (Figure 1.1; Schwob, 2002). Apical layers of the OE are occupied by OSNs and sustentacular cells (SCs). SCs are tissue-specific microvillus-containing glia cells, which provides support to the OE (Farbman, 1992). In rodents, cell bodies of SCs are organized into a single row, which is localized to the apical-most layer of the OE and forms the tightly sealed border of the tissue (Vogalis *et al.*, 2005). Below this layer, mature OSNs can be found, with younger, more recently formed OSNs in more basal layers. Mature OSNs exhibit a particular bipolar organization: they extend dendrites from their apical sides, which protrude above the layer of SC bodies and contain cilia to sense odorant information, whereas at their basal side they extend an unmyelinated axon that conveys sensory information to the olfactory bulb (Farbman, 1992).

Two functionally and structurally distinct cell populations form the major pool of stem/progenitor cells of the OE and are located in the basal layers of the tissue: horizontal basal cells (HBCs) and globose basal cells (GBCs; Graziadei and Graziadei, 1979). HBCs are mitotically quiescent, have a flat-shaped morphology and are located in the basalmost layers (Leung *et al.*, 2007). HBCs share many molecular and morphological features with basal cells of other epithelial tissues as they co-express cytokeratins 5 and 14 (Schwartz Levey *et al.*, 1991), intercellular adhesion molecule 1 (ICAM 1; Carter *et al.*, 2004), and the transcription factor tumor protein 63 (tp63; Packard *et al.*, 2011). It has been shown that HBC proliferation is triggered when the integrity of the OE is disrupted, either if OSNs are destroyed, or if the cell-to-cell connections between SCs and HBCs are lost (Herrick *et al.*, 2017). Therefore, HBCs form a reservoir of long-lasting progenitor cells, or reserve stem cells, that is capable of generating both neuronal and nonneuronal cells of the OE by transient proliferations upon injury (Leung *et al.*, 2007).

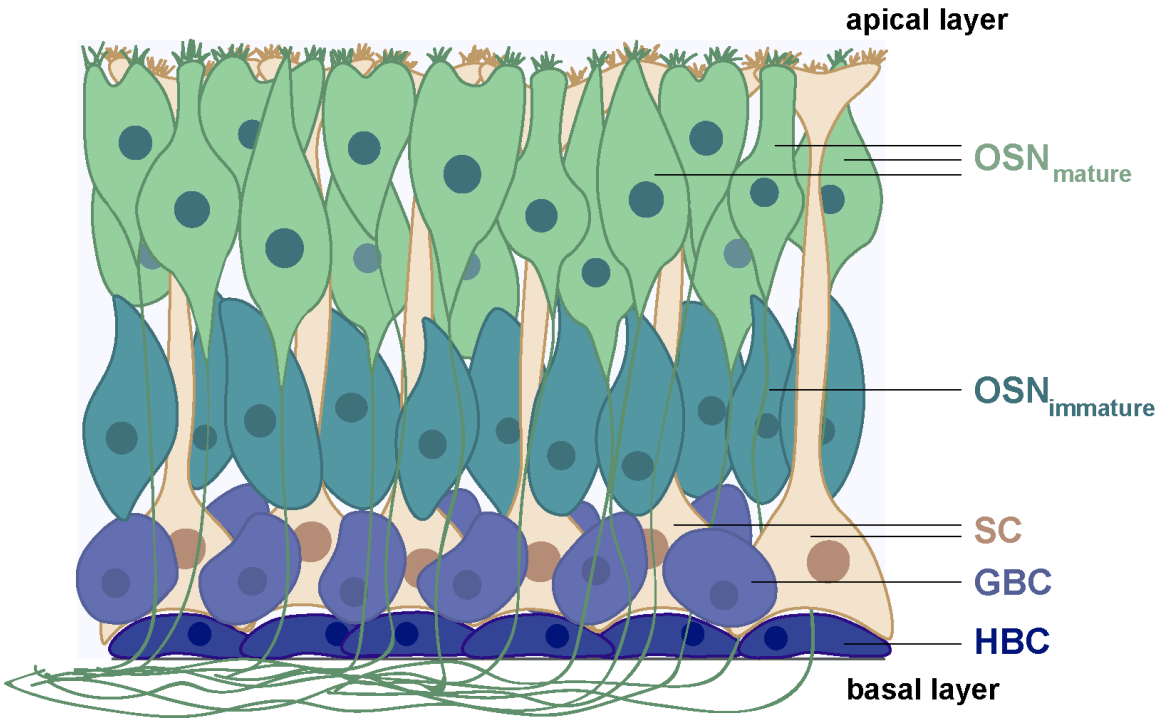

Figure 1.1. Cellular anatomy of the zebrafish peripheral OE. Representation of horizontal basal cells (HBCs), globose basal cells (GBCs), sustentacular cells (SCs), immature and mature olfactory sensory neurons (OSNs).

GBCs, on the other hand, are a round-shaped heterogenous cell population located in more apical positions directly above HBCs. Different from HBCs, GBCs are mitotically active stem/progenitor cells that contribute to the regular turnover of OSNs by constitutive proliferation. GBCs are distinguished by several transcription factors that are expressed temporarily and sequentially during different stages of OSN generation: Sox2 and Pax6 double-positive GBCs generate transit-amplifying cells (Guo *et al.*, 2010; Packard *et al.*, 2016) that express the basic helix-loop-helix transcription factor Ascl1 (Krolewski *et al.*, 2012), while immediate neuronal precursors co-express NeuroD1 and Neurog1 and directly give rise to differentiating OSNs (Cau *et al.*, 1997). Thus, the rodent OE contains two distinct progenitor populations, the GBCs and HBCs, which are triggered by different factors or conditions and which predominantly supply maintenance and repair neurogenesis, respectively. The interrelationship between HBCs and GBCs appears to be complex and interconversion of cell types may be possible under different circumstances.

1.3.2. The structure of the olfactory epithelium in zebrafish

Olfactory organ development in zebrafish begins with the emergence of the olfactory placode at 18 hpf. About 33 dpf, the initially flat OE begins to fold extensively onto itself to form a rosette-like structure. The adult OE has dimensions of 350-600 μm in length and 250-350 μm in width and includes between 10 to 20 lamellae, depending on age, that project radially from a central midline structure (Figure 1.2; Bayramlı, 2016). Each lamella is formed from two epithelial sheets that are facing each other at their basal surfaces but are separated by blood vessels for nutrient transmission to the cells and axon bundles (Hansen and Zeiske, 1993). The apical sides of neighboring lamellae face other each but are not in direct contact and the gap in between allows OSNs to recognize the odorants carried by water flow. OSNs occupy the inner two-thirds of a lamella starting from the midline of OE at the interlamellar curves (ILCs), while the peripheral part of a lamella contains non-neuronal respiratory cells. The region occupied by OSNs is referred to as the sensory region, while the peripheral aspects form a non-sensory region. The relatively sharp sensory/non-sensory border (S/NS) can be visualized by immunostaining against neuronal markers, such as HuC/D (Kim *et al*., 1996).

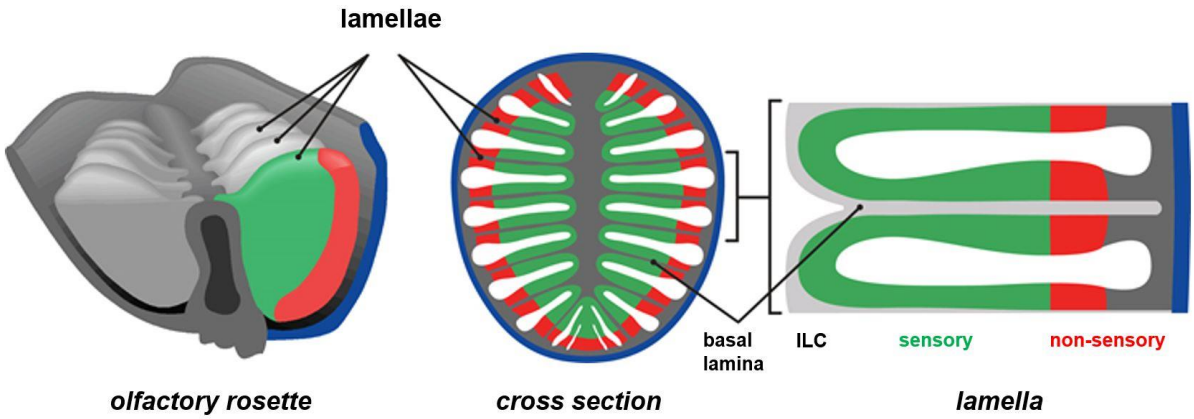

Figure 1.4. Schematic overview of the adult zebrafish OE which forms a rosette like structure divided into three main sections: interlamellar curve (ILC), the sensory region (green), and the non-sensory region (red).

Despite the general molecular and structural similarities between the zebrafish OE and the OE of mammals, the zebrafish OE exhibits a variety of distinctive features. The detection of pheromones is achieved by vomeronasal receptors in the vomeronasal organ in some vertebrates. Among them, only bird and fish lack of vomeronasal organ; however, fish can still sense pheromones, since the expression of vomeronasal receptors is associated with microvillous sensory neurons (Saraiva *et al*., 2015; Silva and Antunes, 2017). Therefore, while some vertebrates have two separate olfactory organs, fish have a single organ that contains both cell types. Another major difference between the zebrafish and mammalian OE is the position of SC cell body. Our research group has found that in zebrafish the position of SC, which are immunoreactive to cytokeratin type 2, is inverted and that their cell bodies reside in the basal layer of the OE (Bali, 2015) contrary to forming an apical border in the rodent OE (Vogalis *et al.*, 2005).

As explained above, GBC and HBC stem cell populations reside within the basal layer of the rodent OE and differentiation and migration of OSNs proceeds in the basal to apical direction (Schwob *et al*., 2017). In contrast, the zebrafish OE has two distinct areas of active maintenance

neurogenesis in the intact tissue, which are located at the ILC and S/NS border. Newborn OSNs that are generated at the ILC and S/NS border then migrate towards the center of the lamella (Bayramli *et al.*, 2017). Thus, the ILC and S/NS border are the main neurogenic areas in which the stem/progenitor cells contribute to maintenance neurogenesis. To identify the stem cell niche that contributes to repair neurogenesis in the zebrafish OE, lesion studies can be performed. A commonly used method to damage the OE of aquatic organisms is nasal irrigation with the nonionic detergent Triton X-100 (Çapar, 2015; Iqbal and Byrd-Jacobs, 2010). These studies showed that stem/progenitor cells located along the entire length of the lamellae respond to acute injury with increased mitotic activity, resembling HBC responses. Importantly, cell proliferation under damage conditions includes the sensory region of the OE, which shows little to no proliferative activity in the intact tissue. During the degeneration phase, almost the entire neuronal population is lost by the end of first-day post-injury, which can be detected by the loss of HuC/D-positive cells (Iqbal and Byrd-Jacobs, 2010). Strikingly, the entire OE can regenerate within 5-7 days post-injury (Iqbal and Byrd-Jacobs, 2010; Çapar, 2015; Kocagöz, unpublished).

1.3.3. Olfactory system in regenerative studies

The peripheral OE is relatively unprotected within the nasal cavity and directly exposed to the outside environment, which makes it prone to be injured by toxic chemicals. For this reason, the OE has an unusually high regenerative capacity, which is advantageous for studies of nerve cell regeneration. Nerve transection or bulbectomy are common approaches to induce retrograde degeneration of neurons. Retrograde degeneration results in rapid loss of neurons by apoptosis, and eventually, the loss of functional synapses in the olfactory bulb as demonstrated in the OEs of hamsters (*Mesocricetus auratu*; Costanzo, 1985) and monkeys (*Saimiri sciureus*; Monti Graziadei *et al.*, 1980). Following various and species-specific recovery times, OSNs are regenerated and can successfully reestablish synaptic connections in the olfactory bulb. As an alternative approach, olfactotoxic chemicals such as methyl bromide, zinc sulfate, and the detergent Triton X-100 are commonly used to stimulate anterograde degeneration of OSNs. In a study using the chemical injury method it has been observed that the rat OEs treated with

methyl bromide gas are able to fully restore their neuronal population within 8 weeks (Schwob *et al.*, 1995). The zebrafish OE has a similar regenerative capacity but de- and regeneration occur much faster and reconstitution of almost the entire OSN population can be completed within only 5 days upon nasal irrigation with Triton X-100 (Iqbal and Byrd-Jacobs, 2010). Taken together, these findings suggest that the peripheral OE is a powerful model to study mechanisms of neurogenesis because of its remarkable regeneration capacity. Thus, it is interesting to understand how the peripheral OE is capable to exhibit such a high regenerative potential in contrast to more restricted regenerative abilities in the CNS and mammalian species.

1.4. Molecular regulation of the dynamics of neurogenesis

Understanding the dynamics and molecular signals that control neurogenesis and CNS regeneration is intriguing and important for the development of new therapeutic strategies for traumatic injuries, or neurodegenerative and neuropsychiatric diseases. Most of our current knowledge on how the activities of neuronal precursor cells, such as the terms of proliferation, differentiation, migration, and quiescence, comes from adult neurogenesis studies in mammals. In order to shed light onto these mechanisms, the molecular regulations of relevant stem cell niches should be examined. However, there are many drawbacks since stem cell activity may be driven by complex and interdependent signaling cascades. Among these cascades, several have been shown to contribute to regeneration but also to embryonic development, such as Notch, FGF, BMP, Wnt, and cytokine signaling.

It has long been established that Notch and its ligand Delta regulate cell fate decisions in neurons and glial cells in the CNS (Cau and Blader, 2009; Fortini, 2009; Fortini and Artavanis-Tsakonas, 1993) and in neural precursors in the zebrafish embryo (Haddon *et al.*, 1998; Park and Appel, 2003). Recent work showed that overexpression of the Notch intracellular domain leads to increased dormancy of progenitors in the zebrafish telencephalon, while blocking Notch signaling enhance their proliferation rate (Chapouton *et al.*, 2010). Therefore, the findings of this study suggest that the proliferative status of telencephalic progenitors may be negatively

regulated by Notch signaling. Similarly, BMP signaling has also been shown to inhibit adult neurogenesis in mammalian brains (Bonaguidi, 2005; Colak *et al*., 2008; Mira *et al*., 2010). Thus, these signaling pathways may be essential to sustain the stemness of neuronal progenitors in the adult brain and Notch and BMP signaling may control the balance between the quiescent and proliferation states of neural stem cells.

On the other hand, FGF signaling, which is a fundamental pathway controlling proliferative activity of many cell types, has been shown to upregulate proliferative activity of cerebellar and telencephalic progenitors in the adult zebrafish brain (Ganz *et al.*, 2010; Kaslin *et al*., 2009). In addition, epidermal growth factor (EGF) has also been established as an important factor for neuroregeneration. EGFR has been reported to play a crucial role in the development of oligodendrocytes and remyelinations of axons (Aguirre *et al.*, 2007). In several studies, heparin binding-epidermal growth factor (HB-EGF) has also been shown to stimulate oligodendrocytogenesis and mobilization of subventricular zone progenitors in the injured adult mouse brain (Cantarella *et al.*, 2008; Scafidi *et al*., 2014), and generation of progenitors derived from multipotent Müller glia cells both in the uninjured and injured zebrafish retina (Wan *et al.*, 2012).

More recently, a link between regulation of neurogenesis and inflammation has been established and cytokine signaling is one of the most relevant pathways that has a role in neurogenesis and regeneration. Infections or damage of the nervous system may result in activation of microglia cells, which are macrophages of the CNS (Das and Basu, 2008). Activated microglia have two major roles in de- and regeneration: eliminating dying or damaged neurons and triggering a local neuroinflammatory response (Rock *et al*., 2004). During neuroinflammation, different proinflammatory factors are released such as chemokines, cytokines, and reactive oxygen species which are vastly neurotoxic. Cytokines are immunological mediators that play a role in cell-to-cell communication in various cells and tissues and have been shown to be associated with certain cellular activities such as cell survival and proliferation (Das and Basu, 2008). As an example of proinflammatory cytokine produced

by microglia and astrocytes upon injury, TNF-α inhibits the proliferative activity of neural stem cells in the adult mouse hippocampus both in the intact and pathological brain (Iosif, 2006). Apart from TNF-α, other key proinflammatory modulators, such as interleukin-6 and -18, resulted in a decrease in the proliferation of neural stem cells and defects in neuronal differentiation but increased glial differentiation (Liu *et al.*, 2005; Monje, 2003; Vallières *et al.*, 2002). Contrasting findings have been made in the injured zebrafish retina, in which the cytokines IL6, IL11 and leptin synergistically stimulate repair neurogenesis from Müller glia cells through activation of STAT and β-catenin signaling (Wan *et al.*, 2014; Zhao *et al.*, 2014).

1.4.1. The contribution of Wnt/β-catenin signaling pathway on neurogenesis

The canonical Wnt/β-catenin pathway is activated by the binding of extracellular ligands of the Wnt protein family to a membrane receptor complex containing a Frizzled protein and the Lrp5/6 co-receptors (Figure 1.3; Tran and Zheng, 2017). The interaction between the Wnt protein and Frizzled results in the recruitment of the β-catenin destruction complex containing Axin, adenomatous polyposis coli (APC), and glycogen synthase kinase-3β (GSK3β), and its subsequent inhibition by the Dishevelled protein. Upon inhibition of the destruction complex, β-catenin is prevented from being phosphorylated by GSK3β, and eventually from being degraded by ubiquitin-mediated proteasomal activity. As a consequence of accumulation in the cytoplasm, β-catenin can translocate into the nucleus where it functions as a transcriptional coactivator of a transcription factor from T-cell factor/lymphoid enhancer factor (TCF/LEF) family.

Previous studies in mammals showed that the canonical Wnt/β-catenin signaling has numerous roles in the nervous system such as proliferation and differentiation of precursor cells (Lie *et al.*, 2005), neuronal migration (Chenn and Walsh, 2003), and synaptogenesis in the adult hypothalamus (Bamji *et al.*, 2003). The Wnt pathway is highly conserved among vertebrates and its contribution to early development is incontrovertible since it plays crucial roles in cell

fate specification and body axis organization (Clevers and Nusse, 2012). Intriguingly, it has been shown that Wnt3 is highly expressed in hippocampal neurogenic areas, and consistently, overexpression of Wnt3 is sufficient to trigger stem/progenitor cells to generate new neurons in the adult hippocampus (Lie *et al*., 2005). Consistently, inhibition of Wnt signaling resulted in the total inhibition of adult neurogenesis in the mouse brain. Wnt signaling has also been shown to be a principal regulator during mammalian neuronal development, as β-catenin had decisive roles on progenitors as switching between differentiation and proliferation status of the progenitors (Lie *et al*., 2005). Apart from its role in mammalian brains, Wnt signaling pathway has also been shown to regulate the neurogenesis and precursor cell activity in the mouse OE (M. Chen *et al*., 2014; Wang *et al*., 2011). Studies by Wang *et al.* showed that the stimulation of Wnt signaling with activators such as Wnt3a resulted in promoted differentiation of progenitor cells and thereby generation of neuronal and non-neuronal epithelial cells.

Moreover, Wnt expressing Sox2-positive basal cells in the mouse OE have been shown to increase in number upon injury by methimazole (Chen *et al*., 2014). Consistently, Wnt signaling has been revealed to enhance neuroregeneration by maintaining the proliferation of Lgr5-positive stem/progenitor cells, which can regenerate both in intact and injured OE conditions. These results show that canonical Wnt/β-catenin signaling is triggered upon OE injury, and subsequently, it causes increased proliferative activity of stem/progenitor cells during regeneration events in the mouse OE. Even though zebrafish OE has remarkable regenerative capacity compared to the mammalian counterpart, the contribution of Wnt/β-catenin signaling has not been addressed in zebrafish OE yet. This study aims to reveal the roles of Wnt/β-catenin signaling on the neurogenesis in the zebrafish OE by pharmacological manipulation of Wnt activity and identification of cells in which the pathway is activated upon injury.

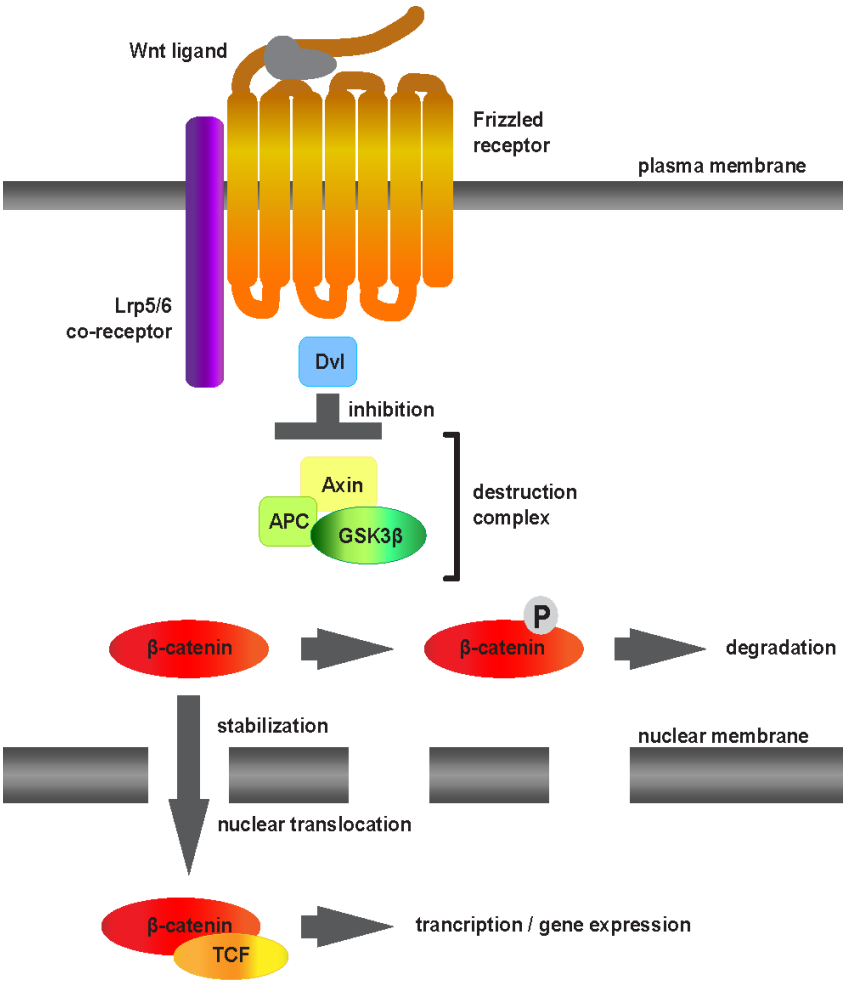

Figure 1.7. Schematic overview of the canonical Wnt/β-catenin signaling pathway. Activation of Frizzled receptor by a Wnt ligand causes the inhibition a destruction complex containing APC, Axin and GSK3β, and thereby results in the stabilization of β-catenin in the cytoplasm and in the nucleus.

2. PURPOSE

While adult neurogenesis is well characterized in the rodent OE, much less is known about the stem/progenitor cell populations or signaling pathways that contribute to OSN maintenance and OE repair in zebrafish. Transcriptome profiling by RNA-seq analysis revealed a prominent role for the Wnt/β-catenin signaling pathway during de- and regeneration of the zebrafish OE. In the framework of this thesis, I intended to provide an in-depth examination of the contribution of the canonical Wnt/β-catenin signaling pathway to zebrafish OE maintenance and regeneration.

As the first aim of this study I wanted to examine whether Wnt/β-catenin signaling is both necessary and sufficient to trigger repair neurogenesis in the zebrafish OE. In order to build a functional link between stem/progenitor cell proliferation and activation of Wnt signaling, a comprehensive set of experiments was devised, which is based on pharmacological pathway manipulation and analysis of changes in cell proliferation by BrdU incorporation assays.

As a second aim, I wanted to confirm that exogenous pharmacological manipulation indeed activates components of the Wnt pathway. For this purpose, changes in mRNA levels of a restricted set of downstream target genes and components of Wnt signaling pathway were analyzed by semi-quantitative RT-PCR.

As a final aim, I wished to identify in which cell populations Wnt/β-catenin activity is triggered upon tissue damage in the zebrafish OE and whether the same cells are responsive to pharmacological activation of the Wnt pathway. To assess this issue, Wnt activity was detected by β-catenin immunoreactivity.

3. MATERIALS AND METHODS

3.1. Materials

3.1.1. Fish

Adult Zebrafish (*Danio rerio*) used in all experiments throughout this study were obtained from a local pet shop. The maintenance of the fish was carried out in the zebrafish facility at Vivarium of Boğaziçi University Center for Life Sciences and Technologies.

3.1.2. Equipment and supplies

The list of chemicals and equipment used in this study can be found in Appendix A and Appendix B.

3.1.3. Buffers and Solutions

The buffers and solutions used in molecular biology experiments, such as RNA purification, cDNA reverse transcription, and polymerase chain reaction were obtained from molecular reaction kits unless otherwise stated. All solutions used for zebrafish studies were prepared as described by Westerfield (1995).

3.2. Methods

3.2.1. Maintenance of fish

Fish were kept in a room with constant 28°C temperature and 14 hours light/10 hours dark cycle. Fish were kept either in 1, 3, or 10 l tanks in groups of maximum 5, 15, or 50 fish, respectively. The tanks were connected to an automated zebrafish housing system in which the circulated fish water passes through a system including five-stage filtration, aeration, UV sterilization and temperature controlling functions. 100 l fish water was supplied with a mixture of 2 g sea salt, 0.84 g calcium sulphate, and 7.5 g sodium bicarbonate. While fish were fed twice a day on weekdays with dry flake food in the morning and with live brine shrimp two-days old larvae (*Artemia sp.*) in the evening, on weekends fish were fed once with *Artemia* and flake food.

3.2.2. Dissection of the olfactory epithelium

To dissect olfactory epithelia, fish were euthanized by submersion in 0-4°C ice-water for at least 10 minutes. After the opercular movement ceased, fish were decapitated by using a surgical blade. Then, the head was transferred into the dissecting dish filled with ice-cold phosphate saline buffer. By using fine forceps, zebrafish eyeballs were first removed under a stereo microscope. After removal of the epithelial, tissue covering the OEs were removed and the OEs were carefully detached from the bones followed by the disruption of the axon bundle which connects the OE to the olfactory bulb.

3.2.3. Sectioning of the OE

After dissecting the tissue, OEs were embedded in molds filled with optimal cutting temperature medium OCT. After molds were completely frozen at -20°C, the tissue blocks was transferred to a cryostat, which is precooled to -22°C. Tissue slices were cut at 12µm-thickness and immediately transferred to positively charged slides. Then, slides were dried in an oven at 60°C for 1 hour. Dried slides were either used immediately for immunohistochemistry experiments or stored at -80°C.

3.2.4. Immunohistochemistry on OE sections

Slides containing OE tissue sections that were stored at -80°C were warmed up to room temperature for 10 minutes before staining. Oven-dried sections were first rehydrated with 1X PBS and then framed with a liquid-repellant slide marker pen, PAP pen to prevent leakage of solutions over the edge of the slide. The sections were fixed with 4% cold-paraformaldehyde (PFA) in PBS (pH 7.4) for 10 minutes within a closed humidity chamber. Then, slides were transferred to glass Coplin jars and washed 3 times 5 min with 0.1% (v/v) Triton X-100 in 1x PBS (PBST) at room temperature (RT) on an orbital shaker. After removal of PFA and washing in PBS, an additional step of antigen retrieval was performed for BrdU incorporation in which the slides were transferred to Coplin jars filled with 4N HCl and incubated for 15 min at RT on the shaker. Then, the slides were washed with 0.1% PBST for 3 times 5 min. For blocking of unspecific binding, the sections were incubated with 3% (w/v) bovine serum albumin (BSA) in 0.1% PBST for 1 hour in a humidity chamber at RT. The blocking solution was gently poured off and the sections were incubated with primary antibodies which were freshly prepared in 3% BSA solution for overnight incubation at 4°C in a humidity chamber. The concentrations of the primary antibodies used in this study were as follows: mouse anti-human neuronal protein HuC/D (1:500) and rat anti-BrdU (1:500). After overnight incubation with the primary antibodies, slides were washed with 0.1% PBST for 4 times 5 min at 4°C. Then, the sections were incubated with secondary antibodies, which were freshly prepared in 3% BSA solution, in

the dark for 2 hours at RT in a humidity chamber, followed by washing 4 times 5 min with 0.1% PBST at RT. The concentrations of the secondary antibodies used in this study were as follows: anti-mouse Alexa Fluor 488 (1:800) and anti-rat Alexa Fluor 555 (1:800). Stained sections were visualized under a TCS-SP5 AOBS laser-scanning confocal microscope.

3.2.5. Heat induced antigen retrieval for anti β-catenin immunostaining

After dissection, OEs were directly fixed overnight at 4°C with 4% cold-PFA in 2 ml Eppendorf tubes on an orbital shaker. After fixation, the OEs were rinsed and washed 3 times for 10 min each with 0.1% PBST and then embedded in OCT medium. After the molds were completely frozen at -20°C, 12 µm-thick sections of the OEs were cut at the cryostat and transferred to positively charged slides. The slides were dried for 2 hours in an oven at 60°C and stored at -80°C if needed for later use.

For immunostaining, slides were rehydrated in 1x PBS for 10 min at RT before the antigen retrieval step. For antigen retrieval, a glass beaker filled with 200 ml of trisodium citrate buffer (10 mM sodium citrate, 0.05% Tween® 20, pH 10.0) was heated to 95°C on a hot plate and the temperature was set between 90-95°C. To prevent folding or detachment of the sections from the slides, an uncharged slide was used to cover the by clipping the two slides at one end with a paperclip as described by Vinod *et al.* (2016) and a minimum gap between the slides were kept by putting plastic coverslips to both ends which were cut into small strips to avoid contact with the sections. Then, the covered slide was placed into hot buffer at a 25°-45° angle, and the sections were incubated for 30 min at 90-95°C. After this step, the slides were immediately transferred to cold water and cooled for 10 min. Then, the uncharged slide was gently removed, followed by an air-dry step for 5-10 min. Next, the slide was washed with 0.1% PBST for 3 times 5 min. An additional 4N HCl treatment was performed for 15 min, followed by washing with 0.1% PBST for 3 times 5 min. For the blocking step, the slide was framed with a PAP pen and transferred to the humidity chamber. The sections were blocked with freshly prepared 3% BSA in 0.1% PBST for 1 hour at RT. Then, they were incubated with mouse anti-β-catenin

antibody (1:250) overnight at 4°C in a humidity chamber, followed by washing with 0.1% PBST for 4 times 5 min at 4°C. For the secondary antibody incubation, anti-mouse Alexa Fluor 488 was freshly prepared in 3% BSA solution and the sections were incubated with the secondary antibody solution for 2 hours at RT in the dark, followed by washing with 0.1% PBST for 4 times 5 min. Then, the sections were imaged under a laser-scanning confocal microscope.

3.2.6. BrdU incorporation assay

Fish were incubated for 24 hours in fish water containing 30 mg/L 5-Bromo-2'-deoxyuridine (BrdU) to allow BrdU incorporate into replicating DNA of dividing cells. An additional 4N HCl treatment was required for BrdU immunostainings to denature the hydrogen bonds in DNA which enables the anti-BrdU antibody to recognize BrdU antigen (Tang *et al.*, 2007).

3.2.7. Intraperitoneal injection of pharmacological agents

Fish were anesthetized with MS-222 solution until opercular movements slowed down and then placed onto a sponge soaked with fish water. Chemicals were injected in the direction of the anterior to posterior fin into the midline of the abdomen in a maximum volume of 50 µl using 0.5 ml U100 insulin syringes with 30G needle. Then, the needle was gently pulled back avoiding any damage and the fish was placed back to fish water.

3.2.8. Chemical lesion on the OE with Triton X-100

After anesthesia in MS-222 and slowed down gill movements, fish were transferred into a petri dishes and wrapped between wet tissue papers. 1% (v/v) Triton X-100 solution in 0.1M PBS supplemented with 0.1% (v/v) phenol red was prepared and filled into a pulled-out glass

capillary tube. Approximately 1 µl of Triton X-100 solution was administered directly into the nasal cavity 2 times with 45 sec intervals under a stereo microscope using an electronic microinjector. The Triton solution was washed out from the nasal cavity after 90 sec by a gentle stream of fish water from a Pasteur pipette and the fish was placed back into tank water for recovery.

3.2.9. RNA purification

RNA purifications were performed using TRIzol® reagent by following the protocol supplied by the manufacturer. The concentration of purified RNAs was measured using a NanoDrop® spectrometer and the purified RNAs were immediately stored at -80°C for later use.

3.2.10. cDNA reverse transcription reaction

cDNA synthesis was performed using Transcriptor First Strand cDNA Synthesis Kit by following the manufacturer's protocol. Each reaction was carried out by using 400 ng of RNA template and cDNA templates were kept at -20°C.

3.2.11. Polymerase Chain Reaction (PCR)

For semi qRT-PCR experiments, PCR was performed by using OneTaq® polymerase according to the instructions of the manufacturer. Each reaction contained cDNA template, 0.5µM of each primer, 0.2 mM deoxynucleotide mix, and 1x OneTaq® reaction buffer. A typical PCR program comprises 3 min of initial denaturation at 95°C, followed by 25 cycles of 30 sec of denaturation at 95°C, 30 sec of annealing at 2ºC below the melting temperature of the primer pairs (see Appendix Table D.1.), which were calculated by using NEB online tool (https://tmcalculator.neb.com), 1 min of elongation at 72°C, and a final elongation for 5 min at

72°C. The PCR products were stored either at 4°C or -20°C or directly run on agarose gels for visualization.

3.2.12. Agarose gel electrophoresis

PCR products were separated and visualized on 1-2% (w/v) agarose gels prepared in 1x TAE buffer depending on the size of the predicted product. Agarose gels were supplemented with 0.5μg/ml ethidium bromide (0.01%, v/v) for visualization of DNA. Samples were mixed with 6x loading dye and loaded into wells. Gels were run at 80-120V until the dye passed two thirds of the gel. Gels were visualized under UV either under a Bio-Rad Geldoc XR System or Syngene.

3.2.13. Data analysis

In immunohistochemistry experiments, quantifications of BrdU-positive cells in the entire OE was performed using a custom macro in Fiji image analysis software (Fuss, Appendix F and Appendix G). In semi-qRT-PCR experiments, quantifications of the band intensities on agarose gel were performed using the measurement function of Fiji. Each band was set with equal rectangular regions of interest and measured as cumulative integrated density. Graphs were drawn in GraphPad software where the statistical significance was assessed by Mann Whitney U Test.

4. RESULTS

Recent studies have demonstrated the importance of Wnt/β-catenin signaling for the regulation of stem/progenitor cell activity during neurogenesis and regeneration of the rodent OE (M. Chen *et al*., 2014; Wang *et al*., 2011), however, the contribution of Wnt/β-catenin signaling during regeneration of the zebrafish OE has not been investigated. Gene expression analysis at the transcriptome level by RNA sequencing on regenerating OE tissue following Triton-X-100 injury revealed an upregulation of genes associated with the Wnt/β-catenin signaling pathway and showed an induction of pathway genes during the early phase of regeneration.

Based on these findings, I wished to establish a direct link between Wnt/β-catenin pathway activation and stem cell proliferation in the zebrafish OE during regeneration. In the framework of this thesis I devised a comprehensive set of experiments to examine whether exogenous activation of the Wnt/β-catenin pathway is sufficient to mimic the native response of the OE to damage, which is characterized by a proliferation pattern with increased mitotic activity in the otherwise quiescent sensory OE, and whether inhibition of the pathway may silence baseline proliferation or diminish mitotic activity during the regeneration of the damaged OE. I reasoned that pharmacological manipulation of the pathway with small molecule agonists could, in principle, induce strong mitotic activity in the OE. Thus, if Wnt/β-catenin pathway activation would be sufficient to induce stem/progenitor cell proliferation it may trigger a pattern of repair neurogenesis, which resembles the proliferation pattern of the native OE response to tissue damage. For this purpose, I utilized two different agonists that are strong and selective activators of Wnt signaling: lithium chloride (LiCl), and the small molecule agonist CAS 853220-52-7. LiCl is a commonly used activator of Wnt signaling, since it directly inhibits GSK3β, the negative regulator of the pathway. In several studies, LiCl has been shown to have strong effects on development, cell fate determination and glycogen metabolism (Klein and Melton, 1996), and, consequently, therapeutic potential for many diseases such as diabetes, bipolar disorder, and Alzheimer's disease (Cohen and Goedert, 2004). The small molecule

agonist CAS 853220-52-7 is a cell permeable compound mimicking the effect of extracellular Wnt ligand by binding to the Frizzled receptor complex, and therefore induces β-catenin stability and its transcriptional activity without inhibiting the activity of GSK3β (Liu *et al*., 2005).

In addition to the hypothesis that Wnt/β-catenin may be sufficient for the induction of neurogenesis, either during maintenance of the tissue or during regeneration, I wanted to examine whether Wnt/β-catenin signaling is strictly required to trigger repair neurogenesis. Therefore, I aimed to examine if the increase in the cell proliferation after traumatic damage and/or the base level of proliferation that is observed during the maintenance of the OSN population could be diminished by utilizing a panel of antagonists of Wnt/β-catenin signaling: IWR-I, Quercetin, and iCRT-14. IWR-I has been shown to stabilize Axin1, which is a part of β-catenin destruction complex (Wehner *et al*., 2017), thereby preventing β-catenin stabilization in the cytoplasm. The second chosen antagonist of Wnt/β-catenin signaling was Quercetin which is a polyphenolic flavonoid constituent in many dietary foods (Formica and Regelson, 1995) with potential anti-cancer (Amado *et al*., 2014) and neuroprotective effects (Sabogal-Guáqueta *et al*., 2015). Quercetin also acts as a Wnt/β-catenin antagonist since it blocks binding between β-catenin and TCF via direct interaction with β-catenin (Park *et al*., 2005). Being a potent thiazolidinedione inhibitor of β-catenin responsive transcription (CRT) genes, the last antagonist used was iCRT-14, which has been reported to reduce the amount of Dishevelled and to disrupt both TCF binding to DNA and the interaction between TCF and β-catenin (Gonsalves *et al*., 2011) .

4.1. Functional characterization of Wnt activity in the zebrafish OE

Exogenous activation and silencing of the pathway is necessary to conclude whether Wnt/β-catenin signaling is sufficient and/or necessary to trigger repair neurogenesis during OE regeneration. For this purpose, BrdU incorporation assays were performed following the application of small molecule agonists and antagonists in order to visualize the frequency and

tissue distribution of proliferating cells. Pilot experiments that included the application of drugs to the fish water and trials using nasal irrigation did not result in observable or consistent effects (data not shown). This was possibly due to variability in chemical uptake by the body of the fish, or inefficient penetrance of the small molecules into the OE tissue. Naturally, the apical layer of cells of the intact OE forms a tight barrier that does not permit the entrance of foreign reagents into the underlying tissue. Therefore, an alternative protocol was developed to standardize efficient introduction of Wnt pathway modulators by intraperitoneal (IP) injection. This route of drug administration is commonly used in animal studies, since the drug is absorbed efficiently through the peritoneal membrane and enters to systemic blood circulation, eventually reaching to target cells in the OE.

In total the effects of Wnt pathway modulators were compared among five different experimental groups that received IP injections. A PBS vehicle-injected group (n=3) served as control group and the number of BrdU-positive cells of this control group was compared to four experimental groups that were treated with agonists or antagonists of the Wnt/β-catenin pathway. The first experimental group of fish was IP-injected with 250 mg/kg of LiCl per fish dissolved in 50 µl PBS (n=3), the second received 50 µM CAS 853220-52-7 per fish dissolved in 50 µl PBS containing 1% DMSO (n=3), the third were injected with 25 µM iCRT-14 dissolved in 50 µl PBS containing 0.1% DMSO (n=3), and the fourth received 100 mg/kg of Quercetin per fish in 50 µl PBS with 20% DMSO (n=3). Following three consecutive days of IP injection at 24 hours intervals, the fish were incubated in tank water containing the thymidine analogue BrdU for 24 hours and analyzed by immunohistochemical staining against the pan-neuronal marker HuC/D, and BrdU. In all five experimental groups, OE sections with an intact-typical HuC/D pattern resembling an undamaged zebrafish OE have been selected to analyze the functional effects of the drugs.

4.1.1. Wnt/β-catenin signaling is sufficient to induce OE neurogenesis

Following the experimental protocol described above, immunohistochemical staining of the OE from fish treated with either one of the two Wnt activators (LiCl, CAS 853220-52-7) displayed a strong increase in proliferative activity across the entire OE when compared to PBS-injected control fish (Figure 4.1, Appendix C). The induced mitotic activity resembled the proliferation profile that is typically observed after tissue lesion by nasal irrigation with 1% Triton X-100. In contrast, PBS-injected fish showed the characteristic pattern of cell proliferation during maintenance neurogenesis in the intact OE, which is characterized by high proliferative activity predominantly at regions of the interlamellar curve (ILC) and the sensory/non-sensory (S/NS) border (Bayramli *et al*., 2017). As shown in Figure 4.1, BrdU-positive cells were exclusively located at the ILC and non-sensory periphery, yet the sensory region of the OE, highlighted by HuC/D staining, was largely devoid of proliferating cells. In contrast, fish in which the OE was damaged by nasal irrigation with the detergent Triton X-100 showed a severely reduced and highly fragmented HuC/D pattern due to the degeneration of OSNs. Because tissue damage in the OE triggers repair neurogenesis (Iqbal and Byrd-Jacobs, 2010; Çapar, 2015; Kocagöz, unpublished), the OE showed an increased number of BrdU-labeled cells, including the dense and even distribution of mitotic cells across the sensory OE.

Injection of LiCl to the fish increased the number of proliferating cells at the sites of maintenance neurogenesis at the ILC and S/NS border but also induced additional mitotic activity within the sensory OE, similar to the tissue response during regeneration. It appeared that proliferation within the ILC and the peripheral ring outside of the sensory region was also higher in number of BrdU-positive proliferating cells compared to untreated control fish. Similar to the application of LiCl, treatment with the Wnt agonist CAS853220-52-7 had the same effect and resulted in a dramatic increase in the number of BrdU-positive cells within the sensory OE as well as ILC and non-sensory periphery. Therefore, exogenous activation of the Wnt/β-catenin pathway resulted in a robust proliferation response in the intact OE similar in magnitude and pattern that is observed upon tissue damage by Triton X-100 but without

affecting the neuronal population and the integrity of OE.

In order to quantitatively and describe the effect of Wnt agonists on proliferative activity, BrdU-positive cells were counted across the entire OE (Figure 4.2A), ILC only (Figure 4.2B) and sensory area only (Figure 4.2C). A custom macro (Appendix F and Appendix G) was developed in ImageJ to quantify the cell numbers for segments of the OE between the ILC and the non-sensory periphery. In order to represent the data in a more reliable way, cell counts

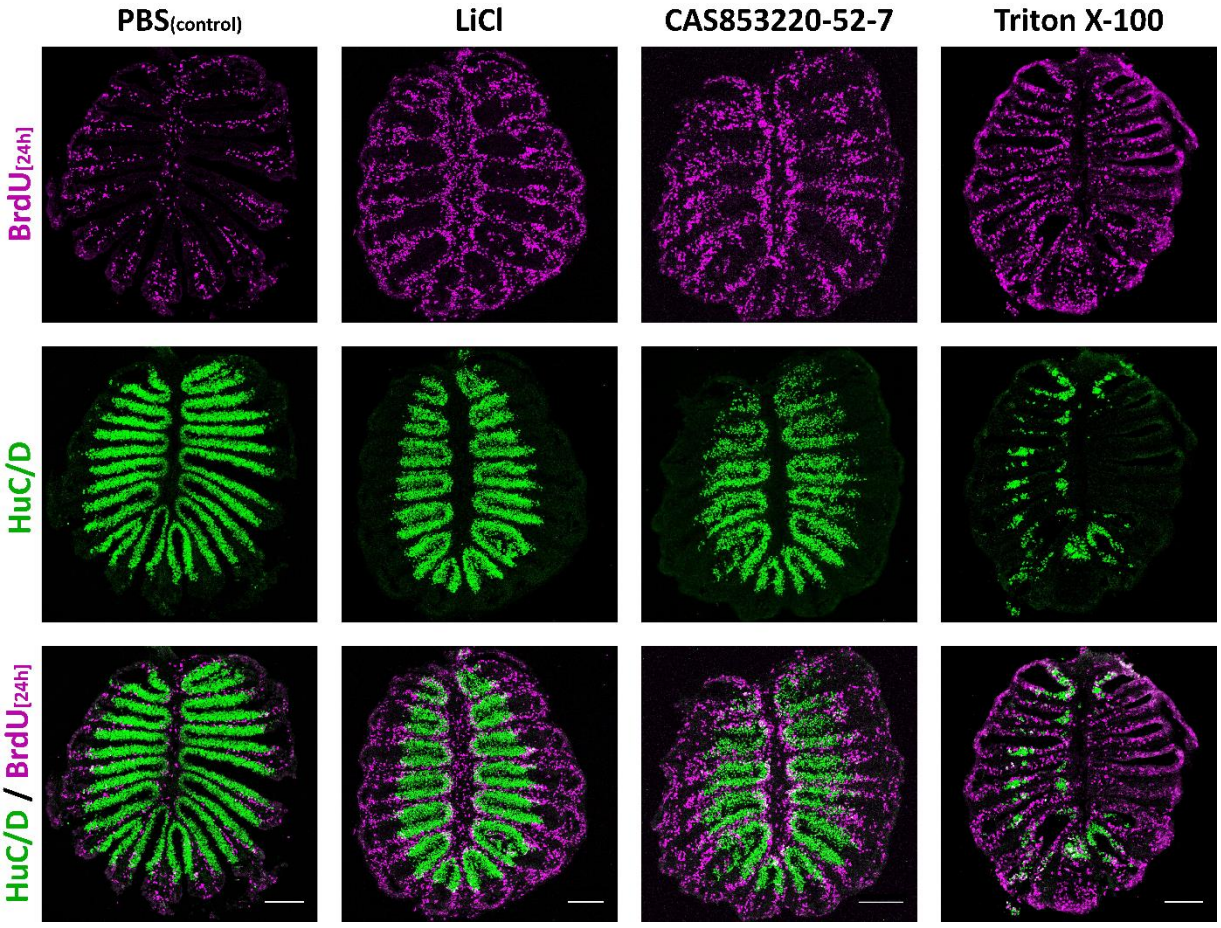

Figure 4.1. Effect of LiCl and Wnt agonist on cell proliferation in the zebrafish OE. Immunohistochemistry against BrdU (magenta) and HuC/D (green) in PBS control fish, fish injected with LiCl, Wnt agonist CAS853220-52-7 and the fish in which the OE has been damaged by Triton-X-100 (last column). Scale bars: 100 μm.

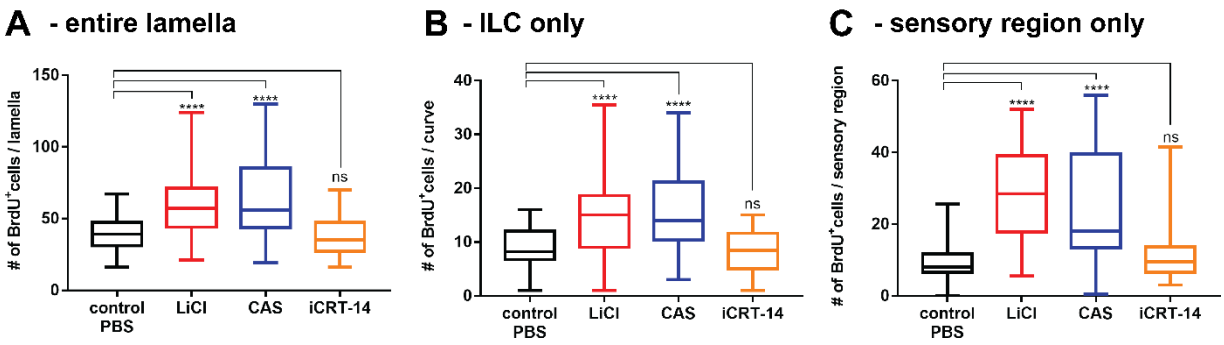

Figure 4.4. Effect of Wnt agonists and the Wnt antagonist iCRT-14 on proliferation rate in the OE. Box and whisker plot represents the quantification of BrdU-positive proliferating cells (A) in the entire OE, (B) in ILC only, and (C) in sensory OE only regarding the treatments. ****p<.0001

were plotted as box plots with Tukey style whiskers; bar in the bounding box indicates median, while bounding box represents second and third quartile, and the whiskers stand for maximum and minimum values in the data sets, which includes 54 measurements from 3 fish for each experimental group (3 sections per OE and 6 lamellae per section).

Across the entire OE (Figure 4.2A), an average of 40.44 ± 1.7 (mean ± SEM) BrdU-labeled cell could be observed per lamella for PBS-injected control fish. Activation of the Wnt/β-catenin pathway by LiCl or CAS853220-52-7 resulted in an increased number of proliferating cells and 60.2 ± 2.8 or 63.5 ± 3.6 cells were observed per lamella, respectively. In order to test for statistical significance of the observed difference in proliferation, cells counts were analyzed with the non-parametric Mann-Whitney U test, which indicated that LiCl- (*Mdn* = 57, $p<.0001$) and CAS853220-52-7-injected fish (*Mdn* = 56, $p<.0001$) contained a significantly higher number of BrdU-positive proliferating cells than PBS-injected control (*Mdn* = 39).

The overall increase in the number of BrdU-positive cells across the entire OE suggests that both activators trigger mitotic activity within progenitor cells. However, analysis across

the entire lamella structure does not reveal selective effects on progenitors that contribute to maintenance neurogenesis at the ILC and S/NS border or to repair neurogenesis within the sensory OE. To get initial insight into spatial differences of the Wnt agonist-induced proliferation response the number of mitotic cells where scored separately for the ILC and sensory OE.

When counting cells within the ILC only, in which the progenitor cells predominantly divide during maintenance of the neuronal population, an overall increased mitotic activity could be observed in agonist-treated animals. An average of 14.7 ± 0.9 BrdU-positive cells per ILC could be observed for for LiCl-injected fish (*Mdn* = 15) and 24.45 ± 2.0 cells for CAS853220-52-7-injected fish (*Mdn* = 14), while only 8.6 ± 0.5 cells were labeled BrdU-positive in PBS-injected controls (*Mdn* = 8.2). Therefore, IP injection of both agonists significantly increased the mean number of BrdU-positive cells about two-fold within the ILC ($p<.0001$; Mann-Whitney U test), denoting that the progenitor cells residing in ILC region may be sensitive for the exogenous activation of Wnt signaling.

Cell proliferation in the inner sensory OE occurs exclusive during repair neurogenesis and an accordingly low number of 9.42 ± 0.6 BrdU-positive cells per sensory region was observed for PBS control fish (*Mdn* = 8). Interestingly, a three-fold increase to 28.1 ± 1.8, and 24.45 ± 2.0 cells could be detected for LiCl-injected (*Mdn* = 28.5) and CAS853220-52-7-injected fish (*Mdn* = 18), respectively. Thus, application of LiCl and CAS853220-52-7 had a strong effect on mitotic activity also within the sensory OE. The 2- to 3-fold difference in the number of proliferating cells between experimental and control group was significant for both comparisons ($p<.0001$; Mann-Whitney U test), suggesting that dormant progenitor cells residing within the sensory region can be effectively stimulated by Wnt agonists ($p<.0001$).

In summary, the quantitative analysis of cell proliferation in the OEs showed that exogenous activation of Wnt signaling with two different agonists, LiCl and CAS853220-52-

7, resulted in increased mitotic activity. This effect was regardless of the segment of OE, as increased activity was observed both in the ILC and sensory OE. This observation indicates that Wnt signaling may induce mitotic activity in GBC- and HBC-like progenitors, which preferentially contribute to maintenance and repair neurogenesis, respectively.

4.1.2. Inhibition of the Wnt does not prevent maintenance neurogenesis

An additional assumption was that silencing of Wnt signaling may diminish the background rate of cell proliferation in the intact OE and/or block repair mechanisms in the injured OE. To test this hypothesis the iCRT-14 and Quercetin antagonists were used, which both were reported to disrupt efficient interaction between β-catenin and TCF (Quercetin), or to decrease Dishevelled protein levels (iCRT-14). Similar to the experiments described for Wnt agonists, 25 μM iCRT-14 and 100 mg/kg Quercetin was injected intraperitoneally during three consecutive days before analysis.

Intact fish that have been injected with iCRT-14 showed a pattern of BrdU-positive cells that largely resembled the proliferation pattern of PBS-injected control fish (Figure 4.3). Immunochemistry staining against BrdU showed that iCRT-14-injected fish had a subtle decrease in the number of BrdU-positive cells compared to PBS control. However, iCRT-14 did not fully inhibit the base level proliferation of maintenance neurogenesis occurring at the ILC and S/NS border. In the presence of the inhibitor, the majority of the BrdU-positive cells were found at the ILC and peripheral ring outside of the sensory OE, and rarely within the sensory area. Quantification of the BrdU-positive cells revealed that iCRT-14-injected fish had on average of 37.9 ± 1.9 cells (*Mdn* = 35) per lamella across the entire OE (Figure 4.2A), 8.5 ± 0.5 cells (*Mdn* = 8.5) per lamella within the ILC (Figure 4.2B), and 11.1 ± 0.9 cells (*Mdn* = 9.5) per lamella within the sensory OE only (Figure 4.2C). These numbers were similar to the numbers of BrdU-positive cells in PBS-injected control fish with 40.4 ± 1.7 cells per lamella (*Mdn* =39), 8.6 ± 0.5 cells per ILC (*Mdn* = 8.2), 9.4 ± 0.6 cells per sensory OE (*Mdn* = 8) and statistical

analysis showed that iCRT-14 did not significantly affect the proliferative activity in the intact OE, regardless of the OE segment (Mann-Whitney U, $p>0.05$).

However, inconsistent results were obtained for Quercetin treatment, and both decreases and increases in the number of proliferating cells were observed. Thus, I opted to exclude Quercetin for further experiments.

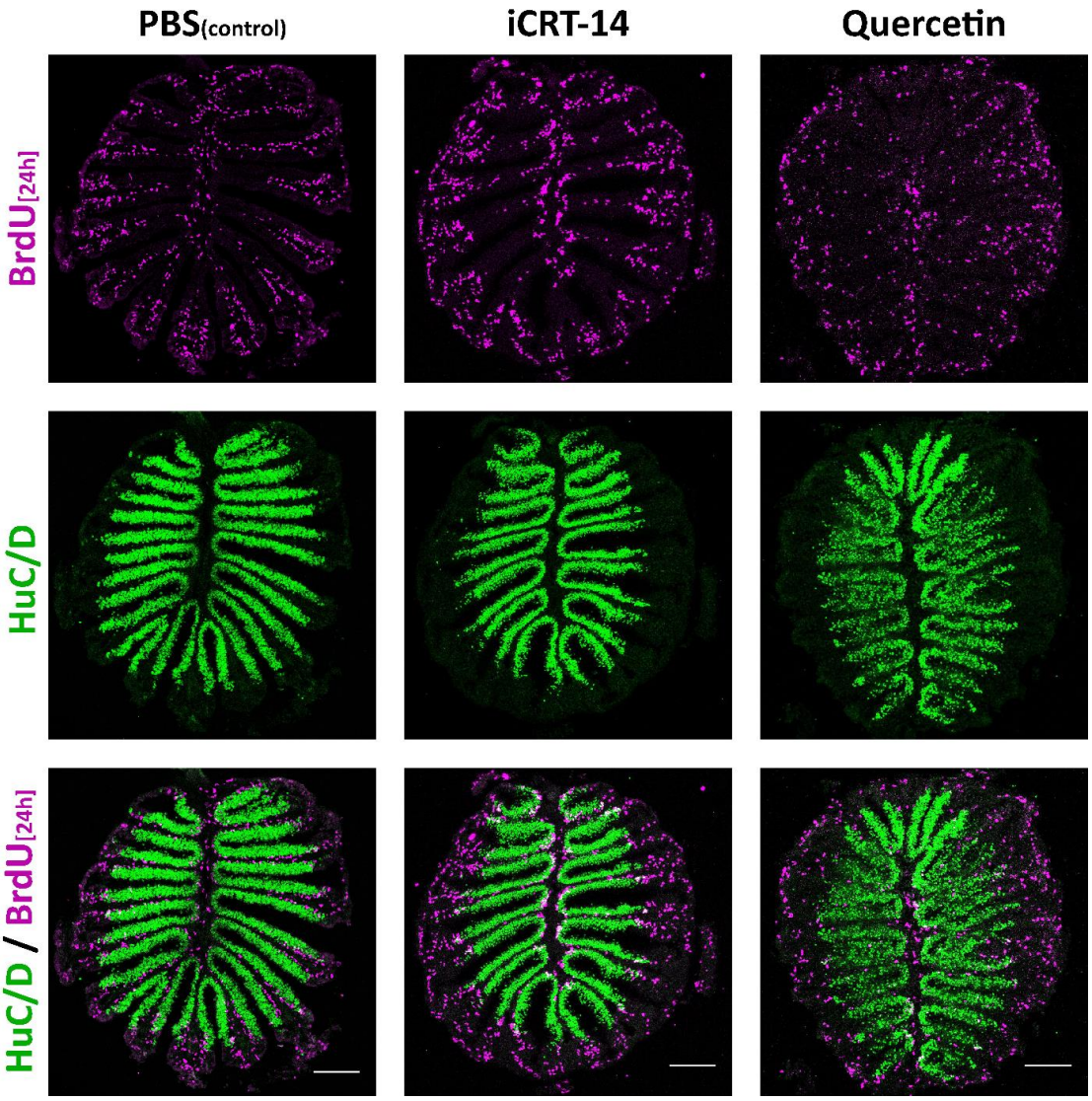

Figure 4.7. Effect of iCRT-14 and Quercetin on maintenance neurogenesis. Immunohistochemistry against neuronal marker HuC/D (green) and proliferating cell marker BrdU (magenta), control fish injected with PBS, and fish injected with antagonists iCRT-14 and Quercetin. Scale bars: 100 μm.

4.1.3. Wnt agonists affects both repair and maintenance neurogenesis

Previously it has been shown that injury to OSNs in zebrafish OE elicits a strong repair neurogenesis response throughout the entire OE. However, OE damage stimulates specific mitotic activity from a distinct pool of dormant progenitor cells that are functionally and molecularly different from the progenitors contributing to maintenance neurogenesis (Çapar, 2015; Kocagöz, unpublished). During progressive degeneration of the OE upon injury, those dormant progenitor cells are triggered to proliferate exclusively within the sensory OE, as they have distinct tissue distribution, while maintenance progenitors are exclusively located at the ILC and periphery (Bayramli *et al*., 2017).

In order to more precisely quantify changes in the spatial distribution of proliferating cells, the presence of BrdU-positive cells was scored at regular intervals along the radial dimension of the OE (from the tip of ILC to the non-sensory periphery) by a custom macro developed in ImageJ. High-resolution images were cropped as individual lamellae for each experimentally-induced OE and the relative positions of BrdU-positive cells across the central to peripheral dimension were determined. Radial distribution analysis includes 54 measurements for each interval along the OE segments (3 fish, 3 sections per OE and 6 lamellae per section).

In the intact OE (Figure 4.4; grey line), cells predominantly divide at the ILC (radial index = 0.1) and peripheral ring outside of the OE (radial index $\geq$ 0.65). Spatial analysis of proliferating cells demonstrates that about 80% of total BrdU-positive proliferating cells were found at those regions, while only 20% of proliferating cells were located within the inner sensory area. In contrast, the lesioned OE (black line) that has been irrigated with 1% Triton X-100 shows a uniform pattern of BrdU-positive cells along the entire OE one day after the manipulation. The response to injury results in increased mitotic activity, which is up to 6-fold higher throughout the entire OE, especially within the sensory OE.

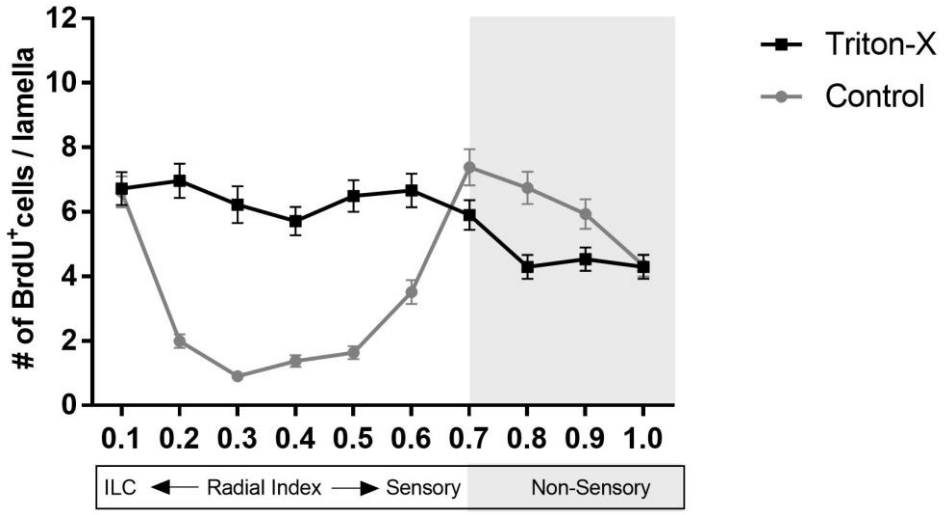

Figure 4.10. Changes in the spatial distribution of BrdU-positive proliferating cells along the central to peripheral dimension (radial index) of the intact OE (grey) and 1-day post lesioned OE (black) that have been damaged by 1% Triton X-100. Data represents mean ± SEM of 54.

A similar analysis was then performed for the OEs injected with Wnt agonists in order to examine if systematic difference in the distribution pattern of BrdU-positive cells occur (Figure 4.5). Application of LiCl stimulated statistically significant increases up to 5-fold preferentially in the inner sensory OE (radial index 0.2 – 0.6, $p<.0001$, Mann-Whitney U), whereas there was no noticeable change within the ILC or non-sensory regions (Figure 4.5A). In contrast, CAS853220-52-7-stimulated OE displayed an even increase of proliferation in the entire OE including the maintenance proliferation sites at the ILC and S/NS border (Figure 4.5B). CAS853220-52-7 had a robust effect across the entire OE as it induced about 1.5-fold increase both within the ILC ($p = .0032$) and S/NS border ($p = .0064$), and up to 4-fold increase in the sensory OE ($p<.0002$) (Figure 4.5B'). Thus, it became evident that both LiCl and CAS853220-52-7 change the proliferation pattern in a particular way that resembles tissue damage by increasing proliferation within the sensory region. CAS853220-52-7 stimulation appeared to induce both progenitor cells responsible for maintenance and repair neurogenesis, whereas LiCl stimulation may preferentially induce the progenitors contributing to repair neurogenesis.

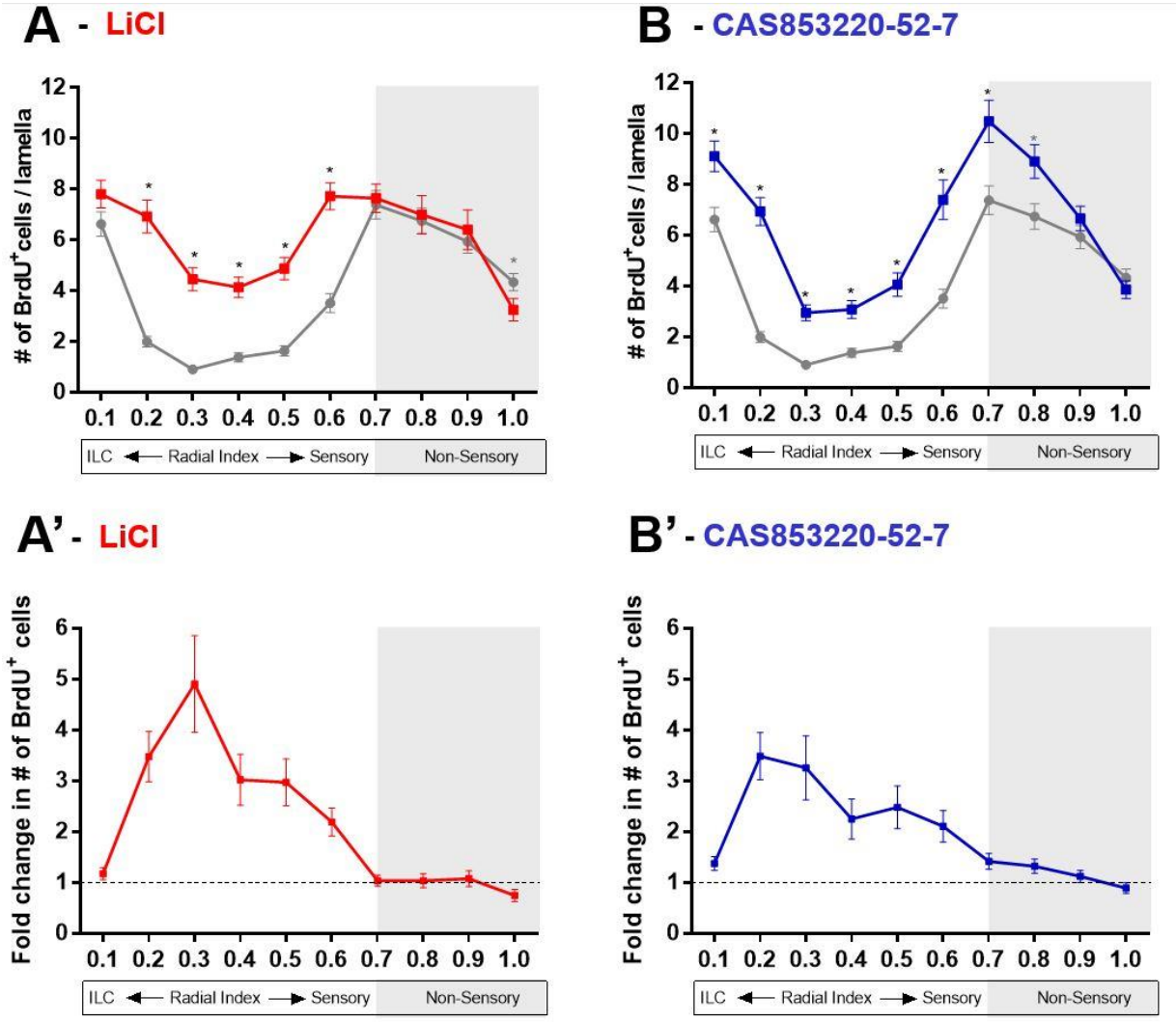

Figure 4.13. Changes in the spatial distribution of BrdU-positive proliferating cells along the lamella of intact zebrafish OE (grey line) and LiCl- (A) and CAS853220-52-7-injected OE (B). Fold changes are plotted for LiCl- (A') and CAS853220-52-7-injected OE (B'). (*: statistically significant points)

4.1.4. Wnt/β-catenin signaling is necessary to trigger repair neurogenesis

After showing that exogenous activation of Wnt signaling is sufficient to induce maintenance and repair neurogenesis, I aimed to investigate whether Wnt/β-catenin signaling is also necessary for the induction of repair neurogenesis by examining whether inhibition of Wnt

signaling could block, at least in part, the induction of mitotic activity after tissue injury. For this aim, fish were primed with IP injections of 25 μM iCRT-14 at 24 hours intervals over three consecutive days. Those injections were followed by tissue damage with 1% Triton X-100 and an additional injection of the antagonist 12 hours after the damage. Following the injury, fish were incubated in BrdU water for 24 hours to determine mitotic activity (n = 3).

Intact OE of iCRT-14-injected fish displayed little to no suppressive effect on the proliferation pattern compared to intact OE of PBS control fish (Figure 4.6). On the other hand, nasal irrigation with Triton X-100 resulted in a distributed pattern of BrdU-positive cells across the entire OE for iCRT-14 treated fish similar to PBS controls. However, the overall number of proliferating cells appeared to be slightly decreased, albeit the similarity of the proliferation pattern.

Quantitative measurements of proliferation revealed that in intact PBS-injected control fish an average of 47.6 ± 1.4 (mean ± SEM) BrdU-labelled cells per single lamella (*Mdn* = 47), 14.7 ± 1.0 cells per ILC (*Mdn* = 15) and 12.3 ± 0.8 cells per sensory OE (*Mdn* = 11.5) could be detected, while in intact iCRT-14 treated OE there were 52.3 ± 1.8 cells per lamella (*Mdn* = 52.5), 10.4 ± 0.8 cells per ILC (*Mdn* = 10) and 14.6 ± 0.8 cells per sensory OE (*Mdn* =14) could be observed (Figure 4.7A,B,C). Thus, in intact OE of iCRT-14 treated fish, the change in the proliferative activity showed significant reduction only at the ILC (radial index 0.1, $p = 0.002$, Mann-Whitney U) compared to PBS control. Moreover, spatial distribution of BrdU-positive cells in the iCRT-14 treated OE displayed a similar pattern to the pattern of PBS-injected control fish with a small but significant reduction at ILC ($p = 0.005$) (Figure 4.7B, D). Thus, it seems that iCRT-14 does have a small, if any, effect on suppressing maintenance neurogenesis at the ILC and the S/NS border.

On the other hand, in the damaged OE of PBS control fish, an average of 57.8 ± 2.5 (mean ± SEM) BrdU-labelled cells could be found per single lamella (*Mdn* = 60), and 13.7 ± 0.8 cells

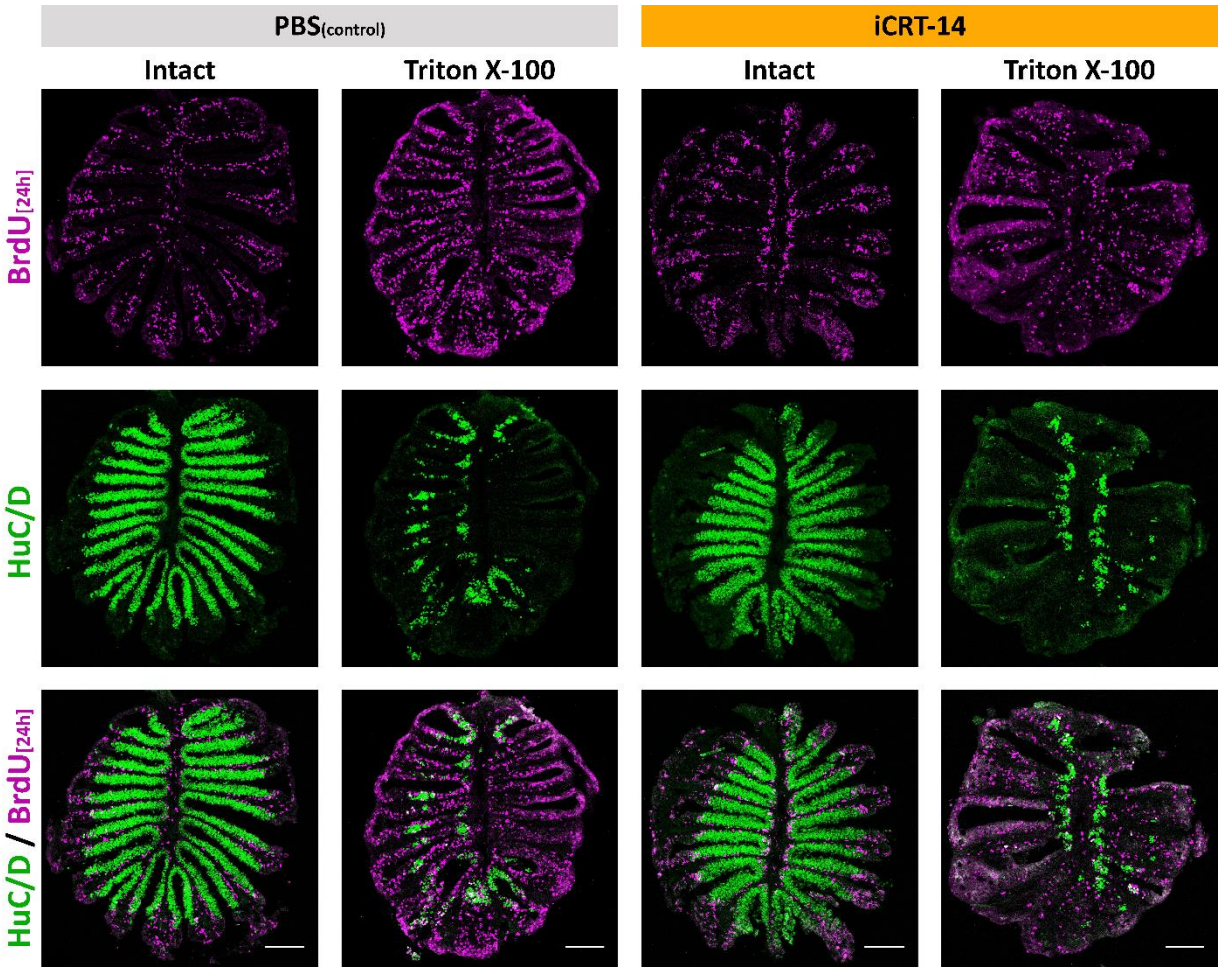

Figure 4.16. Effect of iCRT-14 on repair neurogenesis. Immunohistochemistry against BrdU (magenta) and the neuronal marker HuC/D(green) in PBS-injected control fish (left panels) and in iCRT-14-injected fish (right panels) following Triton X-100 damage compared to intact OEs. Scale bars: 100 μm.

per ILC (*Mdn* = 14.7), and 32 ± 1.6 cells per sensory OE (*Mdn* = 31), while in damaged OE of iCRT-14 treated fish were 44 ± 2.2 cells per lamella (*Mdn* = 41), 8.7 ± 0.5 cells per ILC (*Mdn* = 8) and 23.2 ± 1.3 cells per sensory OE (*Mdn* =21.5) (Figure 4.7A,B,C). Thus, mitotic activity in iCRT-14-treated fish was reduced across the entire OE including both ILC and sensory OE ($p<.0001$) compared to PBS-injected controls. This observation is supported by the change in spatial distribution of dividing cells (Figure 4.7E). It became evident that the reduction in mitotic activity occurred predominantly at the ILC and inner sensory region, while the number

of BrdU-positive cells in the peripheral non-sensory region was not significantly different ($p<0.05$) in comparison to control fish. Therefore, in addition to maintenance neurogenesis, inhibition of Wnt signaling by iCRT-14 treatment may also result in reduction of mitotic activity during repair neurogenesis.

Taken together, iCRT-14 had an overall significant inhibitory effect on regenerating OE but little to no effect on the intact OE. iCRT-14 treatment resulted in strong decrease in proliferating cell numbers both at the ILC and along the sensory region, while a small but significant decrease in proliferative activity could be observed only at the ILC of the intact OE denoting the maintenance neurogenesis.

In additional experiments, the alternative antagonist IWR-I was used, which has been reported to be effective when applied to the tank water instead of IP injection. For an efficient treatment, fish were incubated during a priming period in IWR-I-containing water for one day before damage by nasal irrigation with 1% Triton X-100. Following the tissue damage, fish were incubated in fresh BrdU- and IWR-I-containing water for an additional 24 hours before determination of mitotic activity. The chemicals and fish water were changed once a day until assays.

DMSO-treated vehicle control fish displayed the characteristic proliferation pattern of maintenance and repair neurogenesis of intact and damaged OEs, respectively (Figure 4.8). Immunohistochemistry against BrdU showed that intact OE of IWR-I-treated fish had a proliferation pattern that closely resembled the untreated intact OE. On the other hand, IWR-I-treated fish had high proliferative activity across the entire OE one day post lesion, similar to DMSO controls. Accordingly, IWR-I appeared to have a weak, if any, inhibitory effect on both intact and damaged OE.

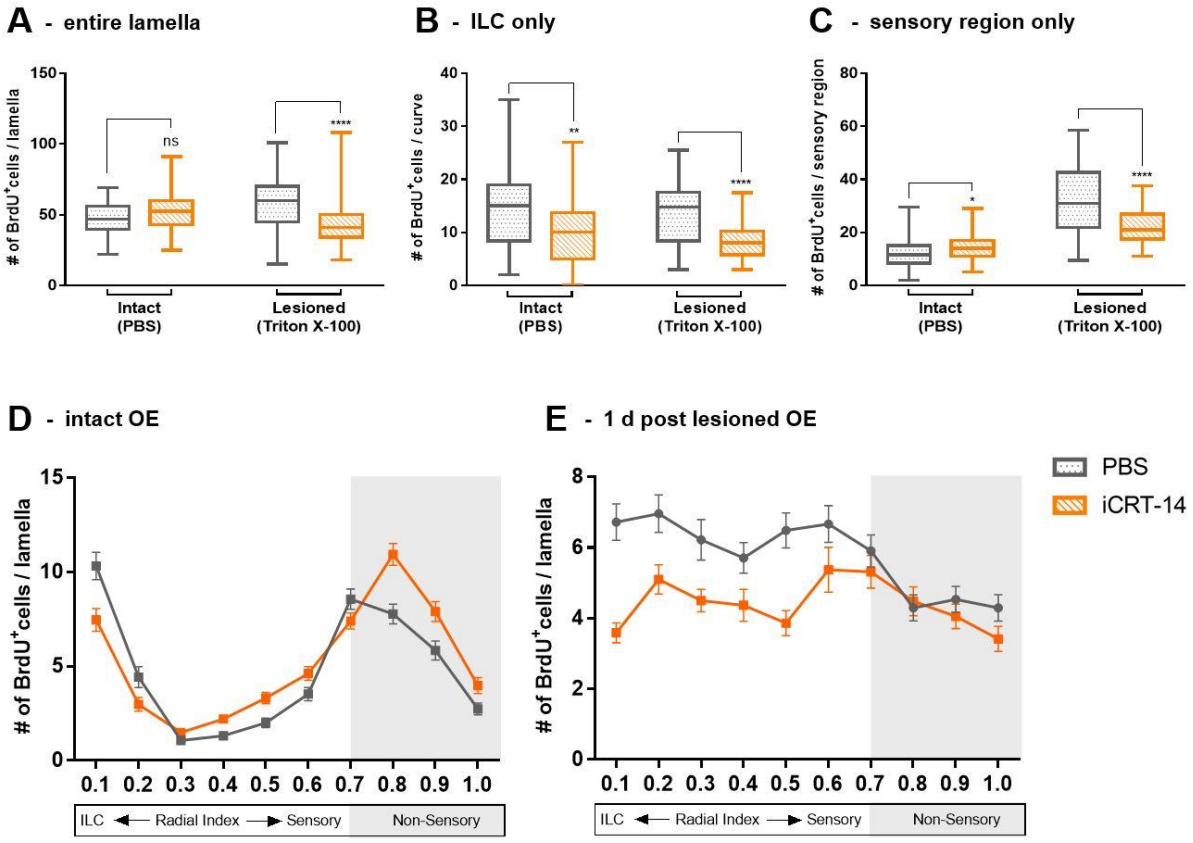

Figure 4.19. Effect of iCRT-14 on proliferation rate and pattern in intact and 1 day post lesioned OE. (A) Box and whisker plot represents the BrdU-positive cells in the entire lamella, (B) within the ILC, (C) within the sensory OE ($^{*}p<0.05$, $^{****}p<.0001$). Changes in the spatial distribution was plotted across the entire lamella (D) in intact, (E) and damaged OE.

Detailed quantification of the proliferation activity revealed that in intact DMSO control fish, there were average of 29.9 ± 1.4 (mean ± SEM) BrdU-labelled cells per single lamella (*Mdn* = 27.5), 9.1 ± 0.6 cells per ILC (*Mdn* = 8) and 6 ± 0.4 cells per sensory OE (*Mdn* = 5), while in intact IWR-I treated OE there were 28.1 ± 2.0 cells per lamella (*Mdn* = 21.5), 8.6 ± 0.7 cells per ILC (*Mdn* = 7.5) and 6.1 ± 0.7 cells per sensory OE (*Mdn* =3.2) (Figure 4.9A,B,C). Thus, IWR-I appears to have no significant effect on maintenance neurogenesis (Mann-Whitney U). This result was supported by spatial distribution analysis comparing the intact OEs of DMSO and IWR-I treated fish, which showed that the proliferation pattern of the IWR-1-treated OE closely resembled the pattern of DMSO control fish (Figure 4.9D), however there

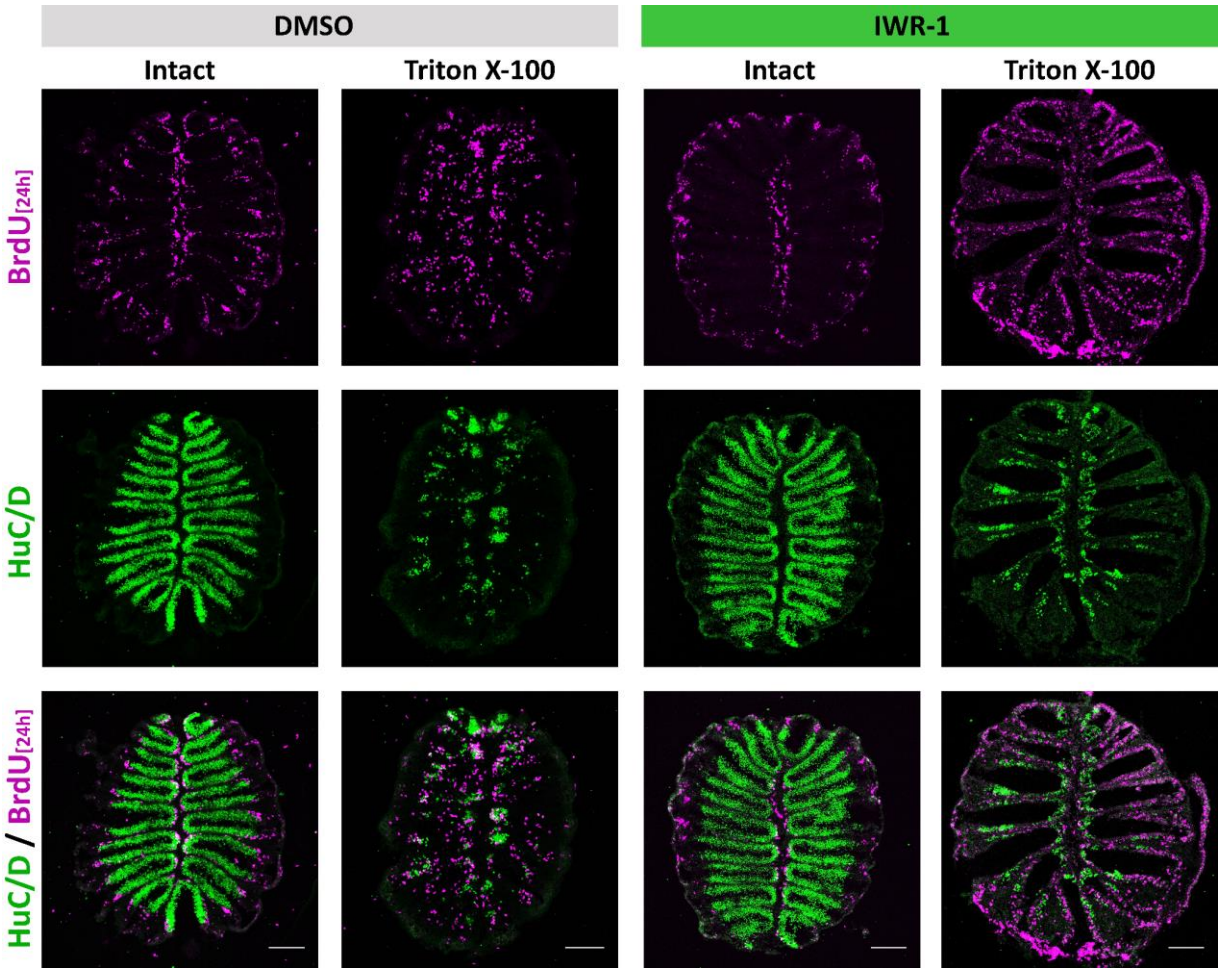

Figure 4.22. Effect of IWR-I on proliferation rate in intact and 1 day post lesioned OE. (A) Box and whisker plot represents the BrdU-positive cells in the entire lamella, (B) within the ILC, (C) within the sensory OE ($^{*}p<0.05$, $^{**}p<.005$). Changes in the spatial distribution was plotted across the entire lamella (D) in intact, (E) and damaged OE.

was up to 0.6-fold significant decrease at the S/NS border (Figure 4.9D, radial index 0.6-0.7, $p<0.005$, Mann-Whitney U).

In the damaged OE of DMSO control fish, there were on average of 26.9 ± 1.2 (mean ± SEM) BrdU-labelled cells per single lamella (*Mdn* = 27), 10.3 ± 0.4 cells per ILC (*Mdn* = 10.2) and 14.9 ± 0.8 cells per sensory OE (*Mdn* = 13), while in damaged IWR-I treated OE there

were 36 ± 2.2 cells per lamella (*Mdn* = 36.5), 8.9 ± 0.6 cells per ILC (*Mdn* = 8) and 14.2 ± 1.0 cells per sensory OE (*Mdn* =12). Therefore, a small but significant decrease of BrdU-positive cells at the ILC of damaged IWR-I-treated OE ($p = 0.03$, Mann-Whitney U test) was conflicted by an overall increase over the entire lamella ($p = 0.002$). Spatial distribution of proliferating cells in both DMSO and IWR-I-treated lesioned OE did not show the characteristic pattern of cell proliferation as it is observed in lesioned controls. Thus, results of damaged OE may be inconclusive for the effect of IWR-I on the repair neurogenesis.

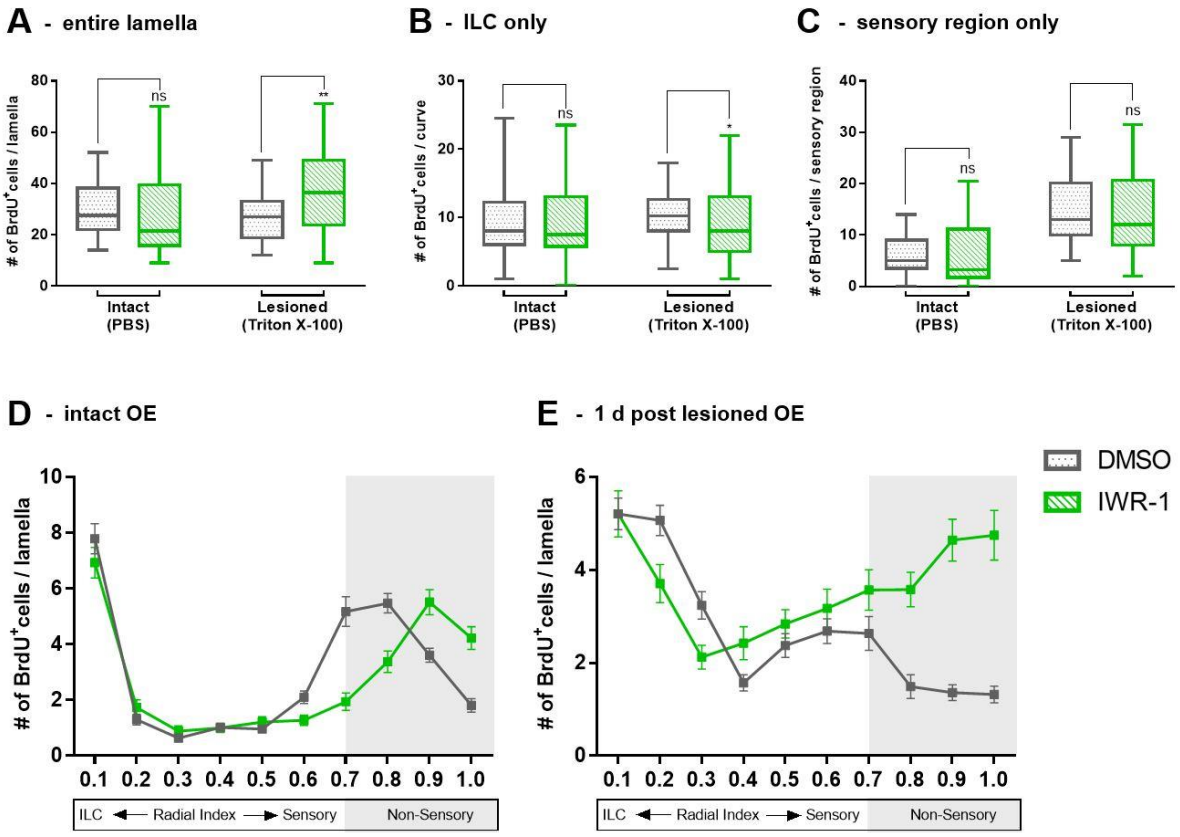

Figure 4.25. Effect of IWR-I on repair neurogenesis. Immunohistochemistry against BrdU (magenta) and the neuronal marker HuC/D (green) in DMSO-treated control fish (left panels) and in IWR-I-treated fish (right panels) following Triton X-100 damage compared to intact OEs. Scale bars: 100µm.

In summary, quantitative analysis revealed that IWR-I treatment during the regenerating phase did not result in a significant reduction in proliferative activity, either at the site of maintenance or of regions characteristic for repair neurogenesis. IWR-I had no significant inhibitory effect on the intact OE except at the S/NS border.

4.2. Characterization of Wnt-responsive cell population in the OE

As the second part of this study, I aimed to reveal exactly which cell populations in the OE respond to damage conditions or pharmacological activation of Wnt pathway and result in increased proliferative activity. Since β-catenin expression is increased in the cytoplasm and nuclear translocation occurs in Wnt-activated cells, I expected to observe Wnt-responsive cell populations in the zebrafish OE by immunohistochemical staining against β-catenin. Apart from its function in the Wnt signaling pathway, β-catenin has an essential role in cell-cell junctions by binding to the cytoplasmic domain of E-cadherin, which in turn recruits α-catenin to bind to the actin cytoskeleton (Nelson and Nusse, 2004). Thus, in the absence of Wnt ligand, the protein levels of β-catenin is kept low in the cytoplasm by the Axin/APC/GSK3β destruction complex and is in excess at the plasma membrane. In the presence of Wnt signaling, β-catenin is stabilized and accumulated in the cytoplasm as well as in the nucleus where it acts as a co-activator of the transcription factor TCF/LEF (Cadigan and Nusse, 1997). In order to observe the β-catenin expression pattern in damaged OE and Wnt agonist-treated OE, three experimental groups were prepared. One group served as a control that has not been treated with any chemical and therefore had an intact OE. In order to determine the responding cell populations during the damage conditions, fish in which the OE had been damaged by nasal irrigation with the detergent 1% Triton X-100, were analyzed 24 hours after the damage. Another group of fish were injected intraperitoneally with CAS853220-52-7 during three consecutive days and analyzed 24 hours following the last injection. After several optimization trials for the immunohistochemistry against β-catenin, I succeeded to obtain reliable β-catenin signals by using a modified antigen retrieval protocol (see Methods 3.2.5).

In the intact OE, β-catenin signals localized at the cell-cell junctions and most abundantly at the non-sensory region. Interestingly and consistent with the regions in which proliferative activity is high during maintenance neurogenesis in the intact OE, nuclear and cytoplasmic β-catenin signals could be observed predominantly in the basal layers of the ILC and S/NS border and occasionally within the sensory region (Figure 4.10). This observation suggests that the flat and horizontal-shaped basal cells within the ILC and at the S/NS correspond to cells in which the Wnt pathway is active. The spatial distribution of these cells is consistent with the pattern of cell proliferation in the intact tissue.

In the Triton X-100 lesioned OE, additional cells that showed increased β-catenin immunoreactivity could be detected. Different from β-catenin immunoreactivity in the intact OE, the entire lamella of damaged OE contained a large number of β-catenin-positive cells. Interestingly, β-catenin signals at the plasma membrane and within the non-sensory region were diminished in the damaged OE. Interestingly, at higher resolution, strong β-catenin signals could be detected in a speckle formation within the nucleus. Taken together, it appears that during the regenerative phases, the OE shows increased nuclear and cytoplasmic β-catenin signals throughout the entire lamella.

In the experiments above, I could show that the Wnt agonist CAS853220-52-7 strongly induces proliferative activity across the OE. To further investigate if the observed effect is indeed due to activation of Wnt signaling immunohistochemistry against β-catenin was also performed on the OE of CAS853220-52-7-injected fish. Similar to the results of damaged OE described above, CAS853220-52-7-treatment induce a large number of β-catenin-positive cells across the entire OE. Again, cytoplasmic and nuclear β-catenin expression could be found throughout the entire lamella, and the expression at the cell-cell junctions and in the non-sensory region was reduced. Also, speckle formation within the nucleus could be detected at higher power views.

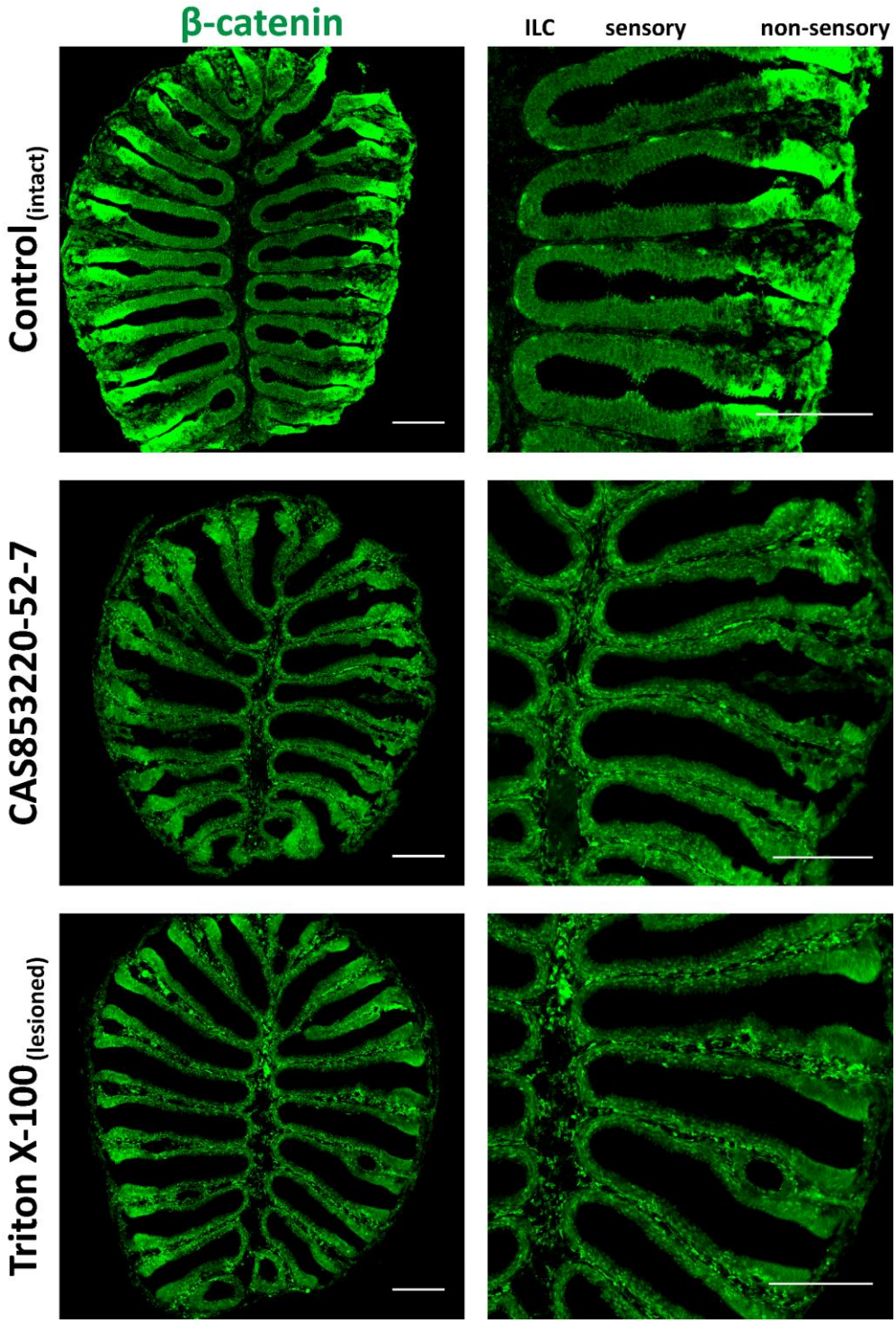

Figure 4.28. Expression profile of β-catenin (green) in the intact OE (top), CAS853220-52-7-injected OE (middle) and 1 day post lesioned OE (bottom) that have been damaged by 1% Triton X-100. Left: whole OE sections. Right: Close-up on ILC, sensory and non-sensory regions. Scale bars: 100 μm.

To summarize, in intact OE, anti-β-catenin immunohistochemistry as an indicator of active Wnt-signaling cells has been found to be restricted to ILC and SNS border in accordance with the zones of high proliferative activity during maintenance neurogenesis. Interestingly, damaged and CAS853220-52-7-treated OE showed a higher number of nuclear and cytoplasmic β-catenin signals throughout the entire OE, including speckles within the nucleus.

4.3. Molecular characterization of Wnt activation by semi qRT-PCR

As an additional aspect of the work described in this thesis, I aimed to confirm the activation and inhibition of Wnt/β-catenin pathway by molecular analysis to verify the specificity and efficiency of the pharmacological agonists that I used above. In order to show the Wnt-specific effects of small molecule agonists and antagonists in zebrafish OE tissue, I opted for a semi-quantitative PCR to examine changes in the mRNA levels of the components and downstream target genes of Wnt signaling. For this purpose, specific oligonucleotide primer pairs were selected to detect the changes in the expression of core components of the Wnt pathway and best-known target genes: *axin1, axin2, bmp2k, β-catenin1 (ctnnb1), β-catenin2 (ctnnb2),* a natural Wnt inhibitor *dickkopf3b (dkk3b), frizzled7b (fzd7b), neuroD1, neuroD2, neuroD4, neurogenin1 (ngn1), wnt11r*. To enable quantitative analysis, the eukaryotic translation elongation factor 2b (*eef2b*) was selected as a housekeeping control gene for the normalization of the changes in the expression levels of selected genes.

For the semi-quantitative RT-PCR analysis, the expression levels of target mRNAs were measured and analyzed on ethidium bromide-stained agarose gels in which the band intensity reflects the amount of amplified transcripts. As a first step, target transcripts were amplified from cDNAs derived from intact control OE (0h, n=20 fish) and OEs at different time points (4, 12, 24 and 120h, n=20 fish) after nasal irrigation with the 1% Triton X-100 (Figure 4.11). Reactions with the same primer pairs were carried out at the same time, and each set of reactions contained a no-cDNA negative control (NC). In these experiments, different numbers of amplification cycles, ranging from 20 to 35 cycles, were tested for the *eef2b* primer pair to

establish a reliable method that enables the visualization of low-expressed transcripts but avoids reaching a plateau for high-expressed transcripts (data not shown). As a result of these pilot studies, 25 cycles were determined to be optimal with respect to the band intensities of the amplified PCR products. Qualitative representation of the PCR products of target mRNAs showed that in 4h-post lesioned OE, band intensities denoting the expression levels decreased in comparison to the intact OE (0h) for most genes except for *dkk3b, axin2* and *eef2b*. However, at 12h after the damage band intensities of target mRNAs generally increased, except for *axin2*. Target transcript levels showed different changes at 24 hours after the damage, yet, largely turned back to their initial band intensities at 120h-post lesion, except for *ctnnb2*. Moreover, the expression levels for *axin2, neurod2, ngn1* and *dkk3b* at 120h time point after damage were even increased when compared to the initial expression levels at 0h time point.

Since the qualitative representation is not sufficient for satisfactory conclusions, changes in the expression levels of target mRNAs were plotted for quantitative analysis by normalizing the band intensities of each time point to the housekeeping control gene respectively. After the first normalization, expression levels of each target mRNA have been also normalized to the expression levels at 0h time point (intact OE), thereby the calculated value of intact OE (0h) for each target mRNA was considered as equal to 1.

Then, the means of three independent technical replicates were plotted for each transcript. In order to examine whether the semi qRT-PCR protocol is reliable or not, the results were compared to the levels of gene expressions previously measured by RNA sequencing at different time points after the damage by Triton X-100 (Figure 4.12, see Appendix Table E.1). According to the quantitative analysis, in 4h-post lesioned OE, all the selected target mRNAs were up to 0.8-fold downregulated except *dkk3b* in which the expression level increased nearly 1.5-fold in comparison to the 0h time point. The downregulation at 4h time point was well correlated with the changes in the expression levels of target mRNAs measured by RNA-seq except *axin2, bmp2k, ctnnb2,* and *neurod1*. For the 12h time point, the transcripts of *axin2* and *bmp2k* were up to 0.6-fold downregulated, while only *dkk3b* showed nearly 1.2-upregulation. Moreover, the

expression levels of each transcript were downregulated up to 0.7-fold at 24h time point, and *fzd7b, neurod1,* and *bmp2k* were consistent between the RNA-seq results and RT-PCR. On the other hand, at 120h time point, none of the genes was found to correspond to the RNA-seq results regarding the changes in the expression levels except *axin2*.

In summary, the expression levels of some of Wnt-related target mRNAs were successfully assessed by semi qRT-PCR of OEs and showed dynamic changes over different time points after damage. The quantitative analysis of the band intensities of target mRNAs showed that *axin2, fzd7b* and *dkk3b* were more reliable because of their better correlation between RT-PCR and RNA-seq results. However, the transcripts *bmp2k, ctnnb1, ctnnb2, neurod1,* and *neurod4* has shown inconclusive expression profiles that conflicted with the RNA-seq results.

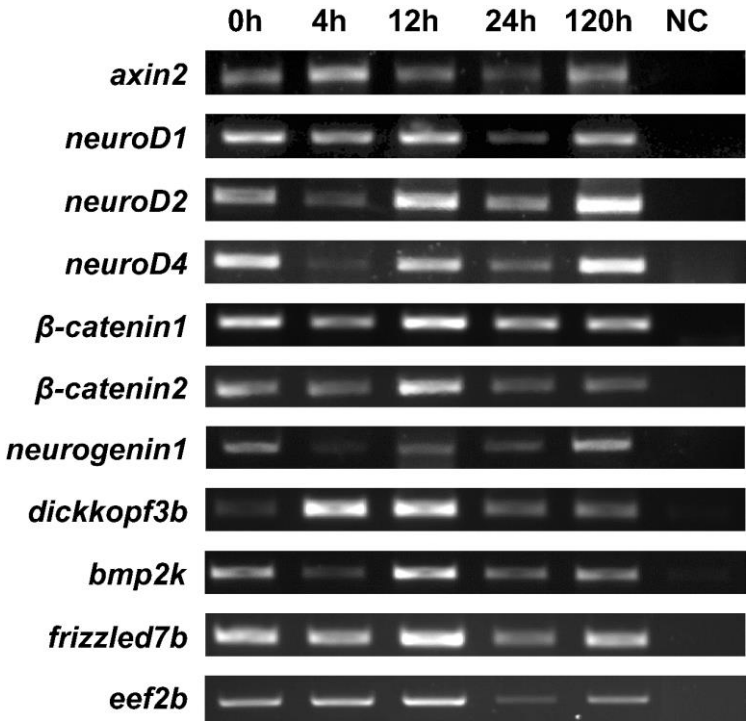

Figure 4.31. Representation of RT-PCR products of target transcripts *axin2, neurod1, neurod2, neurod4, ctnnb1, ctnnb2, ngn1, dkk3b, bmp2k, fzd7b* and *eef2b* on cDNA derived from intact OE (0h) and 4h, 12h, 24h, 120h-post lesioned OE. NC: negative control.

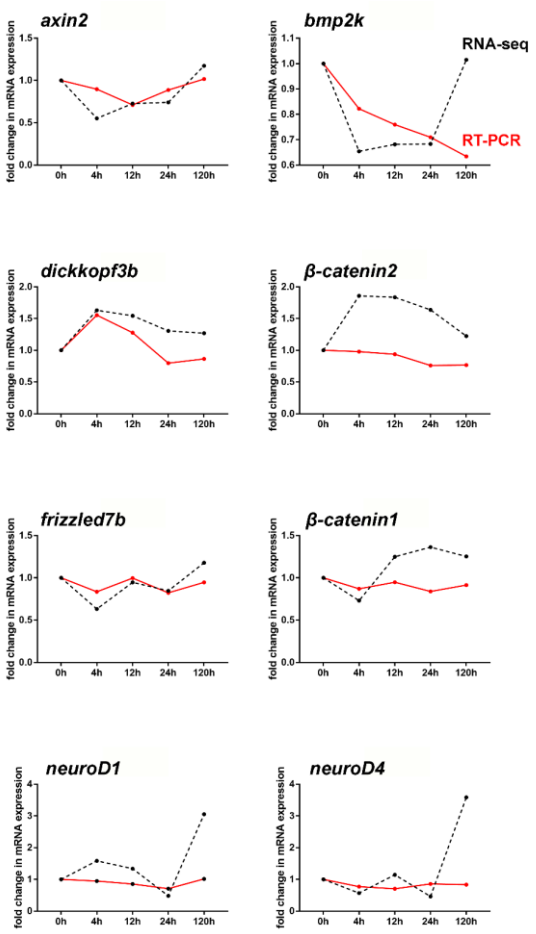

Figure 4.34. Changes in the mRNA levels of *axin2*, *ctnnb1*, *ctnnb2*, *bmp2k*, *fzd7b*, *neurod1*, *neurod4* and *dkk3b* genes in intact OE (0h) and in damaged OEs at different time points (4h, 12h, 24h, 120h) after the damage. Each point represents the mean of the normalized values from three replicates for RT-PCR (red lines) and RNA-seq (black dotted lines).

Similar to the protocol described above, a semi qRT-PCR approach was used to observe the direct effect of LiCl and CAS853220-52-7 on the expression levels of components of Wnt signaling and downstream target genes to ensure that administration of small molecule agonists specifically activates the Wnt/β-catenin pathway. For this purpose, LiCl, CAS853220-52-7 and PBS were IP injected over three consecutive days, and samples were collected 24 hours after the last injection (n=5 fish). RT-PCR reactions were carried out with specific primer pairs for

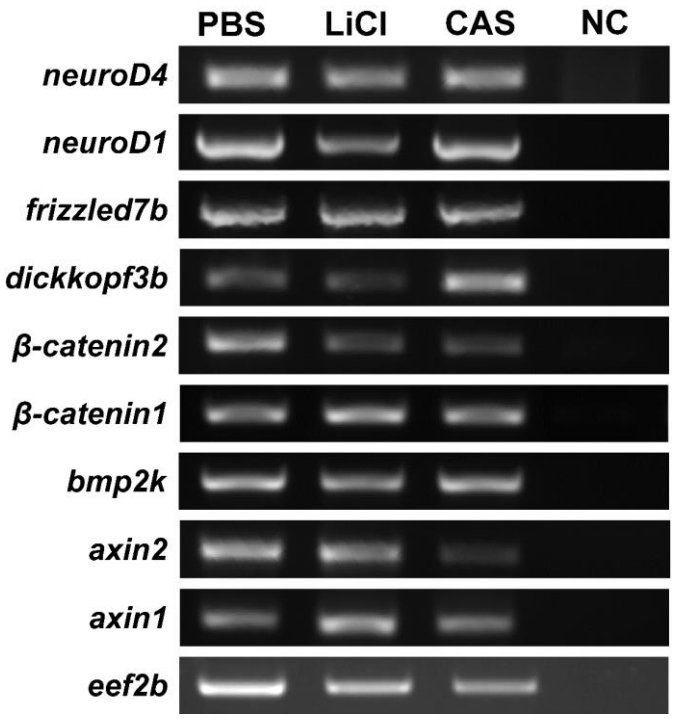

Figure 4.37. Representation of RT-PCR products of the transcripts *neurod4, neurod1, fzd7b, dkk3b, ctnnb2, ctnnb1, bmp2k, axin1, axin2* and housekeeping control gene *eef2b* on cDNA derived from PBS-injected control OE, LiCl- and CAS853220-52-7-injected OE. NC: negative control.

wnt11r, neurod1, neurod4, fzd7b, dkk3b, ctnnb1, ctnnb2, bmp2k, axin1, axin2 and *eef2b* as a housekeeping control gene. This experiment has been performed only once for each target mRNA and included a no-cDNA negative control. Since the target mRNAs were upregulated during the early regenerative phases of the zebrafish OE, it was expected that these transcripts would be upregulated after the pharmacological activation of Wnt pathway as well.

On the ethidium bromide-stained agarose gel, PBS-injected OEs showed the greatest band intensities for *neurod1, ctnnb2, axin2* and *eef2b* genes (Figure 4.13). In line with expectation, the expression of *ctnnb1* was upregulated in both LiCl- and CAS-853220-52-7-injected OE samples compared to the PBS control OE. However, the expression levels of *neurod1, neurod4* and *bmp2k* were downregulated only in LiCl-injected OE but did not changed in CAS853220-

52-7-injected OEs. While the expression of *dkk3b* has notably increased in CAS853220-52-7-injected OE, the band intensities for *fzd7b* and *axin2* decreased compared to the PBS and LiCl-injected OEs. On the other hand, *ctnnb2* has downregulated after the pharmacological activation by both agonists. In order to determine the changes in the mRNA levels quantitatively, band intensities of LiCl and CAS853220-52-7-injected OE were measured for each target mRNA and normalized to the *eef2b* measurements respectively. Then, normalized values for each mRNA have been also normalized to ones for PBS control OE respectively, and calculated value of expression level in PBS control OE was set to 1.

According to the quantitative analysis, only *ctnnb2, axin2* and *fzd7b* were up to 1.8-fold upregulated in LiCl-injected OE in accordance to the band intensities, whereas the expression levels of *neurod1, neurod4, bmp2k, ctnnb2* and *dkk3b* decreased up to 0.6-fold (Figure 4.14, see Appendix Table E.2). In CAS853220-52-7-injected OE, the expression levels of all transcripts except *ctnnb2* were 1.2-2.5-fold upregulated. Interestingly, the transcript *ctnnb1* have been nearly 0.6-fold downregulated. Taken together, administration of two different Wnt activators seemed to have differential effects on the expression levels of the target mRNAs. Based on the qRT-PCR performed on LiCl and CAS853220-52-7-injected OEs, *ctnnb1, axin2,* and *fzd7b* has been shown to be upregulated, and *ctnnb1* has been downregulated when administered with both activators. Even though the comparative results for the changes in the expression levels after the damage conditions have revealed that primer pairs for *axin2, ctnnb1,* and *fzd7b* transcripts may not be reliable, their expressions have been increased both in LiCl- and CAS853220-52-7-injected OE.

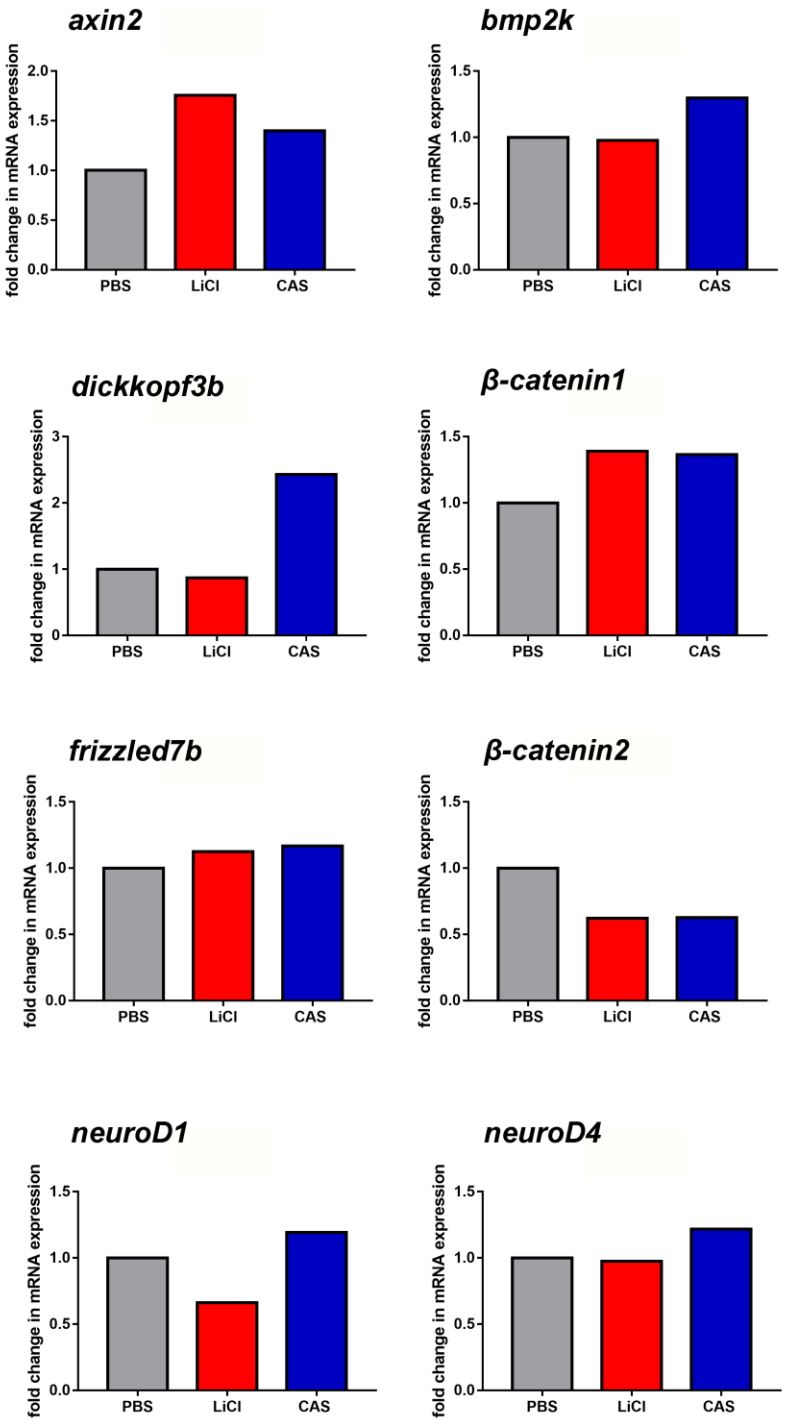

Figure 4.40. Quantitative analysis of RT-PCR for *axin2, ctnnb1, ctnnb2, fzd7b, bmp2k, neurod1, neurod4* and *dkk3b* genes to show the changes in the mRNA levels after the pharmacological activation of Wnt pathway by LiCl and CAS853220-52-7.

5. DISCUSSION

As an exception to the limited regenerative capacity of the nervous system, the peripheral OE has a remarkable capacity to regenerate new cells to replenish neurons that are lost on a daily basis or upon injury. The robust neuroregenerative capacity of the OE also constitutes a powerful experimental system to study adult neurogenesis, which could reveal new insight into mechanisms and signaling pathways that enable nervous system repair. Different from most other neurons that persist for the life of the organism, OSNs have relatively shorter lifespan of 60 to 90 days in rodents (Mackay-Sim and Kittel, 1991; Moulton, 1975; Tsai and Barnea, 2014), and about 30 days in zebrafish (Bayramli *et al.*, 2017). Therefore, the OE undergoes regular turnover of its OSN population and robust mechanisms must be in place to enable constitutive and responsive neurogenesis. The exposed and vulnerable position of the peripheral OE, which directly contacts the chemical environment also obliges it to be able to undergo neurogenesis to replenish neurons that are lost upon injury, infection, or contact with damaging agents.

However, the detailed cell to cell signaling mechanisms that enable the rapid turnover of OSNs, the molecular signals that communicate between the need of the OE tissue to generate more or less OSNs at any moment in time and the underlying cell populations that enable rapid OSN turnover and OE repair are not known in zebrafish. In this study, I performed an in-depth examination of the Wnt/β-catenin signaling pathway, using pharmacological manipulation, immunohistochemistry, and analysis of gene expression. I find that pharmacological activation of Wnt/β-catenin signaling induces massive proliferation from basal progenitor cells across the OE. The observed proliferation pattern closely resembles the native response of the OE to global damage of the OSN population by damaging agents, such as Triton X-100. In contrast, silencing Wnt/β-catenin signaling in the intact OE has a minor impact on maintenance neurogenesis but, at least in part, blocks the unfolding of a full damage response. Importantly, immunohistochemistry against β-catenin reveals immuno-positive cells in previously characterized regions of active maintenance neurogenesis, whereas tissue damage or pharmacological activation induce patterns of β-catenin expression that are distributed across

the OE, similar to the proliferative response observed under these conditions. The results strongly suggest that activation of the Wnt/β-catenin signaling pathway is a critical step in the induction of mitotic activity in neural progenitors in the zebrafish OE.

There are two functionally and morphologically distinct stem/progenitor cell populations in the rodent OE, the HBCs and GBCs (Schwob *et al*., 2017). HBCs are long-lasting and largely dormant progenitor cells that undergoes transient proliferation upon traumatic injury to generate neuronal and nonneuronal cell populations in the OE (Leung *et al.*, 2007). In contrast, GBCs are constitutively mitotically active progenitor cells that contribute to the constant turnover of OSNs (Chen *et al.*, 2004). Thus, these two progenitor cell populations are predominantly active under different conditions: HBCs become active in the injured OE and contribute to repair neurogenesis, while GBCs are active in the intact OE during constitutive maintenance neurogenesis. Consistent with the relative position of these stem/progenitor cells in the zebrafish OE, the pattern of mitotic activity, examined by BrdU incorporation or anti-phospho-histone H3 immunohistochemistry (Bayramli *et al*., 2017; Kocagöz, unpublished) drastically changes during the two modes of neurogenesis. Previously, our research group revealed that cell divisions predominantly occurs at the ILC and S/NS border in the intact zebrafish OE, and only a few exceptional dividing cells can be observed within the sensory region that is occupied by HuC/D-positive OSNs (Bayramli *et al*., 2017). On the other hand, a much more distributed and elaborate pattern of mitotic activity throughout the entire OE can be observed upon nasal irrigation with Triton X-100 (Iqbal and Byrd-Jacobs, 2010; Kocagöz, unpublished). This finding suggests that relevant progenitors for maintenance and repair neurogenesis have different tissue distribution in the zebrafish OE and that these cells become activated under different conditions, thus resembling the behavior of GBCs and HBCs in the rodent OE. In the zebrafish OE, GBC-like cells are located at the ILC and S/NS border, whereas HBC-like cells are evenly distributed throughout the sensory part of the tissue.

Knowledge of the molecular regulations of the stem/progenitor cell activity is necessary to better understand the mechanisms of neurogenesis and to be able to use their innate potential

for nervous system repair. Activation of stem/progenitor cells in the nervous system has been shown to be controlled by a multitude of signaling cascades, such as Notch, BMP, Wnt, cytokine signaling and growth factors (Kizil *et al.*, 2012). An in-depth analysis of differential gene expression by RNA-seq previously performed by our research group (Çapar, 2015; Demirler, unpublished) revealed that a substantial number of genes associated with the Wnt/β-catenin signaling pathway were upregulated following chemical injury of the OE and during regeneration of the tissue. This suggests that the canonical Wnt/β-catenin signaling pathway may play a crucial role in the regulation or in triggering the stem/progenitor cell activity during neurogenesis events in the zebrafish OE.

Building on this result, in this thesis, the role of the Wnt/β-catenin signaling pathway was investigated both for maintenance and repair neurogenesis in the zebrafish OE. As a first step, I aimed to establish a direct link between the Wnt pathway and activity of progenitor cells. For this reason, small chemical agonists (LiCl and CAS853220-52-7) and antagonists (iCRT-14 and Quercetin) were used to manipulate the pathway activity. A set of experiment was devised which includes the intraperitoneal administration of the pharmacological agents during three consecutive days and analysis by immunohistochemistry experiments against pan-neuronal marker HuC/D and the proliferation marker BrdU. As a result of these manipulations of Wnt pathway activity, I expected to observe an increased level of proliferation in agonist-treated OE and decreased mitotic activity in the antagonist-treated OE. As expected, when Wnt pathway agonists were administered, the level of proliferative activity and the pattern of proliferation changed in a way that resembled the regenerative response of the damaged OE. This result suggests that Wnt pathway activation may be sufficient to trigger repair neurogenesis in the zebrafish OE. In contrast, however, administration of antagonists did not significantly change the base level of proliferation in the intact OE. Thus, Wnt pathway activity may not be required for maintenance neurogenesis or the level of inhibition obtained by the antagonists may be too low to detect meaningful changes in baseline activity of GBC-like cells at the ILC and S/NS border. Therefore, an additional set of experiments was designed to examine the effect of Wnt pathway activity during the course of regeneration in the Triton X-100-lesioned OE. Although the administration of the antagonist iCRT-14 resulted in a small and significant reduction in the

level of proliferation in damaged OEs, application of IWR-I did not reduce proliferative activity. Again, the reason for this observation is not known and either HBC-like cells are not strictly dependent on the Wnt/β-catenin pathway or the effectiveness of the pharmacological inhibitors was too low. Yet, iCRT-14 seemed to suppress repair neurogenesis significantly in damaged OE, suggesting that Wnt pathway activity may be required as well.

As a next step, I aimed to reveal which cell populations are Wnt-responsive in damaged OE and Wnt agonist treated OE and if predictable changes in the tissue distribution of β-catenin expression could be observed. Using immunohistochemistry against β-catenin, nuclear β-catenin signals were obtained predominantly located at the ILC and S/NS border and scarcely at the basal layer of the sensory region in the intact OE. The staining pattern is in good agreement with the active proliferation sites during maintenance neurogenesis observed by BrdU experiments. Importantly, a high number of β-catenin-positive cells were detected throughout the entire OE in both damaged and CAS853220-52-7-treated OEs. This pattern again closely matched the pattern of proliferative activity that can be observed in experimentally lesioned OEs. Thus, the results suggests that by administration of Wnt pathway agonists, the same cell populations could be activated that respond with increased Wnt and mitotic activity in the damaged OE.

Additionally, I aimed to verify the efficiency and specificity of pharmacological activators by profiling the expression levels of a list of components and downstream genes of the Wnt pathway through semi qRT-PCR approach. For this purpose, changes in the mRNA levels of target transcripts in damaged, LiCl- and CAS853220-52-7-treated OEs were quantified and compared with their levels in the intact OE. It has been observed that changes in the expression levels of target genes were dynamic over different time points during regeneration after experimental lesion using RNA-seq. Even though many genes showed inconclusive results compared to the RNA-seq results, some components of the Wnt pathway such as *axin2* and *fzd7b* and the endogenous Wnt antagonist *dkk3b* showed matching expression profile. On the other hand, LiCl and CAS853220-52-7 may have differential effects on the OE, since not all

target transcripts showed the same changes at mRNA level. Yet, *axin2, fzd7b,* and *ctnnb1* all displayed an increase in their expression levels in both LiCl and CAS853220-52-7-treated OE, suggesting that pharmacological agonists may indeed specifically activate the Wnt pathway.

5.1. Exogenous activation of Wnt/β-catenin signaling increases cell proliferation

To test whether the Wnt/β-catenin signaling pathway is sufficient to induce neurogenesis in zebrafish OE, I aimed to show that the native response the injury could be mimicked by using pharmacological agonists of the pathway. For this purpose, IP administration of 250 mg/kg of LiCl and 50 μM CAS853220-52-7 were used to activate the Wnt signaling pathway. For an assessment of the physiological effects of these chemicals, a BrdU incorporation assay was performed and proliferating cells were counted across the entire OE, or selectively within the ILC and the sensory region. This would allow me to specifically conclude on the effect of pharmacological manipulation on maintenance neurogenesis, which occurs predominantly at the ILC or repair neurogenesis, which occurs within the sensory OE. To validate whether the proliferation pattern changed in a way that resembles the pattern of the damage response, these results of Wnt pathway activation were compared to the results in OES, which had been injured by nasal irrigation with 1% Triton X-100. Wnt agonists were intraperitoneally injected to the fish over three consecutive days and incubated in BrdU water for an additional 24 hours before analysis. The fish in which the OE was irrigated with 1% Triton X-100 were also incubated in BrdU water for 24 hours, followed by immunohistochemistry against HuC/D and BrdU to detect mitotic activity. To ensure that Wnt activators did not affect the integrity of the neuronal populations and to eliminate bad samples, only OE sections with intact-typical HuC/D pattern were selected to count the BrdU-positive proliferating cells.

Spatial analysis of proliferating cells showed that one day post-lesioned OEs had nearly a seven-fold increase in BrdU-positive cells within the sensory region compared with intact OEs, whereas the number of BrdU-positive cells at the ILC remained the same between intact and damaged OEs. These changes in the proliferation pattern is mainly due to the unique localization

of two progenitor cell populations in the zebrafish OE. In an intact zebrafish OE, the mitotic activity mostly occurs at the ILC and S/NS border, as there are a few proliferating cells within the sensory region. It suggests that GBC-like cells which are constitutively active progenitor cells in the uninjured OE (Chen *et al*., 2004), are predominantly located at the ILC and S/NS border and thereby, maintenance neurogenesis is restricted to these OE segments. On the other hand, the damaged tissue displayed a robust proliferation profile and a uniform pattern throughout the entire OE. Since HBC-like cells, which are transiently triggered to undergo proliferations upon injury (Leung *et al*., 2007), are forming a continuous band of cells in the basal layer around each lamella (Kocagöz, unpublished; Demirler *et al.*, in preparation), the damage response emerges throughout the entire OE including the sensory region. Thus, the sensory region is the characteristic site of proliferation for repair neurogenesis and does not contribute to maintenance neurogenesis.

Quantitative analysis of BrdU-positive cells across the entire OE showed that injection of either LiCl or CAS853220-52-7 results in 1.5-2-fold increase in proliferative activity across the entire OE, within the ILC and the sensory region. Spatial analysis of BrdU-positive cells revealed that the effect of LiCl was stronger than the effect of CAS853220-52-7 within the sensory region (up to 5-fold increase), whereas CAS853220-52-7 is more effective at the ILC compared to the LiCl (1.5-fold increase). As the ILC is the site of maintenance neurogenesis, and the sensory region the site of repair neurogenesis, it can be concluded that both activators induce repair neurogenesis without damaging the OE. In addition, CAS853220-52-7 may also enhance maintenance neurogenesis. As a result, two lines of evidence support that pharmacological activation of the Wnt pathway is sufficient to induce both modes of neurogenesis maintenance and repair neurogenesis.

5.2. Inhibition of Wnt signaling decreases cell proliferation

To test whether Wnt/β-catenin signaling pathway is necessary to induce repair neurogenesis in zebrafish OE, I intended to show that inhibition of the Wnt pathway by using

pharmacological antagonists may suppress or slow down neuroregeneration. To do this, a panel of antagonists was selected: Quercetin, iCRT-14, and IWR-I, which all have different molecular targets, specificities, side effects, and modes of delivery. In order to examine whether the base level of proliferation, which is observed during the regular turnover of OSNs, in the intact OE could be diminished, fish were intraperitoneally administered with 100 mg/kg of Quercetin and 25 μM iCRT-14 over three consecutive days. Following incubation in BrdU water for 24 hours, immunohistochemistry experiments were performed against BrdU and HuC/D to detect changes in the proliferation pattern in the intact OE.

According to the results, IP administration of Wnt inhibitor Quercetin did not suppress the mitotic activity in terms of the number of BrdU-positive cells, but also gave inconsistent results and sometimes and increased proliferation rate. Even though Quercetin has been shown in before to act as an efficient Wnt inhibitor and diminish the cell proliferation through cell cycle arrest in a dose-dependent manner (Casella *et al.*, 2014; Lisi *et al*., 2010; Wang *et al*., 2011; Zhang *et al.*, 2011), the applied dosage might not be sufficient to suppress the mitotic activity in the zebrafish OE. Another explanation for this result could be that the Wnt pathway shows cross-reactivity with other, kinase signaling pathways which are also suppressed by Quercetin (Zhao *et al.*, 2014). For these reasons, Quercetin was excluded during later experiments.

Quantitative and spatial analysis of BrdU-positive proliferating cells showed that iCRT-14 did not affect the proliferation profile in the intact OE. The administration of iCRT-14 showed an unperturbed pattern of maintenance neurogenesis as judged by PBS-injected control fish, so that high proliferative activity mostly occurred at the ILC and S/NS border. According to these results, it can be concluded that inhibition of the Wnt pathway with pharmacological antagonists may not diminish the base level of proliferative activity in intact OE, either by using Quercetin or iCRT-14.

To see if the Wnt pathway is necessary to induce repair neurogenesis in the injured OE, an experimental setup was designed, which includeed both the inhibition of the pathway and damage to the OE. In this procedure, iCRT-14 was administered IP over three consecutive days and the OE was damaged by nasal irrigation with 1% Triton X-100 following the last injection. Fish were incubated in BrdU water for 24 hours and during this course, an additional dose of iCRT-14 was injected 12 hours after the injury. Quantitative analysis of the BrdU-positive proliferating cells showed that iCRT-14 caused a small but significant reduction in the proliferative activity in the entire OE, within the ILC and the sensory region of one day post-lesioned OEs. However, in intact OEs, the level of proliferative activity did not change in iCRT-14-injected fish, regardless which OE segment was considered. Consistent with the quantitative results, a spatial analysis revealed that iCRT-14 resulted in the suppression of the distributed proliferation pattern across the entire damaged OE, whereas the pattern remained the same in the case of uninjured OEs. It suggests that inhibition of the Wnt pathway may slow down the activity of HBC-like cells, which are contributing to the repair neurogenesis, however, the activity of GBC-like cells is not affected during the maintenance neurogenesis. Thus, Wnt/β-catenin signaling pathway may be necessary, at least to some level, to trigger the full repair mechanism in the zebrafish OE.

A similar pharmacological approach was followed to examine the effect of the alternative Wnt inhibitor IWR-I. IWR-I is a water-soluble Wnt inhibitor which has been used in many regenerative studies such as zebrafish tail and spinal cord regeneration (Shimizu *et al.*, 2012; Wehner *et al.*, 2017). In my experiments, fish were incubated in IWR-I water during a priming period of 24 hours before the injury with 1% Triton X-100. Following the damage, fish were additionally incubated in BrdU and IWR-I water for 24 hours and then analyzed by immunohistochemistry against BrdU and HuC/D. The counts of BrdU-positive cells revealed that IWR-I-injected intact OEs had similar proliferative activity with DMSO-control fish. It appeared that administration of IWR-I reduced the number of proliferating cells non-significantly across the entire OE and within the sensory region and could not diminish the activity of stem/progenitor cells within the ILC. Amore precise analysis of the spatial distribution pattern of proliferating cells showed that IWR-I did not change the proliferation

pattern within the ILC and the sensory region of the intact OE, however, it resulted in a significant decrease at the S/NS border, specifically. This result suggests that IWR-I does not completely block maintenance neurogenesis, yet, it may reduce the activity of stem/progenitor cells locating at the S/NS border.

On the other hand, in damaged OEs, IWR-I showed a significant decrease in the number of proliferating cells only at the ILC. Yet, the quantitative analysis was not conclusive when the entire lamella was analyzed since it appears that IWR-I resulted in a significant increase in proliferation. This result may be misguided due to the massive proliferation that could be observed within the outer non-sensory region. Thus, my attempts to inhibit the Wnt pathway with IWR-I showed inconsistent results. Both the damaged OEs of IWR-I or DMSO-control fish had the highest proliferative activity at the ILC with a sharp decrease within the sensory region, suggesting that the damage was not complete in these experiments. Thus, these results may not be conclusive for the inhibitory effect of IWR-I in one day post-lesioned OE.

To summarize, IWR-I and iCRT-14 had differential inhibitory effects on the neurogenesis in zebrafish OE and inhibition of the Wnt pathway resulted in decreased cell proliferation either in uninjured tissue or upon injury. Quantitative analysis of proliferating cells revealed that iCRT-14 did not fully inhibit but suppressed the damage response regarding the decreased mitotic activity across the entire OE. On the other hand, the inhibitory effect of IWR-I in intact OE emerged only at the S/NS border which is one of the proliferative sites for the maintenance neurogenesis. Thus, it may be concluded that Wnt/β-catenin signaling pathway may be necessary, at least in part, to trigger maintenance and repair neurogenesis to some extent.

5.3. Injured zebrafish OE shows increased nuclear β-catenin signaling

To validate whether Wnt/β-catenin signaling is indeed activated by the pharmacological agonists and whether the pathway is indeed upregulated upon traumatic injury,

immunohistochemistry experiments were performed against β-catenin. Expression of β-catenin is most dense at cell-cell junctions since it involves with the adhesion with E-cadherin protein (Nelson and Nusse, 2004) and kept low in the cytoplasm of Wnt-off cells via a destruction complex formed by Axin2, APC and GSK3β (Cadigan and Nusse, 1997). Through the binding of Wnt ligand to its receptor called Frizzled, β-catenin can accumulate in the cytoplasm and nuclear translocation occurs by which it regulates the expression of downstream target genes in a complex with the transcription factor TCF/Lef. Thus, the activation of the Wnt pathway can be indicated by increased cytoplasmic and nuclear levels of β-catenin.

After several attempts to reliably detect β-catenin immunoreactivity, a protocol including a heat-induced epitope retrieval method resulted in positive staining signals. According to the immunohistochemistry experiments, the intact OE displayed nuclear β-catenin signals at the basal-most layer, exclusively at the ILC and S/NS border. A limited number of β-catenin-positive cells could also be detected at the basal layer of the sensory region, suggesting that in an uninjured OE progenitor cells localized within the sensory region have a low tendency to be Wnt-responsive. This exclusive staining pattern is consistent with the sites of maintenance neurogenesis at the ILC and S/NS border. Considering the relative position and the morphology of HBC-like cells along lamellae, within the sensory region the flat shaped β-catenin signals may belong to this cell population. However, further immunohistochemistry experiments are required to ensure this possibility and the HBC marker Tp63 (Packard *et al*., 2011; Kocagöz, unpublished) could be used for co-labeling studies. Thus, it can be suggested that Wnt/β-catenin signaling pathway may play an essential role in regulating the maintenance neurogenesis in the zebrafish OE.

On the other hand, the immunohistochemistry experiments performed in damaged OEs revealed that the expression pattern of β-catenin is completely altered when compared with the intact OE. In this case, cells along the entire OE display a robust increase in the number of nuclear β-catenin signals regardless the OE segments. These β-catenin-positive cells did not appear only at the basal-most layer but also at more apical layer within the lamella, which is

consistent with the disorganized arrangement of Tp63/krt5-positive cells upon injury (Demirler, unpublished). At higher resolutions, speckle signals of β-catenin could be detected within the nuclei, which may also indicate the positions of β-catenin where it binds to DNA together with the transcription factor TCF/Lef to regulate some gene expression. By this indication and consistent with the previously described proliferation pattern in the damaged OE, it may be concluded that Wnt/β-catenin signaling pathway may indeed be involved in the induction of mitotic activity during repair neurogenesis.

To validate whether the Wnt pathway can be effectively activated through pharmacological agonists, immunohistochemical staining against β-catenin was performed in fish which have been administered with CAS853220-52-7 by the previously described procedure. CAS853220-52-7-injected OE showed a very similar expression pattern of β-catenin as the damaged OE. Again, the administration of CAS853220-52-7 resulted in increased induction of β-catenin expression across the entire OE, at the basal-most and more apical layers. The speckle formation of the nuclear signals could also be detected, and membrane-bound signals were diminished to a respectable level. Thus, by utilizing the Wnt agonist CAS853220-52-7, the Wnt/β-catenin signaling pathway can indeed be activated exogenously. Moreover, by two lines of evidence, including the similarity of BrdU proliferation profiles and the β-catenin expression pattern, it can be concluded that the Wnt pathway may be sufficient to induce repair neurogenesis even without damaging the OE.

5.4. Exogenous activation of Wnt signaling causes upregulation of target genes

Based on BrdU incorporation and β-catenin immunoreactivity following the pharmacological manipulation, it has been shown that to some extent, the Wnt signaling pathway is sufficient and necessary for the induction of both maintenance and repair neurogenesis. To ensure that the observed effect on robust activation of neurogenesis is bona fide due to the activation of Wnt/β-catenin signaling pathway, the specificity and efficiency of LiCl and CAS853220-52-7 needs to be verified by examining expression changes in Wnt target

genes. Upon the activation of Wnt/β-catenin signaling pathway, through the interaction with TCF/LEF, β-catenin either downregulates or upregulates the expression of the target genes. Not only the downstream target genes but also Wnt components may be regulated through crosstalk between other signaling pathways. Previously our group revealed upregulation of Wnt target and component genes by RNA sequencing in OEs which are damaged at different time points by nasal irrigation with Triton X-100. To validate the changes in the expression of target genes in LiCl- and CAS853220-52-7-injected OEs, semi qRT-PCR was performed in which the band intensities on ethidium bromide-stained agarose gel reflects the expression of genes. A list of upregulated Wnt-associated genes was selected according to the RNA-seq results and primer pairs for these genes were pre-tested.

Normalized data of the changes in mRNA levels were compared to the RNA-seq results in order to ensure the reliability of the primer pairs. As a result, the changes in the expression of *axin2, dkk3b,* and *fzd7b* were relatively consistent with RNA-seq results, thus, these primer pairs are more reliable. On the other hand, *bmp2k, ctnnb2, ctnnb1, neurod1,* and *neurod4* showed inconsistent results compared to the RNA-seq results. In semi qRT-PCR, the quantitative measurements are dependent on the detectability of the band intensities and the quality of the gel image. Thus, either saturated bands or weak bands may mislead the measurements and give inaccurate results. Therefore, the conflicting result may be, in part, due to the lack of accuracy in the quantitative measurement of the semi qRT-PCR, and less likely the low-specificity of the primer sets. Thus, qRT-PCR approaches using SYBR® Green or TaqMan® may be more accurate to validate the changes in expression of target transcripts.

Axin2 as a negative regulator of the Wnt signaling pathway is a commonly used indicator to verify the activation of the pathway due to its upregulation (Yan *et al.*, 2001). Similarly, *fzd7* as a signaling component of Wnt is also upregulated at downstream of β-catenin (Willert *et al.*, 2002). The secreted natural Wnt antagonist, *dkk1* is upregulated in Wnt-active cells, and thereby, initiating a negative feedback loop (González-Sancho *et al.*, 2005). It should be noted that the activation of the Wnt signaling pathway does not necessarily result in increased mRNA levels

of *ctnnb* (Yu *et al.*, 1998). Yet, its expression level may be altered in a Wnt-independent manner through the crosstalk between other signaling pathways. BMP is one of these pathways and it has been shown that *bmp2* is either upregulated by Wnt or downregulating the Wnt pathway (Li *et al*., 2013; Nakashima *et al.*, 2005; Zhang *et al.*, 2013). The neuronal differentiation gene *neurod1* has been also shown to be upregulated as a direct downstream target and *neurod4* as an indirect target (Kuwabara *et al*., 2009).

In the next step, to verify whether the pharmacological agonists indeed activated the Wnt signaling pathway, the changes in expression of target transcripts were measured by using cDNAs from LiCl- and CAS853220-52-7-injected OEs. Quantitative analysis revealed that in both LiCl- and CAS853220-52-7-injected OE, *axin2, fzd7b,* and *ctnnb1* were consistently upregulated. On the other hand, *dkk3b, bmp2k, neurod1,* and *neurod4* were upregulated only in CAS853220-52-7-injected OEs. The differential expression of genes in LiCl and CAS853220-52-7-stimulated OEs may be due to any complication during the IP administration or the fact that LiCl is a less specific Wnt activator, or that both agonists have different targets within the Wnt cascade. Only *ctnnb2* showed a decreased mRNA level both for LiCl- and CAS853220-52-7-injected OEs, that may suggest the involvement of *ctnnb2* into a negative feedback loop.

These results suggest that the efficiency and specificity of LiCl and CAS853220-52-7 may differ from each other in terms of the regulation of the expression of downstream genes. The consistency of the upregulated target transcripts may indicate that CAS853220-52-7 is a more specific and efficient pharmacological activator of the Wnt signaling pathway. Moreover, it can be concluded that the previous immunohistochemistry experiments display bona fide results of the pharmacological activation of the Wnt pathway. However, further validation of the activation of the pathway should be performed via western blotting approach, since the main indicator of the active Wnt signaling is the increase in intracellular β-catenin levels, thus at protein, not mRNA levels. For this reason, changes in the cytoplasmic/nuclear β-catenin protein levels should be compared between damaged and Wnt-associated OE by using β-catenin

antibody. Preliminary studies in this thesis have successfully established routines for β-catenin staining on western blots.

5.5. What is upstream activator of Wnt/β-catenin signaling in the OE?

The activation of a signaling pathway that is crucial during the early development of organisms and adult homeostasis such as Wnt signaling, is critically regulated by crosstalk with other signaling pathways in a highly coordinated manner (Thompson *et al.*, 2011). To understand the regulatory mechanisms of the activation of the Wnt pathway during repair neurogenesis, firstly the regulation on the secretion of Wnt ligands should be elucidated. Wnt proteins include a large family of hydrophobic glycoproteins which play vital roles in a wide variety of biological processes such as development, cell differentiation, cell division, and wound healing. Pioneering studies in *Drosophila* revealed the segment polarity gene *wingless* as an orthologue of Wnt-1 (Cabrera *et al.*, 1987; Rijsewijk *et al.*, 1987). It was shown that for the proper folding, secretion and activity of *wingless* undergo some post-translational modifications in which the gene *porcupine* plays a role in its N-linked glycosylation and lipid modification by encoding a seven transmembrane receptor in endoplasmic reticulum (Kadowaki *et al.*, 1996; Smolich *et al.* 1993; van den Heuvel *et al.*, 1993). Moreover, the secretion of Wnt proteins from producing cells is mediated by a multipass transmembrane protein called Wntless/Evi (Bänziger *et al*., 2006; Bartscherer *et al.*, 2006; Ching and Nusse, 2006). Thus, downregulation of expression of *porcupine* or Wntless/Evi results in decreased Wnt signaling due to their important roles in the secretion and processing of Wnts. After a Wnt protein is secreted from a producing cell, it mostly associates with cell membranes and extracellular matrix due to its hydrophobic property. For that reason, the navigation of secreted hydrophobic Wnt ligand is facilitated by glycosaminoglycans such as heparin (Reichsman *et al.*, 1996). Thereby, any disruption in the processes of N-glycosylation, lipid modification or in the interaction with glycosaminoglycans causes reduced Wnt signaling activity.

The activity of the Wnt pathway is under control of many other signaling pathways such as TGF-β (Akhmetshina *et al.*, 2012), TLR (Manoharan *et al*., 2014), Sonic hedgehog (Alvarez-Medina *et al.*, 2009), TNFα and IFNγ (Silva-García *et al*., 2014), HB-EGF (Colombres *et al.*, 2008; Wan *et al.*, 2012), and MAPK (Červenka *et al.*, 2011). These signaling pathways regulate the activation of the Wnt signaling by affecting different components of the pathway at different levels, either at transcriptional or at protein levels. Among them, TGF-β, TLR, HB-EGF, and MAPK acts as a positive regulator of Wnt ligand. TGF-β/Smad3 signaling pathway has been shown to upregulate the secretion of Wnt proteins (DiRenzo *et al.*, 2016). Downstream of the MAPK signaling pathway, p38 mediates TGF-β to enhance the Wnt signaling by repressing the natural Wnt inhibitor Dkk-1 through a Smad-independent manner in which p38 (Akhmetshina *et al.*, 2012). In another study, heparin and HB-EGF have been shown to modulate Wnt/β-catenin signaling pathway either through activation of Wnt or inhibition of GSK3β (Colombres *et al.*, 2008; Wan *et al.*, 2012). Interestingly, HB-EGF has recently been found to be activated in the damaged OE and is sufficient to induce massive proliferation similar to Wnt pathway activation (Kocagöz, unpublished).

Upon pathogen invasion, necrosis or stress response, TLRs are activated via PAMPs or DAMPs, and thereby, an inflammatory response is generated. Activation of TLR signaling increases the expression of proinflammatory molecules TNFα and IFNγ, which synergistically enhance the expression of a list of Wnt proteins and Frizzled (Silva-García *et al*., 2014). Apart from TNFα and IFNγ, TLRs also activate PI3K/Akt signaling pathway in which Akt either suppresses GSK3β or enhances β-catenin via phosphorylation. Crosstalk between TLR signaling and Wnt signaling is based on a negative regulatory feedback loop. Increased Wnt ligand and Frizzled receptors result in upregulated β-catenin activity which in turn inhibits the expression of TNFα and IFNγ via interacting with NFκB, suggesting that Wnt/β-catenin signaling pathway acts as a negative regulatory to repress the inflammatory response at late stages.

Cells which undergo traumatic injury or necrosis, elicit DAMP-mediated inflammatory response. Extracellular ATP which is released from necrotic cells acts as a DAMP and results in the activation of purinergic signaling (Vénéreau *et al.*, 2015). A study examining the effect of purinergic signaling on the Wnt signaling pathway showed that activation of P2X receptor upregulates the Wnt/β-catenin signaling pathway through GSK3β inhibition (Grol *et al.*, 2016).

Previously our group showed that activation of purinergic signaling by using extracellular ATP enhances cell proliferation in the zebrafish OE in a way that resembles the native damage response upon traumatic injury, suggesting that purines may play an important role during induction of repair neurogenesis (Sakızlı, 2018). Considering this result and the interactions between the Wnt and other signaling pathways, it is possible to hypothesize that Wnt/β-catenin signaling pathway may be downstream of an inflammatory immune response which includes the activation of TLR or purinergic signaling. Since damaging the OE causes severe loss of cells, the tissue undergoes neuroinflammation in which proinflammatory molecules and DAMPs were released. Either enhanced expression of TNFα and IFNγ or increased extracellular ATP may lead to activation of Wnt/β-catenin signaling pathway in many ways: the secretion of Wnt ligand may be increased, GSK3β activity may be suppressed via phosphorylation, or β-catenin may be stabilized through phosphorylation as well. In any case, the Wnt/β-catenin signaling pathway may be triggered to act on the cell proliferation during repair neurogenesis.

6. CONCLUSION

To summarize, in this thesis, I showed that pharmacological activation Wnt/β-catenin signaling resulted in increased proliferation profile resembling the acute injury response in zebrafish OE and inhibition of the pathway by using small molecular antagonists suppressed the regenerative response in the OE. In addition, by β-catenin immunoreactivity, it was shown that HBC-like cells located exclusively at ILC and S/NS may be Wnt-responsive cell populations in intact OE, however, double labeling with an HBC-marker is required to ensure that. Upon tissue

damage, the entire OE displayed a robust increase in Wnt activity consistent with the proliferation pattern assessed by BrdU incorporation. Exogenous activation of the pathway was validated in agonist treated OEs by either increase in expression level of Wnt target genes or enhanced β-catenin immunoreactivity across the entire OE. These findings indicate that Wnt/β-catenin signaling pathway may have crucial contributory role in mechanisms of either maintenance or repair neurogenesis in zebrafish OE.

REFERENCES

Aguirre, A., Dupree, J. L., Mangin, J. M., & Gallo, V. (2007). A functional role for EGFR signaling in myelination and remyelination. *Nature Neuroscience*, *10*(8), 990–1002. https://doi.org/10.1038/nn1938

Akhmetshina, A., Palumbo, K., Dees, C., Bergmann, C., Venalis, P., Zerr, P., … Distler, J. H. W. (2012). Activation of canonical Wnt signalling is required for TGF-β-mediated fibrosis. *Nature Communications*, *3*, 735. https://doi.org/10.1038/ncomms1734

Altman, J. (1969). Autoradiographic and histological studies of postnatal neurogenesis. IV. Cell proliferation and migration in the anterior forebrain, with special reference to persisting neurogenesis in the olfactory bulb. *The Journal of Comparative Neurology*, *137*(4), 433–457. https://doi.org/10.1002/cne.901370404

Altman, J., & Das, G. D. (1965). Autoradiographic and histological evidence of postnatal hippocampal neurogenesis in rats. *The Journal of Comparative Neurology*, *124*(3), 319–335. https://doi.org/10.1002/cne.901240303

Alvarez-Buylla, A., & Kirn, J. R. (1997). Birth, migration, incorporation, and death of vocal control neurons in adult songbirds. *Journal of Neurobiology*, *33*(5), 585–601. https://doi.org/10.1002/(SICI)1097-4695(19971105)33:5<585::AID-NEU7>3.0.CO;2-0

Alvarez-Buylla, A., Ling, C.-Y., & Yu, W. S. (1994). Contribution of neurons born during embryonic and adult life to the brain of adult canaries: Regional specificity and delayed birth of neurons in the song-control nuclei. *The Journal of Comparative Neurology*, *347*(2), 233–248. https://doi.org/10.1002/cne.903470207

Alvarez-Medina, R., Le Dreau, G., Ros, M., & Martí, E. (2009). Hedgehog activation is required upstream of Wnt signalling to control neural progenitor proliferation. *Development (Cambridge, England)*, *136*(19), 3301–3309. https://doi.org/10.1242/dev.041772

Amado, N. G., Predes, D., Moreno, M. M., Carvalho, I. O., Mendes, F. A., & Abreu, J. G. (2014). Flavonoids and Wnt/β-catenin signaling: potential role in colorectal cancer

therapies. *International Journal of Molecular Sciences*, *15*(7), 12094–12106. https://doi.org/10.3390/ijms150712094

Bali, B. (2015). *The Role of Sustentacular Cells in Adult Neurogenesis*. Boğaziçi University.

Bamji, S. X., Shimazu, K., Kimes, N., Huelsken, J., Birchmeier, W., Lu, B., & Reichardt, L. F. (2003). Role of β-Catenin in Synaptic Vesicle Localization and Presynaptic Assembly. *Neuron*, *40*(4), 719–731. https://doi.org/10.1016/S0896-6273(03)00718-9

Bänziger, C., Soldini, D., Schütt, C., Zipperlen, P., Hausmann, G., & Basler, K. (2006). Wntless, a conserved membrane protein dedicated to the secretion of Wnt proteins from signaling cells. *Cell*, *125*(3), 509–522. https://doi.org/10.1016/j.cell.2006.02.049

Bartscherer, K., Pelte, N., Ingelfinger, D., & Boutros, M. (2006). Secretion of Wnt ligands requires Evi, a conserved transmembrane protein. *Cell*, *125*(3), 523–533. https://doi.org/10.1016/j.cell.2006.04.009

Bayramli, X., Kocagöz, Y., Sakizli, U., & Fuss, S. H. (2017). Patterned Arrangements of Olfactory Receptor Gene Expression in Zebrafish are Established by Radial Movement of Specified Olfactory Sensory Neurons. *Scientific Reports*, *7*(1), 5572. https://doi.org/10.1038/s41598-017-06041-1

Bayramlı, K. (2016). *Neurogenesis and Migration of Specified Chemosensory Neurons in the Adult Zebrafish Olfactory Epithelium*. Boğaziçi University.

Boldrini, M., Fulmore, C. A., Tartt, A. N., Simeon, L. R., Pavlova, I., Poposka, V., … Mann, J. J. (2018). Human Hippocampal Neurogenesis Persists throughout Aging. *Cell Stem Cell*, *22*(4), 589–599.e5. https://doi.org/10.1016/j.stem.2018.03.015

Bonaguidi, M. A. (2005). LIF and BMP signaling generate separate and discrete types of GFAP-expressing cells. *Development*, *132*(24), 5503–5514. https://doi.org/10.1242/dev.02166

Brockes, J. P., & Kumar, A. (2002). Plasticity and reprogramming of differentiated cells in amphibian regeneration. *Nature Reviews Molecular Cell Biology*, *3*(8), 566–574. https://doi.org/10.1038/nrm881

Cabrera, C. V, Alonso, M. C., Johnston, P., Phillips, R. G., & Lawrence, P. A. (1987).

Phenocopies induced with antisense RNA identify the wingless gene. *Cell*, *50*(4), 659–663. https://doi.org/10.1016/0092-8674(87)90039-0

Cadigan, K. M., & Nusse, R. (1997). Wnt signaling: a common theme in animal development. *Genes & Development*, *11*(24), 3286–3305. Retrieved from http://www.ncbi.nlm.nih.gov/pubmed/9407023

Cameron, H. A., Woolley, C. S., McEwen, B. S., & Gould, E. (1993). Differentiation of newly born neurons and glia in the dentate gyrus of the adult rat. *Neuroscience*, *56*(2), 337–344. https://doi.org/10.1016/0306-4522(93)90335-D

Cantarella, C., Cayre, M., Magalon, K., & Pascale, D. (2008). Intranasal HB-EGF administration favors adult SVZ cell mobilization to demyelinated lesions in mouse corpus callosum. *Developmental Neurobiology*, *68*(2), 223–236. https://doi.org/10.1002/dneu.20588

Çapar, S. (2015). *Olfactory Neurogenesis Following Acute Injury*. Boğaziçi University.

Carter, L. A., MacDonald, J. L., & Roskams, A. J. (2004). Olfactory horizontal basal cells demonstrate a conserved multipotent progenitor phenotype. *The Journal of Neuroscience : The Official Journal of the Society for Neuroscience*, *24*(25), 5670–5683. https://doi.org/10.1523/JNEUROSCI.0330-04.2004

Casella, M. L., Parody, J. P., Ceballos, M. P., Quiroga, A. D., Ronco, M. T., Francés, D. E., … de Luján Alvarez, M. (2014). Quercetin prevents liver carcinogenesis by inducing cell cycle arrest, decreasing cell proliferation and enhancing apoptosis. *Molecular Nutrition & Food Research*, *58*(2), 289–300. https://doi.org/10.1002/mnfr.201300362

Cau, E., & Blader, P. (2009). Notch activity in the nervous system: to switch or not switch? *Neural Development*, *4*, 36. https://doi.org/10.1186/1749-8104-4-36

Cau, E., Gradwohl, G., Fode, C., & Guillemot, F. (1997). Mash1 activates a cascade of bHLH regulators in olfactory neuron progenitors. *Development*, *124*(8).

Červenka, I., Wolf, J., Mašek, J., Krejci, P., Wilcox, W. R., Kozubík, A., … Bryja, V. (2011). Mitogen-activated protein kinases promote WNT/beta-catenin signaling via

phosphorylation of LRP6. *Molecular and Cellular Biology*, *31*(1), 179–189. https://doi.org/10.1128/MCB.00550-10

Chapouton, P., Skupien, P., Hesl, B., Coolen, M., Moore, J. C., Madelaine, R., … Bally-Cuif, L. (2010). Notch activity levels control the balance between quiescence and recruitment of adult neural stem cells. *The Journal of Neuroscience : The Official Journal of the Society for Neuroscience*, *30*(23), 7961–7974. https://doi.org/10.1523/JNEUROSCI.6170-09.2010

Chen, M., Tian, S., Yang, X., Lane, A. P., Reed, R. R., & Liu, H. (2014). Wnt-Responsive Lgr5+ Globose Basal Cells Function as Multipotent Olfactory Epithelium Progenitor Cells. *Journal of Neuroscience*, *34*(24), 8268–8276. https://doi.org/10.1523/JNEUROSCI.0240-14.2014

Chen, X., Fang, H., & Schwob, J. E. (2004). Multipotency of purified, transplanted globose basal cells in olfactory epithelium. *The Journal of Comparative Neurology*, *469*(4), 457–474. https://doi.org/10.1002/cne.11031

Chenn, A., & Walsh, C. A. (2003). Increased Neuronal Production, Enlarged Forebrains and Cytoarchitectural Distortions in beta-Catenin Overexpressing Transgenic Mice. *Cerebral Cortex*, *13*(6), 599–606. https://doi.org/10.1093/cercor/13.6.599

Ching, W., & Nusse, R. (2006). A dedicated Wnt secretion factor. *Cell*, *125*(3), 432–433. https://doi.org/10.1016/j.cell.2006.04.018

Chojnacki, A., & Weiss, S. (2008). Production of neurons, astrocytes and oligodendrocytes from mammalian CNS stem cells. *Nature Protocols*, *3*(6), 935–940. https://doi.org/10.1038/nprot.2008.55

Clevers, H., & Nusse, R. (2012). Wnt/β-catenin signaling and disease. *Cell*, *149*(6), 1192–1205. https://doi.org/10.1016/j.cell.2012.05.012

Cohen, P., & Goedert, M. (2004). GSK3 inhibitors: Development and therapeutic potential. *Nature Reviews Drug Discovery*, *3*(6), 479–487. https://doi.org/10.1038/nrd1415

Colak, D., Mori, T., Brill, M. S., Pfeifer, A., Falk, S., Deng, C., … Götz, M. (2008). Adult neurogenesis requires Smad4-mediated bone morphogenic protein signaling in stem cells.

The Journal of Neuroscience : The Official Journal of the Society for Neuroscience, *28*(2), 434–446. https://doi.org/10.1523/JNEUROSCI.4374-07.2008

Colombres, M., Henríquez, J. P., Reig, G. F., Scheu, J., Calderón, R., Alvarez, A., … Inestrosa, N. C. (2008). Heparin activates Wnt signaling for neuronal morphogenesis. *Journal of Cellular Physiology*, *216*(3), 805–815. https://doi.org/10.1002/jcp.21465

Costanzo, R. M. (1985). Neural regeneration and functional reconnection following olfactory nerve transection in hamster. *Brain Research*, *361*(1–2), 258–266. https://doi.org/10.1016/0006-8993(85)91297-1

Das, S., & Basu, A. (2008). Inflammation: A new candidate in modulating adult neurogenesis. *Journal of Neuroscience Research*, *86*(6), 1199–1208. https://doi.org/10.1002/jnr.21585

DiRenzo, D. M., Chaudhary, M. A., Shi, X., Franco, S. R., Zent, J., Wang, K., … Kent, K. C. (2016). A crosstalk between TGF-β/Smad3 and Wnt/β-catenin pathways promotes vascular smooth muscle cell proliferation. *Cellular Signalling*, *28*(5), 498–505. https://doi.org/10.1016/j.cellsig.2016.02.011

Doetsch, F., & Scharff, C. (2001). Challenges for brain repair: insights from adult neurogenesis in birds and mammals. *Brain, Behavior and Evolution*, *58*(5), 306–322. https://doi.org/10.1159/000057572

Ekström, P., Johnsson, C.-M., & Ohlin, L.-M. (2001). Ventricular proliferation zones in the brain of an adult teleost fish and their relation to neuromeres and migration (secondary matrix) zones. *Journal of Comparative Neurology*, *436*(1), 92–110. https://doi.org/10.1002/cne.1056

Eriksson, P. S., Perfilieva, E., Björk-Eriksson, T., Alborn, A.-M., Nordborg, C., Peterson, D. A., & Gage, F. H. (1998). Neurogenesis in the adult human hippocampus. *Nature Medicine*, *4*(11), 1313–1317. https://doi.org/10.1038/3305

Farbman, A. (1992). *Cell biology of olfaction*. Retrieved from https://books.google.com/books?hl=en&lr=&id=74Vv2LPE-xwC&oi=fnd&pg=PR11&ots=SuYCMnk5HD&sig=pIuu2XN0hFxEQ6iaXgGVSTeO4B

o, accessed at December 2018.

Filoni, S., Bernardini, S., & Cannata, S. M. (1995). Differences in the decrease in regenerative capacity of various brain regions of Xenopus laevis are related to differences in the undifferentiated cell populations. *Journal Fur Hirnforschung*, *36*(4), 523–529. Retrieved from http://www.ncbi.nlm.nih.gov/pubmed/8568223

Formica, J. V., & Regelson, W. (1995). Review of the biology of quercetin and related bioflavonoids. *Food and Chemical Toxicology*, *33*(12), 1061–1080. https://doi.org/10.1016/0278-6915(95)00077-1

Fortini, M. E. (2009). Notch signaling: the core pathway and its posttranslational regulation. *Developmental Cell*, *16*(5), 633–647. https://doi.org/10.1016/j.devcel.2009.03.010

Fortini, M. E., & Artavanis-Tsakonas, S. (1993). Notch: Neurogenesis is only part of the picture. *Cell*, *75*(7), 1245–1247. https://doi.org/10.1016/0092-8674(93)90611-S

Ganz, J., Kaslin, J., Hochmann, S., Freudenreich, D., & Brand, M. (2010). Heterogeneity and Fgf dependence of adult neural progenitors in the zebrafish telencephalon. *Glia*, *58*(11), n/a-n/a. https://doi.org/10.1002/glia.21012

García-Verdugo, J. M., Ferrón, S., Flames, N., Collado, L., Desfilis, E., & Font, E. (2002). The proliferative ventricular zone in adult vertebrates: a comparative study using reptiles, birds, and mammals. *Brain Research Bulletin*, *57*(6), 765–775. https://doi.org/10.1016/S0361-9230(01)00769-9

Goldman, S. (2005). Stem and progenitor cell–based therapy of the human central nervous system. *Nature Biotechnology*, *23*(7), 862–871. https://doi.org/10.1038/nbt1119

Goldman, S. A., & Nottebohm, F. (1983). Neuronal production, migration, and differentiation in a vocal control nucleus of the adult female canary brain. *Proceedings of the National Academy of Sciences of the United States of America*, *80*(8), 2390–2394. https://doi.org/10.1073/PNAS.80.8.2390

Gonsalves, F. C., Klein, K., Carson, B. B., Katz, S., Ekas, L. A., Evans, S., … DasGupta, R. (2011). An RNAi-based chemical genetic screen identifies three small-molecule inhibitors

of the Wnt/wingless signaling pathway. *Proceedings of the National Academy of Sciences*, *108*(15), 5954–5963. https://doi.org/10.1073/pnas.1017496108

González-Sancho, J. M., Aguilera, O., García, J. M., Pendás-Franco, N., Peña, C., Cal, S., … Muñoz, A. (2005). The Wnt antagonist DICKKOPF-1 gene is a downstream target of β-catenin/TCF and is downregulated in human colon cancer. *Oncogene*, *24*(6), 1098–1103. https://doi.org/10.1038/sj.onc.1208303

Gould, E., Reeves, A. J., Fallah, M., Tanapat, P., Gross, C. G., & Fuchs, E. (1999). Hippocampal neurogenesis in adult Old World primates. *Proceedings of the National Academy of Sciences of the United States of America*, *96*(9), 5263–5267. Retrieved from http://www.ncbi.nlm.nih.gov/pubmed/10220454

Grandel, H., Kaslin, J., Ganz, J., Wenzel, I., & Brand, M. (2006). Neural stem cells and neurogenesis in the adult zebrafish brain: Origin, proliferation dynamics, migration and cell fate. *Developmental Biology*, *295*(1), 263–277. https://doi.org/10.1016/J.YDBIO.2006.03.040

Graziadei, P. P. C., & Graziadei, G. A. M. (1979). Neurogenesis and neuron regeneration in the olfactory system of mammals. I. Morphological aspects of differentiation and structural organization of the olfactory sensory neurons. *Journal of Neurocytology*, *8*(1), 1–18. https://doi.org/10.1007/BF01206454

Grol, M. W., Brooks, P. J., Pereverzev, A., & Dixon, S. J. (2016). P2X7 nucleotide receptor signaling potentiates the Wnt/β-catenin pathway in cells of the osteoblast lineage. *Purinergic Signalling*, *12*(3), 509–520. https://doi.org/10.1007/s11302-016-9517-4

Guo, Z., Packard, A., Krolewski, R. C., Harris, M. T., Manglapus, G. L., & Schwob, J. E. (2010). Expression of Pax6 and Sox2 in adult olfactory epithelium. *The Journal of Comparative Neurology*, *518*(21), 4395–4418. https://doi.org/10.1002/cne.22463

Hack, M. A., Saghatelyan, A., de Chevigny, A., Pfeifer, A., Ashery-Padan, R., Lledo, P.-M., & Götz, M. (2005). Neuronal fate determinants of adult olfactory bulb neurogenesis. *Nature Neuroscience*, *8*(7), 865–872. https://doi.org/10.1038/nn1479

Haddon, C., Smithers, L., Schneider-Maunoury, S., Coche, T., Henrique, D., & Lewis, J. (1998). Multiple delta genes and lateral inhibition in zebrafish primary neurogenesis. *Development*, *125*(3).

Hansen, A., & Zeiske, E. (1993). Development of the olfactory organ in the zebrafish,Brachydanio rerio. *The Journal of Comparative Neurology*, *333*(2), 289–300. https://doi.org/10.1002/cne.903330213

Herrick, D. B., Lin, B., Peterson, J., Schnittke, N., & Schwob, J. E. (2017). Notch1 maintains dormancy of olfactory horizontal basal cells, a reserve neural stem cell. *Proceedings of the National Academy of Sciences of the United States of America*, *114*(28), E5589–E5598. https://doi.org/10.1073/pnas.1701333114

Iosif, R. E. (2006). Tumor Necrosis Factor Receptor 1 Is a Negative Regulator of Progenitor Proliferation in Adult Hippocampal Neurogenesis. *Journal of Neuroscience*, *26*(38), 9703–9712. https://doi.org/10.1523/JNEUROSCI.2723-06.2006

Iqbal, T., & Byrd-Jacobs, C. (2010). Rapid Degeneration and Regeneration of the Zebrafish Olfactory Epithelium after Triton X-100 Application. *Chemical Senses*, *35*(5), 351–361. https://doi.org/10.1093/chemse/bjq019

Jin, K., Sun, Y., Xie, L., Peel, A., Mao, X. O., Batteur, S., & Greenberg, D. A. (2003). Directed migration of neuronal precursors into the ischemic cerebral cortex and striatum. *Molecular and Cellular Neuroscience*, *24*(1), 171–189. https://doi.org/10.1016/S1044-7431(03)00159-3

Johansson, B. B. (2007). Regeneration and plasticity in the brain and spinal cord. *Journal of Cerebral Blood Flow & Metabolism*, *27*, 1417–1430. https://doi.org/10.1038/sj.jcbfm.9600486

Kadowaki, T., Wilder, E., Klingensmith, J., Zachary, K., & Perrimon, N. (1996). The segment polarity gene porcupine encodes a putative multitransmembrane protein involved in Wingless processing. *Genes & Development*, *10*(24), 3116–3128. https://doi.org/10.1101/gad.10.24.3116

Kaplan, M. S., & Bell, D. H. (1984). Mitotic neuroblasts in the 9-day-old and 11-month-old rodent hippocampus. *The Journal of Neuroscience : The Official Journal of the Society for Neuroscience*, *4*(6), 1429–1441. https://doi.org/10.1523/JNEUROSCI.04-06-01429.1984

Kaplan, M. S., & Hinds, J. W. (1977). Neurogenesis in the adult rat: electron microscopic analysis of light radioautographs. *Science (New York, N.Y.)*, *197*(4308), 1092–1094. Retrieved from http://www.ncbi.nlm.nih.gov/pubmed/887941

Kaslin, J., Ganz, J., Geffarth, M., Grandel, H., Hans, S., & Brand, M. (2009). Stem Cells in the Adult Zebrafish Cerebellum: Initiation and Maintenance of a Novel Stem Cell Niche. *Journal of Neuroscience*, *29*(19), 6142–6153. https://doi.org/10.1523/JNEUROSCI.0072-09.2009

Kim, C.-H., Ueshima, E., Muraoka, O., Tanaka, H., Yeo, S.-Y., Huh, T.-L., & Miki, N. (1996). Zebrafish elav/HuC homologue as a very early neuronal marker. *Neuroscience Letters*, *216*(2), 109–112. https://doi.org/10.1016/0304-3940(96)13021-4

Kirn, J. R., Alvarez-Buylla, A., & Nottebohm, F. (1991). Production and survival of projection neurons in a forebrain vocal center of adult male canaries. *The Journal of Neuroscience : The Official Journal of the Society for Neuroscience*, *11*(6), 1756–1762. https://doi.org/10.1523/JNEUROSCI.11-06-01756.1991

Kirsche, W., & Kirsche, K. (1961). Experimentelle Untersuchungen zur Frage der Regeneration und Funktion des Tectum opticum von Carassius carassius L. *Zeitschrift Fuer Mikroskopisch-Anatomische Forschung*, (67), 140–182.

Kizil, C., Kaslin, J., Kroehne, V., & Brand, M. (2012). Adult neurogenesis and brain regeneration in zebrafish. *Developmental Neurobiology*, *72*(3), 429–461. https://doi.org/10.1002/dneu.20918

Klein, P. S., & Melton, D. A. (1996). A molecular mechanism for the effect of lithium on development. *Proceedings of the National Academy of Sciences of the United States of America*, *93*(16), 8455–8459. https://doi.org/10.1073/PNAS.93.16.8455

Krolewski, R. C., Packard, A., Jang, W., Wildner, H., & Schwob, J. E. (2012). Ascl1 (Mash1)

Knockout Perturbs Differentiation of Nonneuronal Cells in Olfactory Epithelium. *PLoS ONE*, *7*(12), e51737. https://doi.org/10.1371/journal.pone.0051737

Kuhn, H. G., Dickinson-Anson, H., & Gage, F. H. (1996). Neurogenesis in the dentate gyrus of the adult rat: age-related decrease of neuronal progenitor proliferation. *The Journal of Neuroscience : The Official Journal of the Society for Neuroscience*, *16*(6), 2027–2033. https://doi.org/10.1523/JNEUROSCI.16-06-02027.1996

Kuwabara, T., Hsieh, J., Muotri, A., Yeo, G., Warashina, M., Lie, D. C., … Gage, F. H. (2009). Wnt-mediated activation of NeuroD1 and retro-elements during adult neurogenesis. *Nature Neuroscience*, *12*(9), 1097–1105. https://doi.org/10.1038/nn.2360

Leung, C. T., Coulombe, P. A., & Reed, R. R. (2007). Contribution of olfactory neural stem cells to tissue maintenance and regeneration. *Nature Neuroscience*, *10*(6), 720–726. https://doi.org/10.1038/nn1882

Li, Q., Kannan, A., Das, A., Demayo, F. J., Hornsby, P. J., Young, S. L., … Bagchi, I. C. (2013). WNT4 acts downstream of BMP2 and functions via β-catenin signaling pathway to regulate human endometrial stromal cell differentiation. *Endocrinology*, *154*(1), 446–457. https://doi.org/10.1210/en.2012-1585

Lie, D.-C., Colamarino, S. A., Song, H.-J., Désiré, L., Mira, H., Consiglio, A., … Gage, F. H. (2005). Wnt signalling regulates adult hippocampal neurogenesis. *Nature*, *437*(7063), 1370–1375. https://doi.org/10.1038/nature04108

Lisi, S., Botta, R., Lemmi, M., Sellari-Franceschini, S., Altea, M. A., Sisti, E., … Marinò, M. (n.d.). Quercetin decreases proliferation of orbital fibroblasts and their release of hyaluronic acid. *Journal of Endocrinological Investigation*, *34*(7), 521–527. https://doi.org/10.3275/7321

Liu, J., Wu, X., Mitchell, B., Kintner, C., Ding, S., & Schultz, P. G. (2005). A small-molecule agonist of the Wnt signaling pathway. *Angewandte Chemie - International Edition*, *44*(13), 1987–1990. https://doi.org/10.1002/anie.200462552

Liu, Y.-P., Lin, H.-I., & Tzeng, S.-F. (2005). Tumor necrosis factor-α and interleukin-18

modulate neuronal cell fate in embryonic neural progenitor culture. *Brain Research*, *1054*(2), 152–158. https://doi.org/10.1016/j.brainres.2005.06.085

Luskin, M. B. (1993). Restricted proliferation and migration of postnatally generated neurons derived from the forebrain subventricular zone. *Neuron*, *11*(1), 173–189. https://doi.org/10.1016/0896-6273(93)90281-U

Mackay-Sim, A., & Kittel, P. W. (1991). On the Life Span of Olfactory Receptor Neurons. *European Journal of Neuroscience*, *3*(3), 209–215. https://doi.org/10.1111/j.1460-9568.1991.tb00081.x

Manoharan, I., Hong, Y., Suryawanshi, A., Angus-Hill, M. L., Sun, Z., Mellor, A. L., … Manicassamy, S. (2014). TLR2-Dependent Activation of β-Catenin Pathway in Dendritic Cells Induces Regulatory Responses and Attenuates Autoimmune Inflammation. *The Journal of Immunology*, *193*(8), 4203–4213. https://doi.org/10.4049/JIMMUNOL.1400614

Ming, G., & Song, H. (2005). Adult neurogenesis in the mammalian central nervous system. *Annual Review of Neuroscience*, *28*(1), 223–250. https://doi.org/10.1146/annurev.neuro.28.051804.101459

Mira, H., Andreu, Z., Suh, H., Lie, D. C., Jessberger, S., Consiglio, A., … Gage, F. H. (2010). Signaling through BMPR-IA regulates quiescence and long-term activity of neural stem cells in the adult hippocampus. *Cell Stem Cell*, *7*(1), 78–89. https://doi.org/10.1016/j.stem.2010.04.016

Monje, M. L. (2003). Inflammatory Blockade Restores Adult Hippocampal Neurogenesis. *Science*, *302*(5651), 1760–1765. https://doi.org/10.1126/science.1088417

Monti Graziadei, G. A., Karlan, M. S., Bernstein, J. J., & Graziadei, P. P. C. (1980). Reinnervation of the olfactory bulb after section of the olfactory nerve in monkey (Saimiri sciureus). *Brain Research*, *189*(2), 343–354. https://doi.org/10.1016/0006-8993(80)90095-5

Mori, K., Nagao, H., & Yoshihara, Y. (1999). The olfactory bulb: coding and processing of odor

molecule information. *Science (New York, N.Y.)*, *286*(5440), 711–715. https://doi.org/10.1126/SCIENCE.286.5440.711

Moulton, D. G. (1975). Cell renewal in the olfactory epithelium of the mouse. In J. P. Denton, D. A. and Coughlan (Ed.) (Vol. V, pp. 111–114). New York: Academic Press.

Nakashima, A., Katagiri, T., & Tamura, M. (2005). Cross-talk between Wnt and bone morphogenetic protein 2 (BMP-2) signaling in differentiation pathway of C2C12 myoblasts. *The Journal of Biological Chemistry*, *280*(45), 37660–37668. https://doi.org/10.1074/jbc.M504612200

Nakatomi, H., Kuriu, T., Okabe, S., Yamamoto, S., Hatano, O., Kawahara, N., … Nakafuku, M. (2002). Regeneration of hippocampal pyramidal neurons after ischemic brain injury by recruitment of endogenous neural progenitors. *Cell*, *110*(4), 429–441. https://doi.org/10.1016/S0092-8674(02)00862-0

Nelson, W. J., & Nusse, R. (2004). Convergence of Wnt, beta-catenin, and cadherin pathways. *Science (New York, N.Y.)*, *303*(5663), 1483–1487. https://doi.org/10.1126/science.1094291

Packard, A., Lin, B., & Schwob, J. E. (2016). Sox2 and Pax6 Play Counteracting Roles in Regulating Neurogenesis within the Murine Olfactory Epithelium. *PloS One*, *11*(5), e0155167. https://doi.org/10.1371/journal.pone.0155167

Packard, A., Schnittke, N., Romano, R.-A., Sinha, S., & Schwob, J. E. (2011). DeltaNp63 regulates stem cell dynamics in the mammalian olfactory epithelium. *The Journal of Neuroscience : The Official Journal of the Society for Neuroscience*, *31*(24), 8748–8759. https://doi.org/10.1523/JNEUROSCI.0681-11.2011

Park, C. H., Chang, J. Y., Hahm, E. R., Park, S., Kim, H.-K., & Yang, C. H. (2005). Quercetin, a potent inhibitor against β-catenin/Tcf signaling in SW480 colon cancer cells. *Biochemical and Biophysical Research Communications*, *328*(1), 227–234. https://doi.org/10.1016/J.BBRC.2004.12.151

Park, H.-C., & Appel, B. (2003). Delta-Notch signaling regulates oligodendrocyte specification.

Development (Cambridge, England), *130*(16), 3747–3755. https://doi.org/10.1242/DEV.00576

Paton, J. A., & Nottebohm, F. N. (1984). Neurons generated in the adult brain are recruited into functional circuits. *Science (New York, N.Y.)*, *225*(4666), 1046–1048. Retrieved from http://www.ncbi.nlm.nih.gov/pubmed/6474166

Price, J. L. (1990). *Olfactory System. The Human Nervous System* (2nd ed.). New York: Academic Press.

Rakic, P. (2002). Neurogenesis in adult primate neocortex: an evaluation of the evidence. *Nature Reviews Neuroscience*, *3*(1), 65–71. https://doi.org/10.1038/nrn700

Ramon y Cajal, S. (1928). *Degeneration and regeneration of the nervous system. Degeneration and regeneration of the nervous system.* Oxford, England: Clarendon Press.

Reichsman, F., Smith, L., & Cumberledge, S. (1996). Glycosaminoglycans can modulate extracellular localization of the wingless protein and promote signal transduction. *The Journal of Cell Biology*, *135*(3), 819–827. https://doi.org/10.1083/JCB.135.3.819

Richter, W. (1965). Regeneration in the tectum opticum of Leucaspius delineatus (Heckel 1843). *Zeitschrift Fur Mikroskopisch-Anatomische Forschung*, *74*(1), 46–68. Retrieved from http://www.ncbi.nlm.nih.gov/pubmed/5888093

Rijsewijk, F., Schuermann, M., Wagenaar, E., Parren, P., Weigel, D., & Nusse, R. (1987). The Drosophila homolog of the mouse mammary oncogene int-1 is identical to the segment polarity gene wingless. *Cell*, *50*(4), 649–657. https://doi.org/10.1016/0092-8674(87)90038-9

Rock, R. B., Gekker, G., Hu, S., Sheng, W. S., Cheeran, M., Lokensgard, J. R., & Peterson, P. K. (2004). Role of microglia in central nervous system infections. *Clinical Microbiology Reviews*, *17*(4), 942–64, table of contents. https://doi.org/10.1128/CMR.17.4.942-964.2004

Sabogal-Guáqueta, A. M., Muñoz-Manco, J. I., Ramírez-Pineda, J. R., Lamprea-Rodriguez, M., Osorio, E., & Cardona-Gómez, G. P. (2015). The flavonoid quercetin ameliorates

Alzheimer's disease pathology and protects cognitive and emotional function in aged triple transgenic Alzheimer's disease model mice. *Neuropharmacology*, *93*, 134–145. https://doi.org/10.1016/J.NEUROPHARM.2015.01.027

Sakızlı, U. (2018). *The Contribution of Purinergic Signaling to Olfactory Neurogenesis in Zebrafish*. Boğaziçi University.

Saraiva, L. R., Ahuja, G., Ivandic, I., Syed, A. S., Marioni, J. C., Korsching, S. I., & Logan, D. W. (2015). Molecular and neuronal homology between the olfactory systems of zebrafish and mouse. *Scientific Reports*, *5*, 11487. https://doi.org/10.1038/srep11487

Scafidi, J., Hammond, T. R., Scafidi, S., Ritter, J., Jablonska, B., Roncal, M., … Gallo, V. (2014). Intranasal epidermal growth factor treatment rescues neonatal brain injury HHS Public Access. *Nature*, *506*(7487), 230–234. https://doi.org/10.1038/nature12880

Schultz, E. W. (1941). Regeneration of Olfactory Cells. *Experimental Biology and Medicine*, *46*(1), 41–43. https://doi.org/10.3181/00379727-46-11882P

Schwartz Levey, M., Chikaraishi, D. M., & Kauer, J. S. (1991). Characterization of potential precursor populations in the mouse olfactory epithelium using immunocytochemistry and autoradiography. *The Journal of Neuroscience : The Official Journal of the Society for Neuroscience*, *11*(11), 3556–3564. https://doi.org/10.1523/JNEUROSCI.11-11-03556.1991

Schwob, J. E. (2002). Neural regeneration and the peripheral olfactory system. *The Anatomical Record*, *269*(1), 33–49. https://doi.org/10.1002/ar.10047

Schwob, J. E., Jang, W., Holbrook, E. H., Lin, B., Herrick, D. B., Peterson, J. N., & Hewitt Coleman, J. (2017). Stem and progenitor cells of the mammalian olfactory epithelium: Taking poietic license. *Journal of Comparative Neurology*, *525*(4), 1034–1054. https://doi.org/10.1002/cne.24105

Schwob, J. E., Youngentob, S. L., & Mezza, R. C. (1995). Reconstitution of the rat olfactory epithelium after methyl bromide-induced lesion. *The Journal of Comparative Neurology*, *359*(1), 15–37. https://doi.org/10.1002/cne.903590103

Shimizu, N., Kawakami, K., & Ishitani, T. (2012). Visualization and exploration of Tcf/Lef function using a highly responsive Wnt/β-catenin signaling-reporter transgenic zebrafish. *Developmental Biology*, *370*(1), 71–85. https://doi.org/10.1016/J.YDBIO.2012.07.016

Silva-García, O., Valdez-Alarcón, J. J., & Baizabal-Aguirre, V. M. (2014). The Wnt/β-catenin signaling pathway controls the inflammatory response in infections caused by pathogenic bacteria. *Mediators of Inflammation*, *2014*, 310183. https://doi.org/10.1155/2014/310183

Silva, L., & Antunes, A. (2017). Vomeronasal Receptors in Vertebrates and the Evolution of Pheromone Detection. *Annual Review of Animal Biosciences*, *5*(1), 353–370. https://doi.org/10.1146/annurev-animal-022516-022801

Smolich, B. D., McMahon, J. A., McMahon, A. P., & Papkoff, J. (1993). Wnt family proteins are secreted and associated with the cell surface. *Molecular Biology of the Cell*, *4*(12), 1267–1275. Retrieved from http://www.ncbi.nlm.nih.gov/pubmed/8167409

Sohur, U. S., Emsley, J. G., Mitchell, B. D., & Macklis, J. D. (2006). Adult neurogenesis and cellular brain repair with neural progenitors, precursors and stem cells. *Philosophical Transactions of the Royal Society of London. Series B, Biological Sciences*, *361*(1473), 1477–1497. https://doi.org/10.1098/rstb.2006.1887

Song, H.-G., Young Kwon, J., Soo Han, H., Bae, Y.-C., & Moon, C. (2008). First Contact to Odors: Our Current Knowledge about Odorant Receptor. *Sensors*, *8*(10), 6303–6320. https://doi.org/10.3390/s8106303

Sorrells, S. F., Paredes, M. F., Cebrian-Silla, A., Sandoval, K., Qi, D., Kelley, K. W., … Alvarez-Buylla, A. (2018). Human hippocampal neurogenesis drops sharply in children to undetectable levels in adults. *Nature*, *555*(7696), 377–381. https://doi.org/10.1038/nature25975

Tang, X., Falls, D. L., Li, X., Lane, T., & Luskin, M. B. (2007). Antigen-retrieval procedure for bromodeoxyuridine immunolabeling with concurrent labeling of nuclear DNA and antigens damaged by HCl pretreatment. *The Journal of Neuroscience : The Official Journal of the Society for Neuroscience*, *27*(22), 5837–5844. https://doi.org/10.1523/JNEUROSCI.5048-06.2007

Tham, W. W. P., Stevenson, R. J., & Miller, L. A. (2009). The functional role of the medio dorsal thalamic nucleus in olfaction. *Brain Research Reviews*, *62*(1), 109–126. https://doi.org/10.1016/J.BRAINRESREV.2009.09.007

Thompson, M., Nejak-Bowen, K., & Monga, S. P. S. (2011). Crosstalk of the Wnt Signaling Pathway. In *Targeting the Wnt Pathway in Cancer* (pp. 51–80). New York, NY: Springer New York. https://doi.org/10.1007/978-1-4419-8023-6_4

Tran, F. H., & Zheng, J. J. (2017). Modulating the wnt signaling pathway with small molecules. *Protein Science*, *26*(4), 650–661. https://doi.org/10.1002/pro.3122

Tsai, L., & Barnea, G. (2014). A critical period defined by axon-targeting mechanisms in the murine olfactory bulb. *Science (New York, N.Y.)*, *344*(6180), 197–200. https://doi.org/10.1126/science.1248806

Vallières, L., Campbell, I. L., Gage, F. H., & Sawchenko, P. E. (2002). Reduced Hippocampal Neurogenesis in Adult Transgenic Mice with Chronic Astrocytic Production of Interleukin-6. *The Journal of Neuroscience*, *22*(2), 486–492. https://doi.org/10.1523/JNEUROSCI.22-02-00486.2002

van den Heuvel, M., Harryman-Samos, C., Klingensmith, J., Perrimon, N., & Nusse, R. (1993). Mutations in the segment polarity genes wingless and porcupine impair secretion of the wingless protein. *The EMBO Journal*, *12*(13), 5293–5302. Retrieved from http://www.ncbi.nlm.nih.gov/pubmed/8262072

Vénéreau, E., Ceriotti, C., & Bianchi, M. E. (2015). DAMPs from Cell Death to New Life. *Frontiers in Immunology*, *6*, 422. https://doi.org/10.3389/fimmu.2015.00422

Vinod, Jones, D., & Udupa, V. (2016). A simple and effective heat induced antigen retrieval method. *MethodsX*, *3*, 315–319. https://doi.org/10.1016/j.mex.2016.04.001

Vogalis, F., Hegg, C. C., & Lucero, M. T. (2005). Ionic conductances in sustentacular cells of the mouse olfactory epithelium. *The Journal of Physiology*, *562*(3), 785–799. https://doi.org/10.1113/jphysiol.2004.079228

Wan, J., Ramachandran, R., & Goldman, D. (2012). HB-EGF Is Necessary and Sufficient for

Mü ller Glia Dedifferentiation and Retina Regeneration. *Developmental Cell*, *22*, 334–347. https://doi.org/10.1016/j.devcel.2011.11.020

Wan, J., Zhao, X.-F., Vojtek, A., & Goldman, D. (2014). Retinal injury, growth factors, and cytokines converge on β-catenin and pStat3 signaling to stimulate retina regeneration. *Cell Reports*, *9*(1), 285–297. https://doi.org/10.1016/j.celrep.2014.08.048

Wang, Y.-Z., Yamagami, T., Gan, Q., Wang, Y., Zhao, T., Hamad, S., … Zhou, C. J. (2011). Canonical Wnt signaling promotes the proliferation and neurogenesis of peripheral olfactory stem cells during postnatal development and adult regeneration. *Journal of Cell Science*, *124*(9), 1553–1563. https://doi.org/10.1242/jcs.080580

Wehner, D., Tsarouchas, T. M., Michael, A., Haase, C., Weidinger, G., Reimer, M. M., … Becker, C. G. (2017). Wnt signaling controls pro-regenerative Collagen XII in functional spinal cord regeneration in zebrafish. *Nature Communications*, *8*(1), 126. https://doi.org/10.1038/s41467-017-00143-0

Westerfield, M. (1995). *The Zebrafish Book. A Guide for the Laboratory Use of Zebrafish (Danio rerio)* (3rd ed.). Retrieved from https://zfin.org/ZDB-PUB-970327-24

Willert, J., Epping, M., Pollack, J. R., Brown, P. O., & Nusse, R. (2002). A transcriptional response to Wnt protein in human embryonic carcinoma cells. *BMC Developmental Biology*, *2*(1), 8. https://doi.org/10.1186/1471-213X-2-8

Yan, D., Wiesmann, M., Rohan, M., Chan, V., Jefferson, A. B., Guo, L., … Williams, L. T. (2001). Elevated expression of axin2 and hnkd mRNA provides evidence that Wnt/beta -catenin signaling is activated in human colon tumors. *Proceedings of the National Academy of Sciences of the United States of America*, *98*(26), 14973–14978. https://doi.org/10.1073/pnas.261574498

Yiu, G., & He, Z. (2006). Glial inhibition of CNS axon regeneration. *Nature Reviews. Neuroscience*, *7*(8), 617–627. https://doi.org/10.1038/nrn1956

Yoshino, J., & Tochinai, S. (2004). Successful reconstitution of the non-regenerating adult telencephalon by cell transplantation in Xenopus laevis. *Development, Growth and*

Differentiation, *46*(6), 523–534. https://doi.org/10.1111/j.1440-169x.2004.00767.x

Yu, X., Riese, J., Eresh, S., & Bienz, M. (1998). Transcriptional repression due to high levels of Wingless signalling. *The EMBO Journal*, *17*(23), 7021–7032. https://doi.org/10.1093/emboj/17.23.7021

Zhang, L., Cao, Q., Hu, Z., Yan, X., & Wu, B. (2011). Effect of quercetin on neural stem cell proliferation in the subventricular zone of rats after focal cerebral ischemia-reperfusion injury. *Journal of Southern Medical University*, *31*(7), 1200–1203. Retrieved from http://www.ncbi.nlm.nih.gov/pubmed/21764695

Zhang, R. L., Zhang, Z. G., & Chopp, M. (2005). Neurogenesis in the Adult Ischemic Brain: Generation, Migration, Survival, and Restorative Therapy. *The Neuroscientist*, *11*(5), 408–416. https://doi.org/10.1177/1073858405278865

Zhang, R., Oyajobi, B. O., Harris, S. E., Chen, D., Tsao, C., Deng, H.-W., & Zhao, M. (2013). Wnt/β-catenin signaling activates bone morphogenetic protein 2 expression in osteoblasts. *Bone*, *52*(1), 145–156. https://doi.org/10.1016/J.BONE.2012.09.029

Zhao, D., Qin, C., Fan, X., Li, Y., & Gu, B. (2014). Inhibitory effects of quercetin on angiogenesis in larval zebrafish and human umbilical vein endothelial cells. *European Journal of Pharmacology*, *723*, 360–367. https://doi.org/10.1016/j.ejphar.2013.10.069

Zhao, X.-F., Wan, J., Powell, C., Ramachandran, R., Myers, M. G., & Goldman, D. (2014). Leptin and IL-6 Family Cytokines Synergize to Stimulate Müller Glia Reprogramming and Retina Regeneration. *Cell Reports*, *9*(1), 272–284. https://doi.org/10.1016/J.CELREP.2014.08.047

Zupanc, G. K. (2001). Adult neurogenesis and neuronal regeneration in the central nervous system of teleost fish. *Brain, Behavior and Evolution*, *58*(5), 250–275. https://doi.org/10.1159/000057569

Zupanc, G. K. H., & Horschke, I. (1995). Proliferation zones in the brain of adult gymnotiform fish: A quantitative mapping study. *The Journal of Comparative Neurology*, *353*(2), 213–233. https://doi.org/10.1002/cne.903530205

APPENDIX A: EQUIPMENT

Table A.1. List of equipment.

05-090-128 Mini Centrifuges	Fisher Scientific, Korea
-20˚C Freezer	Ugur, Turkey
-20˚C Freezer	Arcelik, Turkey
-86°C ULT Freezer	ThermoForma, USA
Agarose Gel Tank, Mini-Sub Cell GT Cell	BioRad, China
Analytical Balance, ME54	Mettler Toledo, India
Aquatic Habitats	Pentair Aquatic Eco-systems, Inc., USA
Beaker	Isolab, Germany
Brine Shrimp Artemia Cysts (*Artemia franciscana*)	Salt Lake Aquafeed, USA
C1000 Thermal Cycler	Bio-Rad, USA
Capillary glass (1.00 mm x 0.75 mm x 10”)	Sutter Instrument, Co., USA
Centrifuge 5417R	Eppendorf, Germany
Centrifuge 5424	Eppendorf, Germany
Colibri Microvolume spectrometer	Titertek Berthold, Germany
Coplin Staining Jar with Cover	VWR, USA
Cryostat CM3050S	Leica Biosystems, Germany
Dishwasher, Melabor G 7783	Miele, Germany
Dual Intensity Transilluminator	UVP, USA
Electrical Balance	Sartorius, Germany
FemtoJet	Eppendorf, Germany
Filter tips (10, 20, 100, 200, 1000 µl)	Griener Bio-One, Germany
Forceps, FST	Dumont, Switzerland
Gel Doc XR Gel Documentation System	BioRad, China
GELoader tips, 0.5-20 µl	Eppendorf, Germany

Table A.1. List of equipment (cont.).

Glass bottle	Isolab, Germany
Graduate cylinder	Isolab, Germany
Ice Flaker	Brema, Italy
IKA Color Squid magnetic stirrer	IKA works, Inc., USA
Incubated Benchtop Orbital Shaker	Thermo Scientific, USA
Instrument oil, No.29055-00	FST, Switzerland
Laboratory Drying Oven, KD 200	Nüve, Turkey
Magnetic stirrer and heater, RH B 2	IKA workd, Inc., USA
MicroCentrifuge tubes 1.5 ml	Capp ApS, Denmark
Microwave oven	Vestel, Turkey
Orbital Shaker, Rotamax120	Heidolph, Germany
P-97 Micropipette Puller	Sutter Instrument, Co., USA
Parafilm™	Parafilm, USA
PCR® strip Tubes	Axygen, USA
Pellet Pestle Motor	Kimble Kontess, USA
pH-meter, pH315i	WTW, Germany
Refrigerator	Arcelik, Turkey
Rnase-ExitusPlus, A7153,0500	PanReac Applichem, Spain
Serological pipettes (5ml, 10ml, 25ml, 50ml)	Greiner Bio-One, Germany
Shake ‘n’ stack hybridization oven, 6240	Thermo Fisher Scientific, USA
Single channel micropipettes (10, 20, 100, 200, 1000 µl)	Eppendorf, Germany
Sodium Bicarbonate	Aquatic Eco-Systems, Inc., USA
Stemi 2000-C stereomicroscope	Zeiss, Germany
Super PAP Pen	Liquid Blocker, Japan
Superfrost Plus slides	VWR, Germany
Superfrost slides	Thermo Fisher Scientific, USA
Swiftlock Front loading Autoclave	Astell, UK

Table A.1. List of equipment (cont.).

Syngene G:Box Chemi XRQ Chemiluminescence and Fluorescence System	Syngene, UK
Syringe filter, 0.22 µm, 99722	TPP, Switzerland
SZ61 stereomicroscope	Olympus, USA
Tetramin	Tetra, Germany
Tissue-Plus O.C.T compound	Fisher HealthCare, USA
Transcriptor First Strand cDNA Synthesis kit	Roche, Germany
U-100 Insulin Syringes (0.5 ml)	BD Medical, Becton, Dickinson, Co., USA
Universal Incubator	Binder, Germany
Vortex-Genie 2	Scientific Industries, Inc., USA
Waving platform shaker, Polymax 2040	Heidolph, Germany
Whetstone	Dan’s Whetstone Campany,Inc., USA

APPENDIX B: SUPPLIES

Table B.1. List of supplies.

1 kb DNA ladder	New England Biolabs, U.S.A. (N3232)
100 bp DNA ladder	New England Biolabs, U.S.A. (N3231)
5-Bromo-2'-Deoxyuridine BioChemica	AppliChem, Germany (A2139,0005)
6X Loading Dye	New England Biolabs, U.S.A (B7021S)
Agarose Universal PeqGOLD	VWR, USA
Alexa Fluor® 488	Life Technologies, U.S.A.
Alexa Fluor® 555	Life Technologies, U.S.A.
Anti mouse-HuC/D antibody	Life Technologies, U.S.A. (1661237)
Anti mouse-β-catenin antibody	BD Biosciences, U.S.A. (610154)
Anti rat-BrdU antibody	Abcam, UK (AB90484)
Bovine Serum Albumine (BSA)	New England Biolabs, U.S.A. (B9001)
Chloroform	Sigma-Aldrich, Germany (288306-1L)
Dimethyl Sulphoxide (DMSO) Hybri-Max®	Sigma-Aldrich, U.S.A. (D2650 -100 ml)
Dithiothreitol (DTT)	Sigma-Aldrich, Germany (10197777001)
Ethanol Absolute	Sigma-Aldrich, U.S.A. (34870)
Ethidium bromide	Sigma Life Sciences, U.S.A. (E1510-1 ml)
Hydrogen Chloride	Merck Millipore, U.S.A. (K48446817 644)
iCRT14	Sigma-Aldrich, U.S.A. (SML0203-5MG)
IWR-1	Sigma-Aldrich, U.S.A. (I061-5MG)
Lithium Chloride	Sigma-Aldrich, U.S.A. (L9650-500G)
MS-222 (Ethyl 3-aminobenzoate methanesulfonate salt)	Sigma-Aldrich, U.S.A. (A5040-25G)
Onetaq® DNA polymerase	New England Biolabs, U.S.A (M0480L)
Paraformaldehyde	Sigma-Aldrich, U.S.A. (P6148 – 1 kg)
Phenol Red	AppliChem, U.S.A. ((A7615,01001)
Potassium Chloride	Sigma-Aldrich, U.S.A. (P9541)

Table B.1. List of supplies (cont.).

Potassium phosphate monobasic	Fisher Scientific, U.S.A. (BP362-500)
Quercetin	Sigma-Aldrich, U.S.A. (Q4951-10G)
Sodium Chloride	Sigma-Aldrich, U.S.A. (S7653 - 1 kg)
Sodium citrate tribasic dihydrate	Sigma-Aldrich, U.S.A. (C8532 – 1 kg)
Sodium Hydroxide	Sigma-Aldrich, U.S.A. (S8045 - 1 kg)
Sodium phosophate dibasic	Sigma-Aldrich, U.S.A. (S7907 – 1 kg)
Triton X-100	AppliChem, Germany (A4975,0100)
TRIzol™ Reagent	Life Technologies, U.S.A. (84703)
Tween® 20	VWR, USA (437082Q)
Wnt Agonist (CAS853220-52-7)	Santa Cruz Biotechnology, U.S.A.

APPENDIX C: RAW DATA OF BRDU INCORPORATION ASSAY

Table C.1. Cell counts of BrdU-positive cells in PBS Control OE.

		Radial Index												
		0.5	1.5	2.5	3.5	4.5	5.5	6.5	7.5	8.5	9.5	total	ILC	sensory
FISH 1	section 1	5.5	1.5	2	1	0.5	0.5	1	6.5	5.5	3	**27**	**7**	**5.5**
		2	0	1	1	0.5	2.5	6	5.5	5.5	4	**28**	**2**	**5**
		0.5	1.5	1	0	3	5	10	3	8.5	4.5	**37**	**2**	**10.5**
		2	3	0	1	1.5	1	3.5	6	7	1	**26**	**5**	**6.5**
		5.5	1.5	0	2.5	3	1	4.5	6.5	5.5	8	**38**	**7**	**8**
		2.5	1.5	3	0.5	4	1.5	5.5	6.5	4	6	**35**	**4**	**10.5**
	section 2	10.5	2	0.5	2	1	8	15	11.5	6	3.5	**60**	**12.5**	**13.5**
		6	3.5	5	4.5	2	10.5	15	6.5	7.5	6.5	**67**	**9.5**	**25.5**
		9	3	0	2.5	1.5	6	10	9	15.5	7.5	**64**	**12**	**13**
		6	5	3	1	4	5	8.5	6.5	8	6	**53**	**11**	**18**
		10	4	0	2.5	6	9	13	6.5	7.5	5.5	**64**	**14**	**21.5**
		4.5	4	0.5	0.5	1.5	5	15	9	10.5	11.5	**62**	**8.5**	**11.5**
	section 3	1	0	0.5	0.5	0	6	6	9.5	9.5	2	**35**	**1**	**7**
		2	0	1	0	0	5.5	6	9.5	11.5	1.5	**37**	**2**	**6.5**
		0	2	2.5	1.5	0	3.5	10.5	9.5	5	4.5	**39**	**2**	**9.5**
		3	2	0	0.5	0.5	0	7.5	6	5	5.5	**30**	**5**	**3**
		3.5	3.5	1	0	2	2.5	5	7.5	6	9	**40**	**7**	**9**
		1	0	0	5	1	0	8	7	9.5	6.5	**38**	**1**	**6**
FISH 2	section 4	9	1	0	0.5	0.5	5	8.5	6.5	11	4	**46**	**10**	**7**
		10	1	0	1.5	2	2.5	8	9	7	0	**41**	**11**	**7**
		6.5	1.5	1	0	0	1	1	5.5	9.5	5	**31**	**8**	**3.5**
		5.5	1.5	0	0	0.5	4.5	9	8.5	4	7.5	**41**	**7**	**6.5**
		8	0	1	2	0	1	6.5	10	9.5	5	**43**	**8**	**4**
		6.5	0.5	1	0	1	3	4	2	6	3	**27**	**7**	**5.5**
	section 5	2.5	2	2.5	0	2.5	0.5	2	1	0	4	**17**	**4.5**	**7.5**
		4	4	0	0	1	2	1	0	1	4	**17**	**8**	**7**
		4	1	0	0	2	1	0.5	4	2.5	1	**16**	**5**	**4**
		9.5	3.5	3	3	1	2	3	0	4.5	1.5	**31**	**13**	**12.5**
		5	2	1.5	2	1.5	2	6.5	7.5	6.5	7.5	**42**	**7**	**9**
		4	3	0.5	2.5	0	2	2	3.5	7	3.5	**28**	**7**	**8**
	section 6	5	3	0	1	2	1	8.5	11	3.5	4	**39**	**8**	**7**
		7	2	0	1	1.5	6	7.5	6.5	3.5	4	**39**	**9**	**10.5**
		7.5	4	1	0.5	0.5	5	13	3.5	12.5	7.5	**55**	**11.5**	**11**
		4.5	5.5	0	1	0	1.5	1.5	1	5	1	**21**	**10**	**8**
		6	0	0	0	2	7	4.5	4.5	2.5	3.5	**30**	**6**	**9**
		7.5	2.5	1	3	3.5	11	2.5	4	6.5	7.5	**49**	**10**	**21**
FISH 3	section 7	13	0	1	1	2.5	3	6.5	8	2	6	**43**	**13**	**7.5**
		10	0	0	5.5	1	4	9.5	9.5	0.5	1	**41**	**10**	**10.5**
		7	1	1	0	1	0	11.5	8.5	0	3	**33**	**8**	**3**
		2.5	1.5	0	0.5	0.5	1	5	6.5	8.5	4	**30**	**4**	**3.5**
		9	0	2	0	1	0.5	7.5	12	10.5	5.5	**48**	**9**	**3.5**
		11.5	1.5	0	0	1	5.5	2.5	11	5	2	**40**	**13**	**8**
	section 8	5	2	0	2	0	4.5	11.5	4.5	2.5	2	**34**	**7**	**8.5**
		4	3	0	2	0	2	13.5	5.5	4	3	**37**	**7**	**7**
		11.5	0.5	2	2.5	5.5	1	11	3	1	3	**41**	**12**	**11.5**
		6.5	3.5	0	2.5	2.5	4.5	3.5	2	6	1	**32**	**10**	**13**
		12	0	0	0	0	0	13	6	2	6	**39**	**12**	**0**
		12	0	0.5	2.5	1.5	2	3.5	12.5	10.5	1	**46**	**12**	**6.5**
	section 9	11.5	1.5	2.5	4.5	2	6	11.5	2.5	3.5	0.5	**46**	**13**	**16.5**
		13	1	1	1.5	4.5	7.5	13.5	7	4	6	**59**	**14**	**15.5**
		13	3	2	1	5.5	7.5	15	7.5	1.5	4	**60**	**16**	**19**
		9	6.5	0.5	2.5	0.5	5	5	19.5	4.5	10	**63**	**15.5**	**15**
		9.5	2.5	0.5	1	2	2.5	7	15	8.5	3.5	**52**	**12**	**8.5**
		11	4	2.5	0.5	4	3	9	3.5	6.5	3	**47**	**15**	**14**
	AVRG	6.62037	1.990741	0.907407	1.37037	1.638889	3.518519	7.388889	6.740741	5.935185	4.333333	**40.44444**	**8.611111**	**9.425926**
	SEM	0.488014	0.213361	0.148768	0.186194	0.207216	0.371287	0.566053	0.499612	0.458693	0.343467	**1.700009**	**0.524546**	**0.691588**

Table C.2. Cell counts of BrdU-positive cells in LiCl-treated OE.

		Radial Index												
		0.5	1.5	2.5	3.5	4.5	5.5	6.5	7.5	8.5	9.5	total	ILC	sensory
FISH 1	section 1	9	1	2.5	4	5.5	7.5	8	15.5	16.5	4.5	74	10	20.5
		4	5	4	2	3	3	5.5	8.5	6.5	1.5	43	9	17
		1.5	3.5	2.5	2	4	5.5	12.5	11.5	13	3	59	5	17.5
		10	4.5	4.5	1.5	6	8	10.5	11	10.5	1.5	68	14.5	24.5
		10	1.5	2.5	5.5	4.5	13.5	4	13	7.5	2	64	11.5	27.5
		10.5	6	3	6	8	13	13	13	6.5	5	84	16.5	36
	section 2	16.5	4.5	0	0.5	1.5	10	12	10.5	11.5	6	73	21	16.5
		11.5	1.5	2	3	2	9.5	12.5	17	5.5	9.5	74	13	18
		15.5	3.5	3	3	8	16.5	20	19.5	21	14	124	19	34
		10.5	9	2.5	1	1	8.5	9	6	9.5	0	57	19.5	22
		10.5	11.5	4	0	1.5	3	7.5	10	17	1	66	22	20
		11.5	4.5	3.5	4.5	2	7.5	7.5	20	15	9	85	16	22
	section 3	10.5	7	2	4.5	7.5	11	10	14	8.5	4	79	17.5	32
		12	7.5	4	2.5	5	13	9.5	12	14.5	11	91	19.5	32
		12.5	9	9	4.5	7.5	14	17.5	15.5	16.5	5	111	21.5	44
		8	10.5	7	1	2.5	7.5	9	9	12	4.5	71	18.5	28.5
		18.5	17	5	2.5	10	9	13	9	10.5	2.5	97	35.5	43.5
		12.5	22.5	5	4.5	5	13	10.5	7.5	20	5.5	106	35	50
FISH 2	section 4	6.5	5.5	6	3	0	3.5	10.5	7.5	0.5	1	44	12	18
		4	3	3	3	2	10	3	0	2.5	2.5	33	7	21
		5.5	3	5	5.5	7	14.5	4.5	3	1	4	53	8.5	35
		7	8.5	13.5	10.5	9.5	10	8	1	0	0	68	15.5	52
		8	11.5	5.5	4	1.5	9	6.5	2	0	0	48	19.5	31.5
		7	10.5	2.5	2	4	3.5	6.5	1	0	0	37	17.5	22.5
	section 5	6	11.5	11	9	2.5	5.5	12.5	11	3	3	75	17.5	39.5
		11	5	1.5	2	3	11	5.5	1	1	0	41	16	22.5
		11.5	3.5	3	5	9.5	14	4	1	2.5	3	57	15	35
		4.5	7	14.5	6	7.5	9.5	5	0.5	1.5	0	56	11.5	44.5
		7.5	9	2	6	7	4.5	7	2	3.5	3.5	52	16.5	28.5
		16	13.5	8	3.5	5	6	5.5	5	1.5	1	65	29.5	36
	section 6	10.5	15	7	10	3.5	7	6.5	8	2.5	3	73	25.5	42.5
		11.5	11.5	3.5	5.5	7	7.5	2.5	1	3.5	1.5	55	23	35
		7	9	4.5	8.5	10.5	6.5	3	2	6	4	61	16	39
		3.5	11.5	8.5	7.5	6.5	7.5	1	1	5	0	52	15	41.5
		4.5	10.5	4	8	7	5	4.5	0.5	0	0	44	15	34.5
		5.5	14	3.5	2	9	11.5	5	0.5	0	1	52	19.5	40
FISH 3	section 7	7	9	10	9.5	7	12	7	3.5	3.5	2.5	71	16	47.5
		9	9	9	9	10	12	7	1	0.5	0.5	67	18	49
		2.5	11.5	5.5	9	14	8	2	0.5	2	0	55	14	48
		5.5	6.5	4.5	6	8	5.5	1	1	3.5	2.5	44	12	30.5
		4	5	11.5	9.5	6.5	5	2.5	2	2.5	1.5	50	9	37.5
		5	13	9.5	6.5	8.5	10	8	4.5	1.5	0.5	67	18	47.5
	section 8	4.5	2	1.5	2	2	3.5	9	8.5	2.5	1.5	37	6.5	11
		5	1	1	2	2	3.5	5.5	7.5	5.5	2	35	6	9.5
		10	4	1	1	3.5	10.5	16.5	10.5	3.5	4.5	65	14	20
		6.5	1.5	1.5	3	4	5.5	10.5	6	11	3.5	53	8	15.5
		5	0	2	2	0	2	9	15	3	5	43	5	6
		10.5	2.5	1.5	2.5	2	0.5	11.5	10	14.5	1.5	57	13	9
	section 9	0	1	1	0	3	2.5	9	4.5	6	4	31	1	7.5
		3	7.5	3.5	6	2.5	5	2.5	1	0	0	31	10.5	24.5
		5	2	3	0	1	7.5	7.5	15.5	15.5	14	71	7	13.5
		1.5	2.5	0.5	0.5	2	1	2	4.5	4.5	2	21	4	6.5
		2	2	0	0	0.5	3	2	6.5	7.5	5.5	29	4	5.5
		3.5	1.5	1.5	1.5	0	1	8	5	3	7	32	5	5.5
	AVRG	7.805556	6.925926	4.453704	4.138889	4.87037	7.722222	7.648148	6.990741	6.407407	3.240741	60.2037	14.73148	28.11111
	SEM	0.555311	0.647276	0.458547	0.400706	0.440606	0.532977	0.56529	0.754558	0.785682	0.445165	2.87155	0.973475	1.795946

Table C.3. Cell counts of BrdU-positive cells in CAS853220-52-7-treated OE.

		Radial Index												
		0.5	**1.5**	**2.5**	**3.5**	**4.5**	**5.5**	**6.5**	**7.5**	**8.5**	**9.5**	**total**	**ILC**	**sensory**
FISH 1	**section 1**	7	3.5	2.5	3	1	2	1.5	2.5	6	2	**31**	**10.5**	**12**
		5	5	1.5	1.5	1	0	2.5	11	9.5	2	**39**	**10**	**9**
		2.5	0.5	0	0	0	0	0.5	7.5	4.5	3.5	**19**	**3**	**0.5**
		5.5	6	2	3.5	1.5	7	11.5	14	6.5	3.5	**61**	**11.5**	**20**
		9.5	5.5	0	1	0	1.5	8.5	16	14.5	5.5	**62**	**15**	**8**
		8.5	0.5	3.5	3.5	4	7.5	6.5	8.5	5	2.5	**50**	**9**	**19**
	section 2	14.5	10.5	5	5.5	6.5	8.5	11	11.5	10	5	**88**	**25**	**36**
		10	11.5	2	3	6.5	8	16	8	8	8	**81**	**21.5**	**31**
		9	13	3	9.5	6	16.5	18.5	5.5	10	1	**92**	**22**	**48**
		13	15	3	6.5	9	11.5	9.5	6.5	7.5	3.5	**85**	**28**	**45**
		13.5	4.5	2	11.5	12	9.5	8.5	9	7.5	5	**83**	**18**	**39.5**
		12	8.5	1	3.5	4	12	12.5	6.5	4.5	0.5	**65**	**20.5**	**29**
	section 3	9.5	10.5	7	3	5	9	16	10	11	2	**83**	**20**	**34.5**
		16	10.5	2	3.5	13.5	26.5	18	17	4	2	**113**	**26.5**	**56**
		19	14.5	7.5	7.5	8.5	10.5	7	7.5	3.5	1.5	**87**	**33.5**	**48.5**
		12.5	12	7	6.5	3	15	16	11.5	4.5	8	**96**	**24.5**	**43.5**
		25	8	8	6.5	15	10.5	22	20	7	8	**130**	**33**	**48**
		10.5	12	6.5	6.5	4	12.5	25.5	12	8.5	2	**100**	**22.5**	**41.5**
FISH 2	**section 4**	8.5	10.5	7	1.5	9	14.5	15	10.5	5.5	4	**86**	**19**	**42.5**
		9.5	12	4	5.5	7.5	16.5	18.5	11	9.5	5	**99**	**21.5**	**45.5**
		11.5	9.5	5	2.5	5	18	13	7	11	2.5	**85**	**21**	**40**
		19	15	5.5	5.5	9	17.5	13.5	10	10	4	**109**	**34**	**52.5**
		12.5	11.5	7.5	4.5	7	11.5	18	12.5	13	10	**108**	**24**	**42**
		11	18.5	4.5	6	7	20	15.5	12	2	8.5	**105**	**29.5**	**56**
	section 5	4.5	3.5	2	1	4	3	7.5	16	6	3.5	**51**	**8**	**13.5**
		7.5	4.5	2	5.5	2	0.5	11.5	10.5	11.5	9.5	**65**	**12**	**14.5**
		5	5.5	4.5	1	6	7.5	13	18	7.5	5	**73**	**10.5**	**24.5**
		6.5	7.5	2	2.5	1.5	2.5	8.5	10.5	7.5	3	**52**	**14**	**16**
		6	4.5	0.5	0	0	1	13.5	12	7	2.5	**47**	**10.5**	**6**
		6.5	2.5	0	1.5	1.5	0.5	4.5	10	11	7	**45**	**9**	**6**
	section 6	7	1.5	0.5	2	5.5	3	12.5	11	8.5	3.5	**55**	**8.5**	**12.5**
		14	3	2.5	3	4	9.5	28.5	19	11.5	6	**101**	**17**	**22**
		9.5	4.5	0	4	4	2.5	17	11	12.5	7	**72**	**14**	**15**
		5	6	6	2	2	11	11	11	3.5	4.5	**62**	**11**	**27**
		4	2.5	3	2.5	1	4.5	13.5	10	11	10	**62**	**6.5**	**13.5**
		3	2.5	3	0.5	0	5.5	14	9	14.5	5	**57**	**5.5**	**11.5**
FISH 3	**section 7**	8	6	4	3.5	1.5	1.5	10	1.5	4.5	8.5	**49**	**14**	**16.5**
		7	2.5	3.5	0	2	2.5	7	4.5	3.5	2.5	**35**	**9.5**	**10.5**
		10.5	4.5	2.5	3	0.5	2.5	12.5	14.5	1.5	3	**55**	**15**	**13**
		9	4	0.5	2	1.5	3	4.5	7	2.5	1	**35**	**13**	**11**
		8	8.5	1.5	0.5	2	6	9	5.5	2.5	2.5	**46**	**16.5**	**18.5**
		11.5	8.5	1	0	1.5	6	6.5	8.5	6	1.5	**51**	**20**	**17**
	section 8	10	4	3.5	1.5	3	5.5	1.5	0	4	2	**35**	**14**	**17.5**
		12	7.5	0.5	1	3	7	6	0	1	1	**39**	**19.5**	**19**
		6	8	6	6	1	6	11.5	2.5	0.5	1.5	**49**	**14**	**27**
		3.5	3.5	2	1.5	1.5	2	1.5	4	2.5	2	**24**	**7**	**10.5**
		11.5	3	2.5	1	3	8	4.5	3	7	4.5	**48**	**14.5**	**17.5**
		4	7.5	0.5	0	4	4	4	12.5	5	0.5	**42**	**11.5**	**16**
	section 9	6.5	5.5	0	1	1	1	3	2	3	2	**25**	**12**	**8.5**
		5.5	4.5	1	0	2	7	4	1	3.5	1.5	**30**	**10**	**14.5**
		5.5	4.5	0	6	1.5	3	8.5	9.5	3.5	2	**44**	**10**	**15**
		5	4.5	3.5	1.5	5.5	2	2.5	4.5	4.5	5.5	**39**	**9.5**	**17**
		13	3.5	0.5	0	3	9	5	0.5	3.5	0	**38**	**16.5**	**16**
		2.5	8.5	3.5	1.5	5.5	7	5	5	6.5	1	**46**	**11**	**26**
	AVRG	9.111111	6.944444	2.953704	3.083333	4.064815	7.407407	10.49074	8.916667	6.666667	3.861111	**63.5**	**16.05556**	**24.4537**
	SEM	0.602872	0.553494	0.311328	0.350815	0.463342	0.783825	0.839023	0.660043	0.47934	0.357991	**3.60876**	**1.001257**	**2.012191**

Table C.4. Cell counts of BrdU-positive cells in iCRT14-treated OE.

		Radial Index												
		0.5	1.5	2.5	3.5	4.5	5.5	6.5	7.5	8.5	9.5	total	ILC	sensory
FISH 1	section 1	8.5	0.5	0	0	3	3	5	12	11.5	4.5	48	9	6.5
		10	2	1.5	1.5	0.5	5.5	10.5	10	5.5	1	48	12	11
		4.5	9.5	0	1	1.5	11	6	2	1.5	4	41	14	23
		11	4	3.5	0.5	0	4	11.5	14	5.5	2	56	15	12
		7.5	4.5	4	0	3	2	5.5	11	11	2.5	51	12	13.5
		4.5	4	0.5	1	0	1.5	6.5	9	12	0	39	8.5	7
	section 2	2	4	0	1	3.5	1	12	7	6.5	8	45	6	9.5
		0.5	2.5	0.5	1.5	1	1	8	6	5	5	31	3	6.5
		3	0	2	0.5	0.5	0	3	5	6	4	24	3	3
		0.5	0.5	1	1.5	4	1.5	5.5	2.5	4.5	5.5	27	1	8.5
		1.5	0.5	0	1	2	3	0.5	6.5	4.5	3.5	23	2	6.5
		0.5	0.5	0	0	0	3	3	8	4	3	22	1	3.5
	section 3	7	8	5	8.5	9.5	10.5	5	5	4.5	3	66	15	41.5
		5	5	7	2	2.5	9	7.5	5	11.5	7.5	62	10	25.5
		6	2	2	0	0	5.5	9.5	5.5	7.5	1	39	8	9.5
		5	5	1	1	2.5	8	11	9	9.5	9	61	10	17.5
		9	2	0	3	0	8	9.5	10.5	14.5	7.5	64	11	13
		3	2	0	2	3.5	7	9.5	4	7	4	42	5	14.5
FISH 2	section 4	6	3	0	0	1	3.5	0.5	4.5	4.5	6	29	9	7.5
		2.5	2.5	2	0	0	4.5	4.5	5	10	4	35	5	9
		3	8	2.5	2.5	0	1	3.5	0.5	3	3	27	11	14
		4.5	1.5	1	2.5	1.5	4.5	12.5	5	2	3	38	6	11
		8.5	3.5	1	0	2	5	5.5	6.5	7	12	51	12	11.5
		4	0	1.5	0.5	2	4	5.5	3.5	2	1	24	4	8
	section 5	6.5	7	0.5	2.5	0	7.5	11.5	8	10	6.5	60	13.5	17.5
		6	6.5	1.5	1	1.5	5	4.5	9	6	6	47	12.5	15.5
		4.5	2.5	2	0	0	2	3.5	8	7	4.5	34	7	6.5
		11	3.5	2.5	1	2	14.5	8	11.5	13	3	70	14.5	23.5
		9	2	4	1.5	3	10.5	11.5	11	9	7.5	69	11	21
		7.5	5	2	2.5	0	4	10	6	6.5	3.5	47	12.5	13.5
	section 6	9.5	1.5	1	0	1	1	4	5.5	3	2.5	29	11	4.5
		2.5	2.5	0	0	2	4	7	5	2	0	25	5	8.5
		11	2	1	0	0	2.5	1.5	1	1	0	20	13	5.5
		7	1	1	1	0	2	3	6	3.5	3.5	28	8	5
		6	3	1	1	0	1	3	9	7	3	34	9	6
		3.5	4.5	0	0	0	1.5	4	9	4	0.5	27	8	6
FISH 3	section 7	2.5	2.5	5.5	1.5	0	1	4.5	5	2.5	0	25	5	10.5
		4.5	7	1.5	1	0.5	4.5	11.5	7	5.5	1	44	11.5	14.5
		3.5	5.5	1.5	1.5	2	7.5	7	3.5	2	3	37	9	18
		2	2	7	2	1	0	1	0	1	0	16	4	12
		3	5.5	3	1.5	1.5	1.5	9	2	0.5	0.5	28	8.5	13
		6	2	3.5	0.5	-0.5	2	8.5	1	0	1	24	8	7.5
	section 8	3.5	3.5	0	0	0.5	1.5	3	2.5	2.5	2	19	7	5.5
		5.5	3.5	0	1	0	3	6	2	6	3	30	9	7.5
		4	4.5	0.5	0	2	2.5	3.5	1.5	2.5	0	21	8.5	9.5
		3	1	1	0	0.5	1.5	6.5	3	4.5	7	28	4	4
		6	2	2	1	0.5	2	3.5	7	4.5	2.5	31	8	7.5
		6	7.5	1.5	2.5	1.5	3.5	6.5	3.5	6	5.5	44	13.5	16.5
	section 9	7	1	0	0	3	2	7.5	9	3.5	2	35	8	6
		5	0	1	0	1.5	2.5	12	10.5	5.5	5	43	5	5
		5	3	1	1	0	3.5	11	5.5	2	2	34	8	8.5
		3.5	1.5	1	1	4	3.5	1	6.5	10.5	2.5	35	5	11
		9.5	4.5	0	1	2	4	4	12.5	6.5	5	49	14	11.5
		3.5	2.5	2	0	0.5	3	4	2.5	3.5	3.5	25	6	8
	AVRG	5.268519	3.240741	1.564815	1.064815	1.361111	3.916667	6.342593	6.12037	5.583333	3.518519	37.98148	8.509259	11.14815
	SEM	0.372382	0.305623	0.229453	0.180518	0.224302	0.414656	0.456966	0.457736	0.463842	0.351355	1.892968	0.501796	0.905859

Table C.5. Cell counts of BrdU-positive cells in PBS intact OE.

		Radial Index												
		0.5	**1.5**	**2.5**	**3.5**	**4.5**	**5.5**	**6.5**	**7.5**	**8.5**	**9.5**	**total**	**ILC**	**sensory**
FISH 1	**section 1**	2	0	0	1	4.5	2.5	3	10	5.5	4.5	**33**	**2**	**8**
		5.5	2.5	1.5	4	4	9.5	2.5	7	8	3.5	**48**	**8**	**21.5**
		2	0	1	3.5	3	7	5	7	11	5.5	**45**	**2**	**14.5**
		13	8.5	3.5	3.5	0.5	6	3.5	10.5	7.5	2.5	**59**	**21.5**	**22**
		4.5	1.5	1.5	2	2.5	4	5.5	12.5	15	7	**56**	**6**	**11.5**
		3.5	6	1.5	2.5	6.5	4.5	15	12	9	8.5	**69**	**9.5**	**21**
	section 2	6	2	4	3	5.5	8	4.5	9	4.5	3.5	**50**	**8**	**22.5**
		3	0	0	0	4	3.5	8	11	8.5	3	**41**	**3**	**7.5**
		6	1	0	2.5	2.5	5	12	13.5	14.5	3	**60**	**7**	**11**
		6.5	3.5	1	1	4.5	5.5	5	7.5	9	1.5	**45**	**10**	**15.5**
		8.5	2.5	1.5	4.5	2.5	9	3.5	12	17.5	5.5	**67**	**11**	**20**
		5	3.5	0.5	1	4.5	3	4.5	6.5	9.5	6	**44**	**8.5**	**12.5**
	section 3	5	0	0	2	5	7	8.5	8	8.5	1	**45**	**5**	**14**
		6	1	1	2.5	1.5	2	10.5	7.5	11	5	**48**	**7**	**8**
		14.5	3.5	6	4	5	3.5	6.5	7	4.5	0.5	**55**	**18**	**22**
		10	1	0	3	2.5	7	7	11.5	6	1	**49**	**11**	**13.5**
		11	4	1	1.5	2.5	6	5.5	8	12.5	11	**63**	**15**	**15**
		3.5	3	2.5	2	5	4	6	15	7.5	1.5	**50**	**6.5**	**16.5**
FISH 2	**section 4**	12	7	0	1	0	2	8.5	4	8.5	3	**46**	**19**	**10**
		10	4	1	0.5	3.5	1.5	9	2.5	3.5	1.5	**37**	**14**	**10.5**
		20.5	7.5	1	2.5	1.5	0.5	13	12.5	4	1	**64**	**28**	**13**
		20.5	10	1	1	0.5	1.5	4	15.5	2	0	**56**	**30.5**	**14**
		15.5	2.5	0	0	1	0.5	17	7.5	3	3	**50**	**18**	**4**
		20	8.5	0.5	0	0	0	5	4	2	0	**40**	**28.5**	**9**
	section 5	10	12	0	0	0	3.5	4	5	8.5	5	**48**	**22**	**15.5**
		21	2	0.5	4.5	1	6.5	8.5	12	5	5	**66**	**23**	**14.5**
		8.5	16.5	1	0	2	2	7.5	2.5	3	1	**44**	**25**	**21.5**
		7	4	1	0	2	2.5	10	10	1.5	5	**43**	**11**	**9.5**
		4.5	2.5	0	2	2	1	3	6	7	1	**29**	**7**	**7.5**
		15.5	4.5	2	0	1	2.5	5.5	6.5	0.5	2	**40**	**20**	**10**
	section 6	5.5	13.5	0	3	4.5	8.5	10	13	7	1	**66**	**19**	**29.5**
		15	6.5	0.5	0	1	7.5	9	8	4	1.5	**53**	**21.5**	**15.5**
		19.5	15.5	0	0	2	6	5	6	3	0	**57**	**35**	**23.5**
		7.5	7.5	2	0	0	1.5	5.5	11	1	0	**36**	**15**	**11**
		12.5	10.5	0	1	0	2	8.5	19.5	6	1	**61**	**23**	**13.5**
		17	5	1.5	1.5	4	1	10.5	5.5	2	0	**48**	**22**	**13**
FISH 3	**section 7**	15	2	2	0	0	0	11	4	4	1	**39**	**17**	**4**
		12.5	1.5	0	0	2	1	13	4	3	1	**38**	**14**	**4.5**
		8	1	1	1	2.5	4	16	8	5	5.5	**52**	**9**	**9.5**
		10	0	1	0	1	2	10	6.5	6	1.5	**38**	**10**	**4**
		11.5	3.5	1	0	0	0	9	5.5	1.5	2	**34**	**15**	**4.5**
		4	4	0	3	1	2	10.5	7	1.5	3	**36**	**8**	**10**
	section 8	19	0	3	3	4	2	15	3.5	6.5	7	**63**	**19**	**12**
		17.5	0.5	2	0.5	1.5	5.5	12	2.5	4	4	**50**	**18**	**10**
		6	13	0	1	0	-0.5	8	3.5	3.5	3.5	**38**	**19**	**13.5**
		5	1	2	0	0	3	7	5	7.5	1.5	**32**	**6**	**6**
		13	4.5	0.5	0	3.5	6	12	11	4.5	1	**56**	**17.5**	**14.5**
		15	3	1	0	0	7.5	14.5	2	1	1	**45**	**18**	**11.5**
	section 9	15.5	1.5	2	2	0	0.5	19.5	6	2	3	**52**	**17**	**6**
		13.5	1.5	2	0	1	4	11	1.5	7	1.5	**43**	**15**	**8.5**
		10	0	1	0	0	1	12	5.5	6.5	1	**37**	**10**	**2**
		9	5	0	0	0	0.5	2.5	2	2	1	**22**	**14**	**5.5**
		8.5	6.5	0	0	0	2	11.5	7.5	4	4	**44**	**15**	**8.5**
		7.5	7.5	1	0	0	3	9	8.5	5	0.5	**42**	**15**	**11.5**
	AVRG	10.33333	4.425926	1.074074	1.314815	2.009259	3.537037	8.574074	7.777778	5.842593	2.740741	**47.62963**	**14.75926**	**12.36111**
	SEM	0.724593	0.560381	0.157901	0.191242	0.248276	0.358096	0.542028	0.524873	0.505597	0.320146	**1.429**	**1.002033**	**0.79159**

Table C.6. Cell counts of BrdU-positive cells in PBS damaged OE.

		Radial Index												
		0.5	**1.5**	**2.5**	**3.5**	**4.5**	**5.5**	**6.5**	**7.5**	**8.5**	**9.5**	**total**	**ILC**	**sensory**
FISH 1	**section 1**	1.5	2.5	1	5	1	0	0.5	0.5	2	1	**15**	**4**	**9.5**
		0	3	3	0.5	0.5	7	0.5	0.5	0.5	2.5	**18**	**3**	**14**
		0	18	25	11	2	2.5	2.5	8.5	5	8.5	**83**	**18**	**58.5**
		9	8	6.5	7	6.5	5	3.5	8	8.5	2	**64**	**17**	**33**
		8	7	6	4	14.5	5.5	10	3	10	1	**69**	**15**	**37**
		8.5	11.5	7	13.5	11.5	12.5	11.5	4.5	6	14.5	**101**	**20**	**56**
	section 2	3.5	2.5	6	5	3	4.5	1	3	0.5	2	**31**	**6**	**21**
		3	4	4	3.5	4	4.5	6	3.5	1.5	3	**37**	**7**	**20**
		6.5	3.5	10	13.5	9	3.5	9.5	6.5	4	7	**73**	**10**	**39.5**
		3.5	8.5	4.5	4	4.5	7.5	8.5	6	3	1	**51**	**12**	**29**
		2	7	5.5	3	8	1.5	11.5	5	4.5	4	**52**	**9**	**25**
		6.5	13	12.5	6	11	3.5	9.5	9.5	6	2.5	**80**	**19.5**	**46**
	section 3	3	2	2.5	9	5.5	5	3	2	4.5	1.5	**38**	**5**	**24**
		4	0.5	4.5	4.5	3.5	6	4	4.5	4.5	8	**44**	**4.5**	**19**
		1.5	4.5	3	1	1	2	0	1	1.5	3.5	**19**	**6**	**11.5**
		9	8.5	6	6.5	10.5	5	11.5	6.5	6.5	4	**74**	**17.5**	**36.5**
		8.5	9	13.5	11	4.5	4.5	11.5	3.5	7	1	**74**	**17.5**	**42.5**
		10.5	1.5	4	6.5	10.5	14	5	2.5	8	1.5	**64**	**12**	**36.5**
FISH 2	**section 4**	9.5	6.5	5	4.5	3.5	8	9.5	9	9.5	5	**70**	**16**	**27.5**
		5.5	2.5	4	5	2	5	7	7.5	2.5	6	**47**	**8**	**18.5**
		6.5	10.5	3.5	7.5	3	6.5	6.5	8	4.5	9.5	**66**	**17**	**31**
		3.5	6.5	5.5	3	7	7	4.5	7	0	1	**45**	**10**	**29**
		2	6	7	4	2.5	9.5	9.5	6.5	4	6	**57**	**8**	**29**
		11	4.5	8	2.5	1.5	6.5	5	7	1.5	4.5	**52**	**15.5**	**23**
	section 5	3	3.5	4	4	7	6	8	3	5.5	4	**48**	**6.5**	**24.5**
		4	6	3	5.5	4.5	5	10	10	6	6	**60**	**10**	**24**
		2	10	2.5	3.5	1.5	6.5	6	6	9	10	**57**	**12**	**24**
		2.5	1.5	2	9.5	5	1.5	2	7	4	6	**41**	**4**	**19.5**
		4.5	2.5	1	1	4	2.5	1.5	0	1.5	4.5	**23**	**7**	**11**
		4.5	4	4.5	2	1.5	3.5	7	6	4	5	**42**	**8.5**	**15.5**
	section 6	7	6	3	3	2.5	2	3	2	3	3.5	**35**	**13**	**16.5**
		9	14	10	8	5	6	2.5	2.5	2.5	3.5	**63**	**23**	**43**
		10.5	11	12.5	6.5	9.5	5	7	2	10	5	**79**	**21.5**	**44.5**
		12.5	10.5	15	11.5	11.5	8.5	7.5	6	6	5	**94**	**23**	**57**
		5.5	11	13	6.5	5	3.5	4	5	11.5	3	**68**	**16.5**	**39**
		5	10.5	8.5	8.5	9	6.5	8.5	5	5.5	3	**70**	**15.5**	**43**
FISH 3	**section 7**	5.5	3.5	7.5	9.5	10	13	3	3.5	4.5	9	**69**	**9**	**43.5**
		4	11.5	6.5	4.5	7.5	14.5	6.5	3.5	3.5	2	**64**	**15.5**	**44.5**
		9.5	8	5	3.5	14	18.5	7.5	10	4.5	2.5	**83**	**17.5**	**49**
		9	2	1	6	9	3.5	3	1.5	5.5	3.5	**44**	**11**	**21.5**
		5.5	4	5.5	7.5	9	6.5	0	1.5	9	5.5	**54**	**9.5**	**32.5**
		7	3.5	6.5	11	5	10	2.5	5.5	3.5	8.5	**63**	**10.5**	**36**
	section 8	11.5	9.5	5.5	4.5	8.5	12	7	1.5	4.5	3.5	**68**	**21**	**40**
		8	9.5	5.5	5.5	10	13	7.5	3.5	5.5	2	**70**	**17.5**	**43.5**
		9	9	1.5	0.5	6	10	12	3	3	3	**57**	**18**	**27**
		18	6.5	7.5	5	8	4	5	2	1	6	**63**	**24.5**	**31**
		9.5	8	8	7.5	6.5	7	6.5	0.5	0.5	6	**60**	**17.5**	**37**
		6	2	2.5	8.5	6	3	2	4.5	7	1.5	**43**	**8**	**22**
	section 9	9.5	16	4	6.5	6	7	5.5	4	4	2.5	**65**	**25.5**	**39.5**
		11.5	3.5	3	1.5	8	4.5	7	4	2	6	**51**	**15**	**20.5**
		13	11	3	0	5	9	7	0	4	2	**54**	**24**	**28**
		11	9	5.5	6.5	12.5	8.5	1	0	2	1	**57**	**20**	**42**
		5	9.5	10.5	7.5	11.5	8.5	9.5	2	4.5	3.5	**72**	**14.5**	**47.5**
		14	8.5	11	2.5	11.5	14.5	8	3.5	2.5	5	**81**	**22.5**	**48**
	AVRG	6.722222	6.962963	6.222222	5.712963	6.490741	6.666667	5.907407	4.296296	4.537037	4.296296	**57.81481**	**13.68519**	**32.05556**
	SEM	0.516309	0.537013	0.575665	0.437171	0.491088	0.521486	0.457762	0.369099	0.365911	0.372797	**2.48522**	**0.822908**	**1.659897**

Table C.7. Cell counts of BrdU-positive cells in iCRT14 intact OE.

		Radial Index												
		0.5	**1.5**	**2.5**	**3.5**	**4.5**	**5.5**	**6.5**	**7.5**	**8.5**	**9.5**	**total**	**ILC**	**sensory**
FISH 1	**section 1**	13.5	2.5	5.5	4.5	11.5	13	9	8	4	8.5	**80**	**16**	**37**
		6	2	2	3	3.5	3	6.5	11.5	10.5	6	**54**	**8**	**13.5**
		3.5	3.5	3	2.5	5	6.5	5.5	12.5	12	5	**59**	**7**	**20.5**
		10.5	1.5	1	2.5	3.5	7	8	7	9.5	1.5	**52**	**12**	**15.5**
		14	3	1	3.5	2.5	4.5	10	15	11.5	6	**71**	**17**	**14.5**
		11	0	3	2.5	3	7	8.5	6.5	6	2.5	**50**	**11**	**15.5**
	section 2	8.5	4.5	2	3.5	5.5	9.5	11.5	9.5	6	3.5	**64**	**13**	**25**
		9.5	1.5	1	2	5	5	8	5	11.5	5.5	**54**	**11**	**14.5**
		11	2	0	1	5	6	9	3.5	7.5	4	**49**	**13**	**14**
		6	0	0	3	8.5	10.5	8	13.5	10.5	3	**63**	**6**	**22**
		4.5	1.5	3.5	3.5	4.5	9.5	12	7.5	5.5	16	**68**	**6**	**22.5**
		5	2	4.5	4	2.5	5	7	8	2.5	2.5	**43**	**7**	**18**
	section 3	11.5	0.5	6	4.5	3	4.5	8.5	9.5	7.5	4.5	**60**	**12**	**18.5**
		3	2	1.5	2.5	8	6.5	4.5	11.5	5.5	6	**51**	**5**	**20.5**
		2	2	0	2	1	4.5	3	7.5	6	6	**34**	**4**	**9.5**
		5.5	2.5	0	3	4.5	9.5	12	15.5	9	13.5	**75**	**8**	**19.5**
		4	3.5	2.5	2	1.5	7	5	10	5	2.5	**43**	**7.5**	**16.5**
		4	1	0	2	3.5	4.5	3.5	7	6.5	3	**35**	**5**	**11**
FISH 2	**section 4**	4	2	1	3	0.5	4.5	6	25.5	11.5	6	**64**	**6**	**11**
		6	3	0	2	3	5	6.5	21.5	13	2	**62**	**9**	**13**
		0	0	0	3	2	3.5	7.5	5	4	0	**25**	**0**	**8.5**
		5	5	0	2.5	4.5	7	5.5	16	17.5	4	**67**	**10**	**19**
		3	0	2	2	5.5	4.5	8	16	9	3	**53**	**3**	**14**
		18	0	0	0	2	3	5.5	18.5	6.5	5.5	**59**	**18**	**5**
	section 5	4	1	1	1	1.5	2.5	3	11	9.5	5.5	**40**	**5**	**7**
		1	0	1	2	2.5	0.5	5	13.5	4	2.5	**32**	**1**	**6**
		1	0	1	0	4.5	8.5	4	7.5	1.5	1	**29**	**1**	**14**
		7.5	4.5	1.5	1.5	1.5	5.5	7	3	21	7	**60**	**12**	**14.5**
		1	0.5	1.5	0.5	3	1.5	2	9	11	1	**31**	**1.5**	**7**
		3	0	0	1.5	4.5	5.5	3	8	4.5	4	**34**	**3**	**11.5**
	section 6	5.5	4.5	0	1	1	3	10	11.5	10.5	9	**56**	**10**	**9.5**
		2	1	0	3	4.5	4.5	5	12.5	11.5	0	**44**	**3**	**13**
		4	0	1	2	4	2	9.5	9.5	3	2	**37**	**4**	**9**
		3	2	0	2	7	7	3.5	14.5	15	1	**55**	**5**	**18**
		4	0	2	3.5	5	4.5	12	17	8	4	**60**	**4**	**15**
		12	1	0	0	2	2	4	10	10	2	**43**	**13**	**5**
FISH 3	**section 7**	16	11	6	5	4	3	12	14.5	12	7.5	**91**	**27**	**29**
		13	4	1.5	1	2.5	1	5.5	12.5	10	2	**53**	**17**	**10**
		11.5	0.5	0	2	3.5	5.5	5	11	3.5	0.5	**43**	**12**	**11.5**
		5.5	3.5	1	4	3.5	5.5	13	10	5	1	**52**	**9**	**17.5**
		13.5	5.5	2	2	1	2	9	5	2.5	3.5	**46**	**19**	**12.5**
		8.5	8.5	1	1.5	2.5	0	6.5	16	9.5	2	**56**	**17**	**13.5**
	section 8	16.5	5	3.5	2	6.5	5.5	8.5	10.5	4.5	9.5	**72**	**21.5**	**22.5**
		5	6	1	3.5	3.5	2	4	9	7	2	**43**	**11**	**16**
		10	2.5	2	2.5	4	3	9.5	7.5	6	0	**47**	**12.5**	**14**
		5.5	4.5	0	2.5	1	5	7.5	10.5	1.5	2	**40**	**10**	**13**
		11	7	2	0	2	2.5	7	12	4.5	3	**51**	**18**	**13.5**
		7	4	3	2	0	1.5	8	9.5	4	1	**40**	**11**	**10.5**
	section 9	11	9	1.5	3.5	0	1.5	5.5	13.5	6.5	1	**53**	**20**	**15.5**
		7.5	4.5	4	0.5	1.5	2	11.5	8.5	8	2	**50**	**12**	**12.5**
		6	3	0	1.5	3.5	5	17	8.5	9.5	6	**60**	**9**	**13**
		11.5	6.5	0.5	0.5	0	3	4	10	6	3	**45**	**18**	**10.5**
		12	8	1	1	0	2	7.5	10.5	10	3	**55**	**20**	**12**
		15	8	2	2	0	2	12.5	14	9.5	7	**72**	**23**	**14**
	AVRG	7.462963	2.981481	1.490741	2.203704	3.314815	4.62037	7.407407	10.94444	7.907407	3.981481	**52.31481**	**10.44444**	**14.61111**
	SEM	0.611371	0.363351	0.212556	0.162773	0.309125	0.364757	0.422911	0.578339	0.529169	0.430324	**1.822513**	**0.841591**	**0.783562**

Table C.8. Cell counts of BrdU-positive cells in iCRT14 damaged OE.

		Radial Index												
		0.5	1.5	2.5	3.5	4.5	5.5	6.5	7.5	8.5	9.5	total	ILC	sensory
FISH 1	section 1	2	7	6	4	2.5	4.5	9.5	1	3.5	1	41	9	24
		2	3.5	3	3	3	2	7	7	3.5	7	41	5.5	14.5
		2.5	9	2	6.5	2.5	1.5	7	8	5	2	46	11.5	21.5
		4.5	2.5	3	4	3	5	1.5	5	6.5	3	38	7	17.5
		1.5	5	3.5	1	6	0	2	3	1	1	24	6.5	15.5
		1.5	4.5	4	4	4	2.5	5.5	4	1	2	33	6	19
	section 2	4	4.5	4.5	5	4.5	1	2.5	6.5	3.5	2	38	8.5	19.5
		1.5	3.5	4.5	3.5	3	4.5	6	4	3	6.5	40	5	19
		2	3.5	9.5	5	4.5	1.5	9	8	3.5	4.5	51	5.5	24
		4	4	3	3.5	1	2	3.5	3	4	1	29	8	13.5
		2	3.5	5.5	2	6.5	6.5	2.5	2.5	1	2	34	5.5	24
		3	2	5	5.5	2.5	5.5	8	4.5	7.5	2.5	46	5	20.5
	section 3	4	2	0	1	4.5	4	1.5	2	2	0	21	6	11.5
		1	7	5.5	7	6	3.5	2	9	7	5	53	8	29
		1	8.5	4.5	4	0	0	0	1	1	1	21	9.5	17
		6.5	0.5	4.5	4.5	2	2	7	4.5	1	5.5	38	7	13.5
		3.5	3	4.5	3	1.5	5.5	2.5	5.5	3	2	34	6.5	17.5
		6.5	8.5	3	0	2	4	4	7.5	4.5	6	46	15	17.5
FISH 2	section 4	2.5	8	6.5	8.5	5	9.5	3	5.5	7	4.5	60	10.5	37.5
		2.5	2.5	9	9.5	5.5	5.5	3.5	5	2.5	3.5	49	5	32
		3.5	8	7.5	1	4.5	6.5	4	4	4.5	2.5	46	11.5	27.5
		4	3.5	2.5	8.5	8.5	13.5	14.5	3	3	4	65	7.5	36.5
		2	3	3.5	2.5	3.5	2.5	1.5	4.5	9	3	35	5	15
		1	2	7.5	8.5	4.5	11	5	4	6.5	6	56	3	33.5
	section 5	5.5	7	4.5	3.5	4.5	2.5	6.5	5	8	7	54	12.5	22
		3	9	7	5	3	9.5	7.5	5	7	6	62	12	33.5
		2.5	3.5	7	6	3	4.5	5.5	3.5	5	5.5	46	6	24
		2	2	3	0.5	5	7.5	7	1	6.5	7.5	42	4	18
		6	1	6	7	2	4.5	5	6.5	5.5	2.5	46	7	20.5
		3	2.5	1.5	12	4	5.5	2.5	2.5	2.5	5	41	5.5	25.5
	section 6	8.5	8	1.5	0	2	1	10	6.5	6.5	3	47	16.5	12.5
		7	2	8	6.5	4.5	5.5	10.5	5.5	5	10.5	65	9	26.5
		2.5	2.5	2	3.5	2	3	11	7.5	9.5	5.5	49	5	13
		6.5	9.5	1.5	10.5	9	18.5	8	18.5	11	5	98	16	49
		3.5	5.5	6	18	15.5	26	13.5	10	5.5	4.5	108	9	71
		0.5	2.5	1	2.5	6	17	4.5	0.5	2.5	13	50	3	29
FISH 3	section 7	5	5	5	2.5	6.5	1	1	2	0	0	28	10	20
		2	6	3	6	4	3	3.5	5.5	5	3	41	8	22
		2	4.5	2.5	2	7	6.5	4.5	5.5	4.5	1	40	6.5	22.5
		2.5	7.5	5	0.5	2	7.5	8.5	5	4.5	0	43	10	22.5
		2.5	9.5	1	1	3	4	8	1	0	2	32	12	18.5
		6.5	13.5	4	4.5	6.5	4	2.5	3.5	3.5	1.5	50	20	32.5
	section 8	3.5	5.5	2	2	5	3	2	2	3	1	29	9	17.5
		4.5	9.5	7.5	2.5	1.5	6	1.5	1	2.5	0.5	37	14	27
		2	6	5.5	2.5	0	5	2	2	0.5	3.5	29	8	19
		7.5	2.5	2	2.5	1.5	2.5	8	8	4	2.5	41	10	11
		2	5	1	2	6.5	8.5	3.5	1.5	0	0	30	7	23
		8	1.5	11.5	8.5	4.5	3.5	8	3.5	3.5	2.5	55	9.5	29.5
	section 9	3	0.5	6.5	4	1	3	2	1	3	2	26	3.5	15
		4.5	13	6	2	0.5	5.5	4.5	3.5	7.5	5	52	17.5	27
		3	3	3	1.5	2	9	5.5	4.5	4.5	3	39	6	18.5
		4.5	7.5	7	3	0	4	5	5	1.5	1.5	39	12	21.5
		2.5	3.5	4	2	2	0	1	0	1	2	18	6	11.5
		9.5	8	5.5	7	4	5.5	12	3.5	2	1	58	17.5	30
	AVRG	3.592593	5.101852	4.5	4.37037	3.861111	5.37963	5.314815	4.481481	4.055556	3.416667	44.07407	8.694444	23.21296
	SEM	0.283301	0.412714	0.325789	0.453455	0.357032	0.637335	0.4593	0.410126	0.346615	0.353977	2.175725	0.532454	1.356638

Table C.9. Cell counts of BrdU-positive cells in DMSO intact OE.

		Radial Index												
		0.5	1.5	2.5	3.5	4.5	5.5	6.5	7.5	8.5	9.5	total	ILC	sensory
FISH 1	section 1	8.5	0.5	0	1	0.5	2	6	1.5	1.5	0.5	**22**	**9**	**4**
		4	0	0	0	0	4.5	10	4.5	3.5	0.5	**27**	**4**	**4.5**
		6.5	0.5	0	2.5	1.5	2	14	7	7	5	**46**	**7**	**6.5**
		11	2	0	0	1.5	0.5	1.5	3	2.5	0	**22**	**13**	**4**
		8	0	0	1	0	3.5	7	3.5	4	0	**27**	**8**	**4.5**
		6.5	3.5	0	1	1	7	6	7.5	4.5	4	**41**	**10**	**12.5**
	section 2	7	0	0	1	1	3	10	3	1.5	2.5	**29**	**7**	**5**
		12	3	0	1	0	2.5	5	5	3	3.5	**35**	**15**	**6.5**
		4	1	0	0	1	1.5	15	1.5	3	1	**28**	**5**	**3.5**
		8	0	0	0	0	0.5	2.5	4.5	2.5	0	**18**	**8**	**0.5**
		6	0	1	2.5	0.5	4	4.5	5.5	3	2	**29**	**6**	**8**
		3	1	0	0	1	3	3	4.5	1.5	0	**17**	**4**	**5**
	section 3	6	1	1	1	0	1.5	12.5	7.5	2.5	2	**35**	**7**	**4.5**
		8.5	0.5	2	0	0	0.5	6	5	1.5	0	**24**	**9**	**3**
		6.5	0.5	0	0	0	1.5	8.5	4	0.5	0.5	**22**	**7**	**2**
		8	1.5	0.5	0	0	1	4.5	6.5	2.5	0.5	**25**	**9.5**	**3**
		11.5	2	1.5	1	0	2	0.5	5	3.5	1	**28**	**13.5**	**6.5**
		14	1	1	1	1	7.5	9	5.5	3	1	**44**	**15**	**11.5**
FISH 2	section 4	8	6	0	1	0.5	5	10.5	6	3.5	2.5	**43**	**14**	**12.5**
		10	1.5	1.5	0	0	1	4	12	3	4	**37**	**11.5**	**4**
		11.5	2	0.5	0	1	2.5	4.5	5.5	4.5	2	**34**	**13.5**	**6**
		6	0	1	1.5	1.5	2	5	3	1.5	0.5	**22**	**6**	**6**
		6	0	0	3	4	4.5	9	8	2.5	1	**38**	**6**	**11.5**
		9.5	2.5	1	6	1.5	3	7	14	6	1.5	**52**	**12**	**14**
	section 5	8	2	0	0	0	4	6	1	4	2	**27**	**10**	**6**
		15	2.5	1	2.5	2.5	3.5	4	7	6	1	**45**	**17.5**	**12**
		8.5	2	0.5	0.5	1	5	9	8	4	4.5	**43**	**10.5**	**9**
		10	1	0.5	3.5	1.5	0.5	1	4	3	1	**26**	**11**	**7**
		10.5	0.5	0.5	0.5	1	2.5	9	7	6.5	1	**39**	**11**	**5**
		12.5	4.5	1.5	2.5	4	1.5	8	9.5	3	3	**50**	**17**	**14**
	section 6	7	1	0	0	1	3	12	5	1	1	**31**	**8**	**5**
		14.5	0.5	2.5	1	3	2	3	7.5	3.5	3.5	**41**	**15**	**9**
		18.5	6	1.5	0	0.5	2	2	8	3.5	0	**42**	**24.5**	**10**
		9.5	2.5	2	1.5	1.5	2	4.5	3.5	3	2	**32**	**12**	**9.5**
		20	3	2	1	2	3.5	8.5	9	2	1	**52**	**23**	**11.5**
		9	4	1	1	2	1	14	8	6	1	**47**	**13**	**9**
FISH 3	section 7	5.5	0.5	0	1	1	2	2	0.5	2	1.5	**16**	**6**	**4.5**
		5.5	0.5	0	0	0	2	1.5	8.5	5.5	10.5	**34**	**6**	**2.5**
		4.5	1.5	0	1	0	0	1	4.5	6.5	2	**21**	**6**	**2.5**
		8.5	0.5	0	0.5	0.5	1	1	3	3.5	1.5	**20**	**9**	**2.5**
		1	0	1	1	1	1	5	6	4	3	**23**	**1**	**4**
		1	0	0	2	1	0	1.5	1.5	5	3	**15**	**1**	**3**
	section 8	6.5	0.5	0	2	1	0	1	5	3.5	0.5	**20**	**7**	**3.5**
		4	0	0	0	0	1	1.5	3.5	2	2	**14**	**4**	**1**
		3.5	0.5	0	1	1	2	2.5	2.5	2	3	**18**	**4**	**4.5**
		4	1	0.5	1.5	0	1	2	5.5	3	0.5	**19**	**5**	**4**
		6	0	3	1	1	1	1.5	6.5	9	1	**30**	**6**	**6**
		2.5	0.5	2	1	1.5	0.5	1.5	5	6.5	2	**23**	**3**	**5.5**
	section 9	11	3	0	1.5	1.5	0.5	3.5	7	4	1	**33**	**14**	**6.5**
		4.5	0.5	0	0	0	1	3	4	8	2	**23**	**5**	**1.5**
		9	0	0	0	0	0	2	3	1	0	**15**	**9**	**0**
		7	1	1	1	0	2	1	6	2	1	**22**	**8**	**5**
		1	0	0	1	1	1	0.5	8.5	4	6	**23**	**1**	**3**
		3	1	3	1	4	1	1	5	6	1	**26**	**4**	**10**
	AVRG	7.796296	1.305556	0.638889	1.018519	0.962963	2.101852	5.175926	5.481481	3.611111	1.814815	**29.90741**	**9.101852**	**6.027778**
	SEM	0.543151	0.197036	0.113717	0.14928	0.139106	0.223906	0.53386	0.354996	0.251084	0.246476	**1.40479**	**0.674641**	**0.477802**

Table C.10. Cell counts of BrdU-positive cells in DMSO damaged OE.

		Radial Index												
		0.5	1.5	2.5	3.5	4.5	5.5	6.5	7.5	8.5	9.5	total	ILC	sensory
FISH 1	section 1	6.5	3	1	1	2.5	1	0	0	1	2	18	9.5	8.5
		1	3.5	1.5	0	2.5	4	1.5	0	0	1	15	4.5	11.5
		2	3.5	5	0.5	2	3	3	1	1	0	21	5.5	14
		2.5	5.5	4.5	2	0.5	7.5	2.5	0	2.5	3.5	31	8	20
		6	7.5	3.5	4	2	3.5	1.5	2	2	1	33	13.5	20.5
		5.5	5.5	4	3	2	4	2	0	2	0	28	11	18.5
	section 2	9.5	4	0.5	0.5	3	2.5	2	1	0	0	23	13.5	10.5
		4	4.5	1.5	0	0	1	0	0	0	1	12	8.5	7
		3.5	3.5	2.5	1.5	1	3.5	3.5	0.5	1	0.5	21	7	12
		7	6	3	4	6.5	1.5	13.5	0.5	0	0	42	13	21
		5.5	4	0.5	1.5	2.5	9	8.5	0.5	1	0	33	9.5	17.5
		3.5	6	2.5	1.5	1.5	6	6.5	2.5	4.5	1.5	36	9.5	17.5
	section 3	8	0	3	1.5	0.5	4	0	0	0	1	18	8	9
		6.5	6	2.5	0	0	0	0	0	0	1	16	12.5	8.5
		7.5	8	1.5	1.5	3.5	4.5	0.5	1	0.5	0.5	29	15.5	19
		4.5	7	9.5	0.5	7	4	4.5	0	3	0	40	11.5	28
		4.5	6	4	3	4.5	3	9	0	1	0	35	10.5	20.5
		7	8	3.5	1.5	6	5.5	7.5	3	1	1	44	15	24.5
FISH 2	section 4	1	2.5	1.5	1	0	0	2.5	0.5	3.5	4.5	17	3.5	5
		2	0.5	4.5	0.5	2.5	0	0	0	4.5	2.5	17	2.5	8
		5.5	4.5	2	1.5	2.5	2	2.5	0.5	3	4	28	10	12.5
		7.5	5	6.5	0	5	2	4	0	0	1	31	12.5	18.5
		4	6.5	7	0.5	1	1	1	0	1	0	22	10.5	16
		6.5	7.5	8	2.5	4	3	4	7.5	2	4	49	14	25
	section 5	1	8	7	0	2	1	0.5	2.5	0.5	1.5	24	9	18
		3.5	9	5.5	2	2	5	1	0	1	1	30	12.5	23.5
		4	6	7	2	2.5	8	3.5	0	0	1	34	10	25.5
		5.5	6.5	3	1	0	1	2	0	0	0	19	12	11.5
		3.5	7	2.5	1	3	1	1.5	2.5	2	0	24	10.5	14.5
		3.5	8	7	3.5	8	2.5	2.5	1	1.5	2.5	40	11.5	29
	section 6	1	3	5	3.5	0.5	1	0	0.5	0.5	0	15	4	13
		2.5	5	2.5	0	0	1	2	0.5	1.5	0	15	7.5	8.5
		5	12.5	5.5	2	2.5	0.5	0	2.5	0.5	0	31	17.5	23
		5	7	5	1	5.5	2.5	0.5	1.5	2	1	31	12	21
		8	5.5	2.5	1	1.5	1.5	0.5	3.5	3	0	27	13.5	12
		2.5	6.5	5	0	0.5	0.5	0	0	0	0	15	9	12.5
FISH 3	section 7	5	1.5	0.5	2	2	4.5	5.5	3	2	3	29	6.5	10.5
		5.5	4.5	0	0	1	3.5	0.5	0	0	2	17	10	9
		5	6	5	1	0	1	6	1	0	0	25	11	13
		9	3	2	2	0	3	5	3.5	0.5	1	29	12	10
		5.5	1	1	3.5	1	3	5	1	1.5	1.5	24	6.5	9.5
		4.5	3.5	0	0.5	3.5	1.5	2.5	0	0	1	17	8	9
	section 8	4	4	2	1	2	3	1	4.5	2	1.5	25	8	12
		11	6	3.5	5	3	1.5	1	3.5	1.5	3	39	17	19
		3	3	2.5	3	3.5	2.5	4.5	1	2.5	2.5	28	6	14.5
		9.5	4.5	0.5	2	2.5	1	0	2.5	3.5	1	27	14	10.5
		3	3	3	0	1.5	2.5	0	1	2	1	17	6	10
		4	3.5	2.5	1	2	4	3	0	1	2	23	7.5	13
	section 9	3	8.5	3	4	6	3	3	8	4.5	2	45	11.5	24.5
		8.5	5	3.5	2	2.5	0.5	3.5	5.5	1	3	35	13.5	13.5
		8.5	5	0.5	1.5	0.5	3.5	3	4.5	1	5	33	13.5	11
		10	8	2	4.5	3.5	3.5	2.5	4	2	0	40	18	21.5
		8.5	0.5	1	1	2	1.5	0.5	2	0	4	21	9	6
		8	1.5	1.5	0.5	1.5	1	2	0.5	1.5	1	19	9.5	6
	AVRG	5.212963	5.074074	3.240741	1.574074	2.37963	2.685185	2.638889	1.490741	1.361111	1.324074	26.98148	10.28704	14.9537
	SEM	0.34061	0.329038	0.297953	0.176853	0.258907	0.268453	0.36534	0.257431	0.169935	0.18246	1.219832	0.471332	0.831713

Table C.11. Cell counts of BrdU-positive cells in IWR-1 intact OE.

		Radial Index												
		0.5	1.5	2.5	3.5	4.5	5.5	6.5	7.5	8.5	9.5	total	ILC	sensory
FISH 1	section 1	10	1	3	3	2	2.5	6.5	12.5	15.5	14	70	11	11.5
		5	1	2	1.5	2.5	3.5	6.5	6	8.5	5.5	42	6	10.5
		6	2	0	3	1	1	4	7.5	11.5	9	45	8	7
		12.5	2.5	5	1	2.5	2	2.5	8	9	4	49	15	13
		4	1	0	2	4	3	3	5.5	4.5	5	32	5	10
		8	5	0	3	3	2.5	4.5	3.5	2.5	7	39	13	13.5
	section 2	11	2	1.5	2.5	2	3	2.5	3	3.5	5	36	13	11
		16	1.5	3.5	5.5	1.5	5	3.5	4.5	9	11	61	17.5	17
		18	5.5	2.5	2	5	4.5	2	3	9.5	9	61	23.5	19.5
		10	3	2	3	1.5	3	4.5	3.5	3	2.5	36	13	12.5
		8	6	5	2	4.5	3	3	4.5	10.5	6.5	53	14	20.5
		14.5	2.5	0	0	1	2.5	8.5	2	7.5	8.5	47	17	6
	section 3	5.5	3.5	3.5	1.5	2	1.5	4	8.5	5	6	41	9	12
		5.5	2.5	3	2	2	0	9	9	8.5	4.5	46	8	9.5
		16.5	6.5	3.5	3.5	2	3	1.5	5.5	5.5	8.5	56	23	18.5
		12	2.5	4.5	1.5	4	2.5	4	10	5.5	2.5	49	14.5	15
		14	2	2	0	5.5	4.5	0.5	3.5	2	1	35	16	14
		9.5	4.5	0	1.5	3.5	3	4.5	4	4	9.5	44	14	12.5
FISH 2	section 4	6	3	0	0	0	0	0	0	9	5	23	9	3
		3	0	0	1	0	1	0	7	5.5	2.5	20	3	2
		4	0	0	0	0	0	1	1.5	7	3.5	17	4	0
		2	0	0	0	0	0	0	2	9	8	21	2	0
		0	0	0	0	0	0	0	1	7.5	4.5	13	0	0
		1	0	0	0	0	0	1	1.5	7.5	4	15	1	0
	section 5	6	0	0	0	0	0	0	0	2.5	6.5	15	6	0
		5	1	0	0	0	0	1	1.5	4.5	1	14	6	1
		5	1	0	0	0	0	0	1.5	2	1.5	11	6	1
		5	0	0	0	0	0	0	0	4.5	5.5	15	5	0
		7	0	1	1	0	1	0	0	14.5	4.5	29	7	3
		6	0	0	0	0	0	0	1	3.5	6.5	17	6	0
	section 6	7	0	0	0	0	1	0	0	5.5	3.5	17	7	1
		4	3	0	1	0	0	0	0	7	5	20	7	4
		5	1	0	0	0	0	1	1	4.5	2.5	15	6	1
		9	1	0	1	0	0	0	5.5	9.5	8	34	10	2
		8	2	0	0	0	0	1	2	3	3	19	10	2
		5	1	0	0	0	1	0.5	6	3	4.5	21	6	2
FISH 3	section 7	2	0	0	0	0	1	1	2	5.5	0.5	12	2	1
		2	0	1	0	1	1	1	2	4	2	14	2	3
		7.5	1.5	0	0	1	1	1.5	3	5	1.5	22	9	3.5
		2	0	0	2	1	1	0	5	4	3	18	2	4
		2	0	1	0	2	0	4	5.5	2.5	3	20	2	3
		5	10	0	0	1	1.5	1.5	3	8.5	1.5	32	15	12.5
	section 8	5.5	1.5	0	0	0	1.5	4	1.5	3	1	18	7	3
		7	0	0	2	0	0	1.5	1	1.5	0	13	7	2
		3	0	1	3	1	0	1	1.5	7	2.5	20	3	5
		6	2	0	2	3	1	3	4	2	2	25	8	8
		7	1	0	0	0.5	3	0.5	2	1	1	16	8	4.5
		6	4	1	1	1	1	5	4.5	5.5	3	32	10	8
	section 9	4	2	0	1	0	0	0	0	2	0	9	6	3
		13	0	0	-0.5	1.5	0	0	4	1	4	23	13	1
		6	0	0	0	1	1	0	3	1	1	13	6	2
		5	0	2	0	0.5	0.5	0	2.5	1.5	0	12	5	3
		12	1	0	1	1	0	0	1	5	2	23	13	3
		5.5	3.5	0	0	0.5	1.5	1	1.5	3.5	2	19	9	5.5
	AVRG	6.935185	1.740741	0.888889	1	1.212963	1.277778	1.944444	3.37963	5.518519	4.231481	28.12963	8.675926	6.12037
	SEM	0.551536	0.27677	0.195836	0.170732	0.196245	0.18779	0.306443	0.380179	0.448279	0.412367	2.06696	0.708821	0.781839

Table C.12. Cell counts of BrdU-positive cells in IWR-1 damaged OE.

		Radial Index												
		0.5	1.5	2.5	3.5	4.5	5.5	6.5	7.5	8.5	9.5	total	ILC	sensory
FISH 1	section 1	0	3	4.5	7.5	8.5	3.5	12	7	11.5	3.5	**61**	**3**	**27**
		0	4	4.5	5	6	6.5	12	8	11	11	**68**	**4**	**26**
		2	3.5	1.5	5	3.5	7.5	11.5	8.5	4.5	3.5	**51**	**5.5**	**21**
		3	0.5	5	1.5	2.5	2	4.5	4	5	3	**31**	**3.5**	**11.5**
		5	3	0	2	0	1	1	6	6.5	10.5	**35**	**8**	**6**
		5.5	1.5	1.5	0.5	10.5	0.5	1	8	8	12	**49**	**7**	**14.5**
	section 2	6	4	2.5	3.5	3	7.5	5	3.5	13	7	**55**	**10**	**20.5**
		6	2	0	1	3.5	4.5	8.5	8	8	1.5	**43**	**8**	**11**
		16.5	0.5	0	3	3.5	6.5	11	3.5	7	7.5	**59**	**17**	**13.5**
		4.5	0.5	2	2	1	6.5	8	4	9	1.5	**39**	**5**	**12**
		4.5	1.5	0	0	1	1	3	3.5	8.5	9	**32**	**6**	**3.5**
		5	1	3	1	3	4	8	10	4	11	**50**	**6**	**12**
	section 3	5.5	2.5	0.5	0.5	5	2.5	2.5	5	9.5	3.5	**37**	**8**	**11**
		13	5	1	0.5	4	11.5	4	6	11.5	11.5	**68**	**18**	**22**
		11	4	1	3	0	2.5	3	9.5	7	6	**47**	**15**	**10.5**
		13.5	3	2.5	2	5	6	6.5	8.5	5.5	10.5	**63**	**16.5**	**18.5**
		12	1	1	0.5	3	2.5	4.5	5.5	2.5	5.5	**38**	**13**	**8**
		11	7	3.5	4.5	4.5	8	5.5	3.5	7.5	16	**71**	**18**	**27.5**
FISH 2	section 4	7.5	6.5	0	0	3	2	1.5	1.5	2	1	**25**	**14**	**11.5**
		5	12	3	0	1	3	1	2	4.5	3.5	**35**	**17**	**19**
		9	0	1	0	0	4	5.5	3.5	7	7	**37**	**9**	**5**
		7	7	1	1	2	3	2.5	2	8.5	5	**39**	**14**	**14**
		6.5	3.5	6	5	7.5	5	5.5	0.5	1.5	4	**45**	**10**	**27**
		6	2	2.5	2.5	1	0	2	4.5	1.5	2	**24**	**8**	**8**
	section 5	3	1	4.5	13	2.5	3	0	1	1	5	**34**	**4**	**24**
		5	10	8	1.5	4.5	4	4	3	1	6	**47**	**15**	**28**
		3	2.5	5	1.5	0	0	2.5	2.5	4	5	**26**	**5.5**	**9**
		4.5	6	6.5	0.5	2.5	3.5	3.5	3	0	6	**36**	**10.5**	**19**
		4.5	4.5	1	2	3	2	0.5	8.5	8	6	**40**	**9**	**12.5**
		1	5	3	7	2	4	4.5	4.5	6	4	**41**	**6**	**21**
	section 6	2.5	3.5	1	1	1.5	5.5	0.5	3.5	2	2	**23**	**6**	**12.5**
		8	14	2	2.5	1.5	9	4.5	4	1.5	2	**49**	**22**	**29**
		4	5	0	1	0	1.5	3	3.5	5.5	7.5	**31**	**9**	**7.5**
		9	9	2.5	4	5.5	2.5	7.5	3	3.5	3.5	**50**	**18**	**23.5**
		7	6	4	2.5	2.5	3.5	1.5	2	8	16	**53**	**13**	**18.5**
		9	2	1	1	5.5	14.5	6	4	2	8	**53**	**11**	**24**
FISH 3	section 7	2	1	0	0	0	2	0	0	5.5	0.5	**11**	**3**	**3**
		0	2	0	0	0	0	0	0	2.5	4.5	**9**	**2**	**2**
		1	0	3	1	1	0	1	1	0.5	3.5	**12**	**1**	**5**
		5	0	0	2	3	0	0	0	2	0	**12**	**5**	**5**
		5	2	0	4	1	0	1	1	4	0	**18**	**7**	**7**
		5.5	2.5	3	5	5.5	2.5	5	5	1	2	**37**	**8**	**18.5**
	section 8	7	4	2	0	3	1	1	4.5	3	2.5	**28**	**11**	**10**
		0.5	2.5	0.5	3	3	1.5	3.5	1.5	2	4	**22**	**3**	**10.5**
		5	2	1	1	4	0	1	1	5	1	**21**	**7**	**8**
		1	4	1	1	3	3	0	1	3	0	**17**	**5**	**12**
		1	3.5	2	6.5	0	0	1	1	1.5	0.5	**17**	**4.5**	**12**
		2	3.5	0.5	1	2.5	1	1.5	4	4.5	3.5	**24**	**5.5**	**8.5**
	section 9	1	2	0	0	2	2	1.5	1.5	0	0	**10**	**3**	**6**
		1.5	3.5	4.5	7	3	1.5	3	0	2	1	**27**	**5**	**19.5**
		3.5	10.5	4	8.5	5.5	3	2	0	1	4	**42**	**14**	**31.5**
		2	1	3	0	1	0	0	1.5	0.5	1	**10**	**3**	**5**
		6.5	3.5	3	1	0	0	2.5	1.5	2	1	**21**	**10**	**7.5**
		6.5	6	1.5	1	3	0	1.5	0.5	4	0	**24**	**12.5**	**11.5**
	AVRG	5.212963	3.712963	2.12963	2.425926	2.842593	3.175926	3.574074	3.583333	4.648148	4.75	**36.05556**	**8.925926**	**14.28704**
	SEM	0.49649	0.408375	0.257995	0.356309	0.305646	0.41474	0.435561	0.368688	0.450124	0.539387	**2.199953**	**0.679835**	**1.054873**

APPENDIX D: PRIMERS USED FOR SEMI QRT-PCR

Table D.1. The sequences of oligonucleotides used in semi qRT-PCR.

Primer Name	**#**	**Sequence (5’ to 3’)**
axin1_F_1	800	AGGGTTCGACTGGAAGAGGA
axin1_R_2	803	CCATAGTGGTGTTGCTCCGT
axin2_F_1	804	GATAGCCAGACTGGAGCGAC
axin2_R_1	805	AAGTACTGGAATGCCCCAAGG
bmp2k_F_2	807	TCTCAAAGGACCCTCACCAAA
bmp2k_R_2	809	CGCTGTTGCTATCAAGCACAA
ctnnb1_F2	872	CAACGGATTGTCGCCATTATTC
ctnnb1_R2	874	CGATGTCTGCTACTTGCTCTT
ctnnb2_F1	875	TCGCTCAGGCTAAAGGATTG
ctnnb2_R1	877	CATCGTCCTGGTAGTTGATGAG
dickkopf3b_F	812	TGCATCAGATGGAGAACGAGA
dickkopf3b_R	813	TCTGGCAGATTGTTCCCGAC
eef2b_F1	893	CAAGCTGGACACAGAGGATAAG
eef2b_R1	894	GAGGAATGAGACACAGGAATGG
fzd7b_F2	880	CTCCAGATCGGATTTGAGGAATAG
fzd7b_R1	881	GTACTCACACAGCACAGGATAG
neuroD1_F_2	818	CACACCCTAGAGTTCCGACA
neuroD1_R_1	819	GAGGACGGGAATTGTGCAAC
neuroD2_F_2	822	AATCACTCCCTCTGTTCGGC
neuroD2_R_2	824	AAACTCGCTTTGGGCTCATGT
neuroD4_F_1	825	GAACTCCACCTTACGACGGG
neuroD4_R_2	828	TCTCTCAGTGAGCGTTAAGGG
wnt11r_F1	889	GACCTAAAGGACATCGCCATAG
wnt11r_R1	891	CCACACCCAGGCTGAATATAA

APPENDIX E: RAW DATA OF SEMI QRT-PCR RESULTS

Table E.1. Measurements of band intensities of 0h,4h,12h,24h,120h post-injury OEs.

	eef2b	axin2	bmp2k	ctnnb1	ctnnb2	dkk3b	fzd7b	neurod1	neurod4	wnt11r	axin1	neurod2
0h	5368712	3664249	6551579	7778526	7336559	5136623	8621527	10195615	9582890	9582890	8325549	6345897
4h	5852618	3583852	5869427	7377967	7831639	8705935	7848349	10554047	8074541	8074541	6865223	5974167
12h	7031282	3411656	6514836	9663975	9011809	8598159	11255144	11409850	8830951	8830951	7765664	6466213
24h	5383334	3258153	4659735	6550796	5594654	4108386	7112464	7249221	8245561	8245561	5745441	7393121
120h	6226593	4320719	4816688	8244937	6537100	5151545	9473035	12008688	9281905	9281905	7734701	7094674
normalized to eef2b	eef2b	axin2	bmp2k	ctnnb1	ctnnb2	dkk3b	fzd7b	neurod1	neurod4	wnt11r	axin1	neurod2
0h	1	0.682519	1.220326	1.448863	1.36654	0.95677	1.605884	1.89908	1.784951	1.784951	1.550754	1.182015
4h	1	0.61235	1.002872	1.260627	1.338143	1.487528	1.340998	1.803303	1.379646	1.379646	1.173017	1.020768
12h	1	0.485211	0.92655	1.374426	1.281674	1.222844	1.600724	1.622727	1.255952	1.255952	1.104445	0.919635
24h	1	0.60523	0.865585	1.216866	1.039254	0.763168	1.321201	1.346604	1.531683	1.531683	1.067264	1.373335
120h	1	0.693914	0.773567	1.324149	1.049868	0.827346	1.521383	1.928613	1.490688	1.490688	1.242204	1.139415
normalized to 0h	eef2b	axin2	bmp2k	ctnnb1	ctnnb2	dkk3b	fzd7b	neurod1	neurod4	wnt11r	axin1	neurod2
0h	1	1	1	1	1	1	1	1	1	1	1	1
4h	1	0.897191	0.821807	0.87008	0.97922	1.554739	0.835053	0.949567	0.772932	0.772932	0.756418	0.863583
12h	1	0.710912	0.759264	0.948624	0.937897	1.278096	0.996787	0.85448	0.703634	0.703634	0.712199	0.778023
24h	1	0.886758	0.709307	0.839877	0.760501	0.79765	0.822725	0.709082	0.858109	0.858109	0.688223	1.161859
120h	1	1.016695	0.633902	0.913923	0.768267	0.864728	0.947381	1.015551	0.835142	0.835142	0.801033	0.96396

Table E.2. Measurements of band intensities of PBS, LiCl, CAS treated OEs.

	eef2b	axin2	bmp2k	ctnnb1	ctnnb2	dkk3b	fzd7b	neurod1	neurod4	wnt11r	axin1
PBS	22684297	9721363	13333328	10909658	13520274	8580149	13867197	18527065	17452694	10660299	15491131
LiCl	19127718	14394387	10993154	12781738	7078080	6282788	13144303	10362447	14338646	12351304	13458394
CAS	16595048	9964881	12655953	10895299	6189456	15249974	11855510	16166179	15539335	11908846	5498909
normalized to eef2b	eef2b	axin2	bmp2k	ctnnb1	ctnnb2	dkk3b	fzd7b	neurod1	neurod4	wnt11r	axin1
PBS	1	0.42855	0.587778	0.480934	0.596019	0.378242	0.611313	0.816735	0.769373	0.469942	0.682901
LiCl	1	0.752541	0.574724	0.668231	0.370043	0.328465	0.687186	0.54175	0.749627	0.645728	0.703607
CAS	1	0.600473	0.762634	0.656539	0.37297	0.918947	0.7144	0.974157	0.936384	0.717614	0.331358
normalized to PBS	eef2b	axin2	bmp2k	ctnnb1	ctnnb2	dkk3b	fzd7b	neurod1	neurod4	wnt11r	axin1
PBS	1	1	1	1	1	1	1	1	1	1	1
LiCl	1	1.756015	0.977791	1.389444	0.620858	0.8684	1.124116	0.663312	0.974334	1.37406	1.03032
CAS	1	1.401173	1.297487	1.365133	0.625769	2.429523	1.168634	1.192745	1.217073	1.527028	0.485222

APPENDIX F: MACRO SCRIPT USED FOR CELL COUNTING IN FIJI

```
id = getImageID();
path = getInfo("image.directory")
name = getInfo("image.filename");
height = getHeight();
width = getWidth();
result_path = path + "results_of_" + File.nameWithoutExtension;
print("image ID: " + id);
print("file path: " + path);
print("file name: " + name);
print("image height: " + height);
print("image width: " + width);
print(File.nameWithoutExtension);
print(result_path);
segments = getNumber("enter the number of segments", 10);
run("8-bit");
//run("Brightness/Contrast...");
run("Enhance Contrast", "saturated=0.35");
setAutoThreshold("Default dark");
run("Threshold...");
waitForUser("User input", "adjust threshold and press ok to continue");
run("Convert to Mask");
run("Close");
run("Watershed");
roiManager("reset");
for (i=0; i<segments; i++) {
		makeRectangle(i*(width/segments), 0, (width/segments), height);
		Roi.setName(i+1)
		roiManager("add");
  }
makeRectangle(0, 0, width, height);
Roi.setName("total");
roiManager("add");
for (i=0 ; i<roiManager("count"); i++) {
   selectImage(id);
   roiManager("select", i);
   current = Roi.getName();
   run("Analyze Particles...", "size=16-Infinity pixel circularity=0.50-1.00 show=Outlines display clear exclude include summarize");
selectWindow("Drawing of " + name);
File.makeDirectory(result_path);
saveAs("Tiff", result_path + "/ROI_" +  current + "_of_" + name);
close();
}
waitForUser("wait");

roiManager("reset");
for (i=0; i<segments-1; i++) {
		makeRectangle(i*(width/segments), 0, 2*(width/segments), height);
		Roi.setName("combined " + i+1)
		roiManager("add");
  }
for (i=0 ; i<roiManager("count"); i++) {
   selectImage(id);
   roiManager("select", i);
   current = Roi.getName();
   run("Analyze Particles...", "size=16-Infinity pixel circularity=0.50-1.00 show=Outlines display exclude include summarize");
   selectWindow("Drawing of " + name);
   close();
}
selectWindow("Summary");
saveAs("Results", result_path + "/counts_of_" + File.nameWithoutExtension+ ".csv");
selectWindow(name);
saveAs("Tiff", result_path + "/mask" + name)
run("Close");
selectWindow("Results");
```

APPENDIX G: R SCRIPT USED FOR CELL COUNTING

```
file_name <- file.choose()
 data <- data.frame(read.csv(file_name, header=TRUE))
 slices <- 10
 sumofcalc <- 0
 sumofmeas <- 0
 values <- 0
  for(i in 1:10) {
                values[i] <- data$Count[i]
                print(values[i])
   }
  for(i in 1:9) {
                values[i] <- data$Count[i]
                sumofcalc[i] <- data$Count[i] + data$Count[i+1]
                sumofmeas[i] <- data$Count[i+slices+1]
   print(sumofcalc[i])
   print(sumofmeas[i])
     }
diff <- sumofmeas - sumofcalc
diff_half <- diff/2
diff_half_left <- append(diff_half, 0, after=0)
diff_half_right <- append(diff_half, 0, after=9)
corrected_values <- values + diff_half_left + diff_half_right
corrected_values
x <- seq(0.1, 1, 0.1)
plot(x, corrected_values)
output <- data.frame(data$Slice[1], x, corrected_values)
new_file_name <- gsub("counts_of_", "corrected_counts_of_", file_name)
write.csv(output, new_file_name)
```